NEW YORK UNIVERSITY

College of Engineering
RESEARCH DIVISION
University Heights, New York 53, N. Y.

GEOMAGNETIC IMPLICATIONS OF THE COSMIC RAY DIURNAL VARIATION, AND ITS SPECTRUM

by
Donald E. Cotten

Final Project Report

Prepared for
U.S. Army Signal Research and Development Laboratory
and
National Aeronautics and Space Administration
March 1, 1963

NEW YORK UNIVERSITY

College of Engineering

Research Division

GEOMAGNETIC IMPLICATIONS OF THE COSMIC RAY DIURNAL VARIATION AND ITS SPECTRUM

by

Donald E. Cotten

Final Project Report

Approved Arthur Beiser

Arthur Beiser
Project Director

The work described herein was sponsored by the Advanced Research Projects Agency under Order Nr. 163-61, through the U.S. Army Signal Research and Development Laboratory under Contract Nr. DA 36-039-SC-87171, and by the National Aeronautics and Space Administration under Grant No. NsG 108-61.

Acknowledgements

The author wishes to thank Dr. Arthur Beiser for suggesting the problem, and to express his gratitude to Drs. Arthur Beiser, Serge A. Korff, Wallace Arthur, Walter Kertz, Wolfgang Ramm, Jurgen Untiedt and David Stern, and also Thomas Kelsall, for many stimulating and helpful discussions. Thanks are also due to Emmanuel Mehr and Abe Lucas for their assistance in computer programming, to Robert H. Kress for neat tracing of some of the figures in this report, to Joan Santora for her conscientiousness in typing and to my wife Evelyn Cotten for her assistance in preparation of this manuscript and her patience during the course of the research.

ABSTRACT

19946

When the amplitudes n_1 of the diurnal variation (CRDV) in counting rates of all northern and equatorial neutron monitors are averaged over groups of months within the IGY, and some pairs of stations with close values of Quenby-Webber cutoff rigidity P_c are averaged together to smooth the data, then two peaks of $n_1(P_c)$ persist at approximately P_c=1 and 4 BV/C. An expression for n_1, wherein the impact zones as calculated by Kelsall for various rigidities P are expressed as geomagnetic colatitude-dependent integration limits $P_o, \ldots P_4$, is used to solve for the CRDV differential spectrum $(4/3)k(P)\cos \phi$ at those limits without any prior assumption as to the form of k(P). Here k(P) is a fraction of the isotropic cosmic ray flux at infinity and ϕ is the assymptotic longitude with respect to an axis of anisotropy. If the equatorial data is smoothed, then $k(P) = 0.0039 \pm 0.002$ satisfies the equation at $P > 6$ BV/C, and the double peak of $n_1(P_c)$ leads to a single peak of k(P) at $3.8 < P < 5.7$ BV/C, with maximum k(P) = 0.01 to 0.06 at P = 5.4 BV/C. At $P < 3.8$ BV/C, k(P) = 0. Contours are presented showing the CRDV amplitude and phase, and the amplitude of the semi-diurnal variation, as functions of latitude and longitude. These maps display relative extremums which correspond to extremums of geomagnetic field maps, and which indicate that the geomagnetic dipole and quadrupole moments as measured at the earth's surface significantly affect the anisotropic part of the cosmic radiation. An explanation is given for the fact that the semi-diurnal variation has appreciable amplitude only along part of the magnetic equator. The cosmic ray anisotropy introduced by the solar system is found to come from a direction 75° to 100° east of the sun. Small CRDV components dependent on Greenwich time and sidereal time are discussed.

Table of Contents

I. Introduction

A.

A description of the magnetic field at large distances above the earth's surface could be obtained completely from an infinite number of magnetometers distributed over the entire surface if not for the existence of unknown electric currents near the earth. This failure makes it desirable to measure the geomagnetic field far above the surface. Nature provides us at all times with a vast number of charged cosmic ray particles which have probed a large portion of the outer field. Their orbits and points of impact upon the atmosphere near the earth's surface depend on the interplanetary magnetic field, the distant geomagnetic field, and partly on the nearby field. Collisions with atoms or molecules of our atmosphere produce secondary protons, neutrons, mesons, electrons, and photons, any of which may be detected at the earth's surface. The counting rates of the detectors can be related to the primary cosmic ray flux.[1]

In order to gain information about magnetic fields these counting rates must be compared over a large region of the earth, preferably the entire earth. Such comparison can only be made for comparable percentage changes in counting rate which occur over large areas. Forbush-type decreases (FD) of a few percent in the cosmic radiation occur at irregular intervals a few days or weeks apart and provide one means of such comparison. Solar flares produce large increases which permit comparison at even less frequent intervals. These events provide occasional information regarding the kind of disturbance of the interplanetary or geomagnetic field which occurred during the event. In order

---

[1] Quenby, J. J. and Webber, W. R., Phil. Mag. 4, 657 (1959).

to monitor the undisturbed magnetic fields by using cosmic rays it is necessary to study a change in their counting rate which is world-wide and which occurs regularly on geomagnetically undisturbed days. The diurnal variation in cosmic ray nucleon counting rate (CRDV) permits such comparison between stations, provided that a suitable theory is used to relate the observed CRDV to the magnetic fields or other geophysical phenomena. This paper presents a new theory which accounts for all of the general features of the CRDV and also several of its heretofore unnoticed and unexplained details.

I. B. Interplanetary and Geomagnetic Fields

The geomagnetic field is specified at all points on the earth's surface and in nearby space by the spherical harmonic coefficients[2,3] for a magnetic scalar potential chosen to fit magnetometer measurements at a limited number of fixed or mobile observing stations on the surface or in airplanes.[2] Satellite-borne magnetometers have recently carried the measurements out to several earth radii within limited regions of latitude, longitude and altitude.[4,5] Scalar potential analysis is only valid in the region which does not include currents such as in the Van Allen particle belts or an equatorial ring current beyond that.[6] In that analysis the dipole terms dominate to give a dipole moment of 8.1×10^{25} gauss cm^3 oriented at 12° with the rotation axis. The quadrupole moment

---

[2]Vestine, E. H., Transactions A.G.U. 41, 4 (1960).
[3]Finch, H. F. and Leaton, B. R., Roy. Astron.Soc., Mon. Not., Geophys. Suppl. 7, 314 (1957).
[4]Cain, J. C., Shapiro, I. R., Stolarik, J. D. Heppner, J. P., NASA Report X-611-62-128, Aug. 21, 1962, Jour. Geophys. Res. 67, 5055, (1962).
[5]Heppner, J. P., Ness, N. F., Scearce, C. S. and Skillman, T. L. NASA Report X-6---62-125, Jour. Geophys. Res. 68, 1, (1963).
[6]Akasofu, S-I, and Chapman, S., Jour..Geophys. Res. 66, 1321-1350, (1961).

gives a field oriented sc that its maximum strength is attained at four "poles" situated near the dipole equator. Its average strength at the surface is 7% of that of the dipole field,[7] and above the surface it falls off as r^{-4} while the dipole field falls off as r^{-3}, where r is the distance from the earth's center. In the theory of many geophysical phenomena the earth's field is regarded as consisting only of the field of a magnetic dipole located at the center of the earth. When a slightly more detailed model of the field is required a dipole of the same strength is located eccentrically so as to best fit the strength of the dipole plus (rotation) axial quadrupole terms.[8] More detailed models for the field include the remaining four quadrupole terms and then multipole terms of higher order. Calculations for some phenomena, as for example, the guiding of hydromagnetic waves bythe actual field lines, or the location of conjugate points at the two ends of a field line, require the use of as many multipole coefficients as are available. The earth ring currents also make contributions to the observed geomagnetic field.[9]

Some measurements have been made of the strengths of interplanetary magnetic (IP) fields,[5] and various models of the IP field have been proposed to explain the observed strength and infer its direction. One of the more recent proposals[10] is that the plasma called the solar wind continuously expanding from the solar corona carries with it magnetic field lines bent in an Archimedian spiral and co-rotating with the sun. The direction of the IP field lines in the vicinity of the earth is not yet established.

---

[7]Quenby, J. J. and Webber, W. R., Phil. Mag. 4, 90, (1959).
[8]Bartels, J. Terr. Mag. and Atmos. Elec. 41, 225, (1936)
[9]Chapman, S., Akasafu, S. I., and Cain, J. C., J. Geophys. Res. 66, 4013, (1961).
[10]Dessler, A. J., Ahluwalia, H. S. and Gottlieb, B., J. Geophys. Res. 67, 3553, (1962).

Interaction between the solar wind plasma and the geomagnetic field prcduces a geomagnetic envelope[11,12,13] such that the geomagnetic field is compressed somewhat and increased in strength on the solar-windward side or head, and extended and decreased in strength on the opposite side, or tail, of the geomagnetic field.

I. C. Previous Studies of the Cosmic Ray Diurnal Variation

Early in the study of cosmic radiation (CR), indications were found of a very small CRDV with period of one sidereal day[14] and of one mean solar day[15-21], and a CRDV theory was put forth.[22] Altitude dependence of the observed CRDV was small.[23,24] Attempts were made[21,25] to attribute the CRDV to a CR anisotropy produced by a solar magnetic moment of 10^{34} gauss cm^3, or to a beam of particles of CR energy coming from the sun.[26,27] Deflections by the geomagnetic dipole model field were calculated[25, 28-31] for

---

[11]Hurley, J., Doctoral Thesis, New York University, (1961).
[12]Hurley, J., "Interaction Between the Solar Wind and the Geomagnetic Field," NYU Project Report, (March 1, 1961).
[13]Beard, D. B., J. Geophys. Res 65, 3559 (1960); 67, 4895, (1962).
[14]Compton, A. H. and Getting, I. A., Phys. Rev. 47, 817 (1935).
[15]Millikan, R. A. and Neher, H. V., Phys. Rev. 47, 204 (1935); 50, 15 (1936).
[16]Hess, V. F. and Graziadei, H. T., Terr. Magn. 41, 9 (1936).
[17]Forbush, S. E., Terr Magn. 42, 1 (1937).
[18]Schonland, B. F. J., Delatizky, B., Gaskell, J., Terr. Magn. 42, 137 (1937).
[19]Thompson, J. L., Phys. Rev. 54, 93 (1938).
[20]Epstein, P. S., Phys. Rev. 53, 862 (1938).
[21]Vallarta, M. and Godart, O., Rev. Mod. Phys. 11, 180 (1939).
[22]Janossy, L., Zeit. Phys. 104, 430 (1937).
[23]Malmfors, Arkiv. Mat. Astron. Fys. 30A, 12 (1944).
[24]Malmfors, Arkiv. Mat. Astron. Fys. 32, 8 (1945).
[25]Dwight, K. Phys. Rev. 78, 40 (1950).
[26]Alfven, H. Tellus 6, 232-253, (1954).
[27]Dorman, L. I., Cosmic Ray Variations, State Publ. House for Tech. and Theor. Lit., Moscow, 1957.
[28]Schluter, J., E. Naturforsch 62, 613 (1951).
[29]Firor, J., Phys. Rev. 94, 1017 (1954).
[30]Jory, F. S., P hys. Rev. 103, 1068 (1956).
[31]Lust, R., Phys. Rev. 105, 1827 (1957).

particles impacting vertically upon the earth, in order to relate[25,32,33] the local time (LT) of diurnal maximum (peak time) of CR to the assymptotic directions for the CR orbits which are responsible. From the CRDV peak times at a small number of observing stations the direction of the axis of anisotropy was thus found[25] to be a few hours before 18 hours LT and later found to be[33] 16.8 hours LT or[34] 259° = 17.3 hours LT. Local time, LT, is also the longitude with respect to the earth-anti-sun line.

A study[35] of the CRDV at Climax, Colorado and Huancayo, Peru showed that the daily variation (DV) in atmospheric temperature was not its principal cause, and this was later corroborated.[34]

CRDV data from 1937 to 1951 were fitted to a differential spectrum aE^{-1} times that of the omnidirectional CR for energies $E > 7.5$ Bev spectral cutoff and $a = 0$ for $E < 7.5$ Bev.[27] A review article on CR[36] discusses the CRDV.

The daily variation bi-hourly counting rates (DVCR) for CR meson telescopes at Ahmedabad, India, showed[37] that the peak times clustered in two groups at 03 hours and 11 hours LT at Solar minimum in 1954. These peak times increased to 7-8 hours and 15 hours LT in 1956. Days when only the morning peak appeared occurred during a long-term decrease of daily mean intensity, and afternoon peaks were similarly associated with

---

[32] Nagashima, K., Patnis, V. R. and Pomerantz, M. A., Nuovo Cimento 19, 292 (1961).
[33] Duggal, S. P., Nagashima, K. and Pomerantz, M. A., J. Geophys. Res. 66, 1970, (1961).
[34] Thompson, D. M., Phil. Mag. Vol. 6, #64, 573, (1961).
[35] Firor, J., Fonger, W. H. and Simpson, J. A., Phys. Rev. 94, 1031 (1954).
[36] Rose, D. C., Adv. in Electronics and Electron Phys. 9, 129 (1957).
[37] Sarabhai, V. and Bhavsar, P. D., Supp. Nuovo Cim. 8, 299 (1958).

increases. Sandstrom and Lindgren[38] found that rejection of data for days of FD does not greatly affect the long term average n_1 and phase of the reported CRDV. Kane[39,40] has further discussed the affects on the CRDV of changes in the isotropic CR. Parsons[41,42] found that even after FD are excluded, short term irregular CR variations depending on UT may alter the monthly average CRDV by not more than 0.11%. He attributed lack of simple agreement between peak LT's to some unremoved variation with UT.

Directional meson telescopes at Uppsala, Sweden and Murchison Bay, Norway, showed[43-45] that n_1 decreases with assymptotic latitude Λ, and is almost zero for $\Lambda = 82^{\circ}$. Elliot's group has done work on the CRDV.[46-48]. The first and second harmonic CRDV amplitudes and peak times for all IGY neutron monitor stations have been calculated as averaged over the eighteen IGY months and plotted against both geomagnetic and geographic latitude.[49] Although no curves are drawn through the points, a definite latitude dependence is displayed despite much scatter of points for stations of different longitudes. Messerschmidt[50] has presented some of this information. The CRDV has also been studied at low latitudes in India.[51]

---

[38]Sandstrom, A. E. and Lindgren, S., Ark. Fys. 16, No. 12, (1959).
[39]Kane, R. P., Proc. Indian Acad. Sci. 52, 69-79 (1960).
[40]Kane, R. P., Indian J. Phys. 35, 213 (1961).
[41]Parsons, N. R., Tellus 12, (4), 1960.
[42]Parsons, N. R. J. Geophys. Res. 65, 3159 (1960).
[43]Sandstrom, A. E., Dyring, E. and Lindgren, S., Nature 187, 1099 (1960).
[44]Sandstrom, Dyring, E. and Lingren, S., Tellus 12, 332, (1960).
[45]Sandstrom, A. E. Am. J. Phys. 29, 187 (1961).
[46]Elliot, H. and Dolbear, D. W. N, J. Atmos. and Terres. Phys. 1, 205 (1951).
[47]Elliot, H., Progress in Cosmic Ray Physics, 1, p. 453, North Holland Publishing Co., (1952).
[48]Elliot, H. Phil. Mag. 5, 601-619 (1960).
[49]Schwachheim, G., J. Geophys. Res. 65, 3149 (1960).
[50]Messerschmidt, W., Naturforschung 15a, 734 (1960).
[51]Rao, A. and Sarabhai, V., Proc. Roy. Soc. 263, 101, 118, 127 (1961).

The dependence of the CRDV upon longitude and month, as well as latitude and cutoff rigidity was presented by Cotten[52] at the April 1961 meeting of the American Geophysical Union, and was related to the locations of the several impact zones at each rigidity for near-equatorial assymptotic orbits, and to the higher multipoles of the geomagnetic field. Isoplot maps were shown.

McCracken[53] found m = 0 to 1 in a p^{-m} spectrum. Dattner and Venkatesen present some experimental results for the CRDV.[54]

Pomerantz, et al.,[32,33] have presented a theory for the CRDV, taking the amplitude as

$$n_1 = \frac{\Delta I}{I} = \frac{\alpha_o}{I} \sum_z \int_{P_c}^{\infty} S_z(P,x) J_z(P) \left(\frac{P_o}{P}\right)^m (\cos\Lambda)^n \cos(\psi - \psi_E) dP \qquad \text{(eq.1)}$$

where α_o is a normalization constant, n = 1, and I, z, S_z, J_z, x, P, and P_c are as defined in section IV B on pages 30 to 33. The assymptotic directions for CR orbits[29] impacting vertically are the latitude Λ with respect to the axis of anisotropy lying in the equatorial plane, and the longitude difference $(\psi - \psi_E)$ between the axis of anisotropy and the assymptotic orbit. This integral maps a CR anisotropy which is a cosine function of assymptotic longitude into a cosine function of longitude without consideration of the focusing into impact zones accomplished by the geomagnetic field.[55] It yields average deflections $\overline{\psi_E}$ by

---

[52]Cotten, D., J. Geophys. Res. 66, 2522, (1961).
[53]McCracken, K. G., Doctoral Thesis, Univ. of Tasmania, (1958).
[54]Dattner, A. and Venkateson, D., Tellus 11, 116 (1959).
[55]Kelsall, T., J. Geophys. Res. 66, 4047(1961).

the geomagnetic field.[29] From a least squares fit of fourteen pairs of observed CRDV first harmonic coefficients to the values predicted by this theory, it was found[33] that $\alpha_o = 0$ for $P < 7$ BV/c and $m = 0.4$ for $P > 7$ BV/c, with the axis of anisotropy at 16.8 hours LT.

Forbush and Venkatesan[56] studied the yearly mean CRDV for 1937 to 1959 for ionization chamber data for Fredericksburg, Maryland; Huancayo, Peru; and Christchurch, England; and found that the yearly mean CRDV varied with a 22 year period. They established a statistically real CRD/2V but regard it, at least at Huancayo, as probably resulting from a systematic error due to friction at the barograph pen.

Rao, McCracken, Venkatesan, and Katzman[57-60] in their study of the CRDV at 22 stations, performed a harmonic analysis of the uncorrected neutron monitor DVCR and of the DV in atmospheric pressure at each station. They then performed a pressure correction upon the uncorrected CRDV amplitude and phase, by a vector addition of the pressure correction of -.72%/mb corresponding to the amplitude and phase of the pressure DV. The resulting corrected CRDV values agree closely with those obtained by harmonic analysis of the cosmic ray nucleon counting rates which had been pressure corrected individually each bi-hour of each day. These investigators ascribe the second harmonic CRD/2V entirely to the second harmonic of the atmospheric pressure

---

[56]Forbush, S. E. and Venkatesan, D., J. Geophys. Res. 65, 2213 (1960).
[57]Katzman, J., Can. J. Phys. 37, 1207 (1959).
[58]Katzman, J. and Venkatesan, D., Can. J. Phys. 38, 1011 (1960).
[59]Katzman, J., Can. J. Phys. 39, 1477 (1961).
[60]Rao, U., McCracken, K. G. and Venkatesan, D., J. Geophys. Res. 67, 3590 (1962); 68, 345 (1963).

DV. They find that after pressure correction there is a residual CRD/2V at all equatorial stations except Huancayo, and none elsewhere.

D. M. Thompson[34] has studied the CRDV for neutron monitors at Makerere College, East Africa; Hermanus, South Africa; and Herstmonceux, England for 1958 and 1959. No CRDV harmonic he finds could be caused by improper pressure correction due to barograph pen friction because these stations use mercury barometers. He found a significant CRD/2V after pressure correction.

Stern[61] has used power spectral analysis to determine the periodicities present in the CR neutron monitor counting rates at several stations and finds semi-diurnal, diurnal, 27 day, and annual periods. His analysis considers amplitudes only, ignoring peak times. It complements the harmonic analysis of other investigators in that it does not assume a fundamental period of one day, yet finds one.

Dessler, Ahluwalia and Gottlieb[10] have proposed a theory to relate the interplanetary magnetic field direction and strength to a CR anisotropy. Dattner and Venketesan[62] discuss many other possible causes for a CR anisotropy.

---

[61] Stern, D., J. Geophys. Res. 67, 2133 (1962).
[62] Dattner, A. and Venkatesan, D., Tellus 11, 239 (1959).

I. D. Störmer Equations

The equations of motion of a charged particle in a magnetic dipole field were written and solved by Carl Störmer[63] and his followers since 1903. These equations are shown in section VC, page 78, of this report if Q is set equal to zero there. They have solutions in closed form only for orbits in the dipole equatorial plane. Numerical integration is required elsewhere. Because the field has symmetry around the dipole axis, the canonical momentum 2γ conjugate to the magnetic longitude is a constant of the motion. No component of the ordinary angular momentum $\vec{r} \times \vec{p}$ is conserved in general in a dipole field since the Lorentz force is not radial except for special orbits which are concentric circles in the equatorial plane. The magnetic rigidity P of a particle is defined as its momentum per unit charge. The Stormer constant 2γ leads to the identification of allowed and unallowed regions, and to a lower limit for P called the cutoff rigidity $P_c(\lambda, \zeta, \mu)$ such that particles approaching from infinity will not impact upon the earth's surface at a magnetic latitude λ from a zenith angle ζ and azimuth μ unless their $P \geq P_c(\lambda, \zeta, \mu)$. For vertical incidence $\zeta = 0^\circ$ and

$$P_c(\lambda, 0^\circ) = P_c(\lambda) = 14.9 \cos^4 \lambda \quad BV/c. \qquad \text{(eq. 2)}$$

Lemaitre and Vallarta[64-66] have modified the Störmer allowed cones to remove those directions whose orbits would have gone inside the earth at some other place.

---

[63] Störmer, C., The Polar Aurora, Oxford, (1955).
[64] Lemaitre, G. and Vallarta, M. S., Phys. Rev. 43, 87 (1933).
[65] Lemaitre, G. and Vallarta, M. S., Phys. Rev. 49, 719 (1936).
[66] Lemaitre, G. and Vallarta, M. S., Phys. Rev. 50, 49, (1936).

Numerical integrations to determine the points of impact upon the earth for particles of various rigidities along orbits whose assymptotes at infinite distance (assymptotic orbits) have various directions have been performed by Stormer and his pupils,[63] by several other workers for $\zeta = 0^{o}$,[25,28-31] and by Kelsall[55] for $\zeta \leq 90^{o}$. This paper makes use of the impact zones[55] which result from a broad parallel beam of non-interacting charged particles whose assymptotic orbits are at angle α with respect to the dipole axis. If the beam came directly from the sun α would be 90^{o} at the equinoxes, except that the rotation of the earth carries the dipole axis around on a cone of half-angle 12^{o}. In Kelsall's[55] figures 6 it can be seen that for energies of less than 15 Bev there are two impact zones in each hemisphere, an early one at about 03 hrs LT, and a late one at 09 hrs, symmetrical about the equator. For energies higher than 15 Bev there is one zone centered on the equator but with essentially two centers. Both early and late impact zones show impact times later for high latitudes than for low or equatorial latitudes. When $\alpha \neq 90^{o}$ the impact zones shift away from symmetry. Kelsall's results show that the beam is focussed down from a broad area at infinity to much smaller areas of impact on the earth's surface. Focussing factors C (herein called f) are tabulated there.[55]

I. E. Cosmic Rays in a Non-Dipole Geomagnetic Field

Consideration of which orbits can reach the earth from infinity in a field model for the earth which includes some terms beyond the dipole terms has been made by approximately correcting the Störmer cutoff rigidities at vertical incidence (eq. 2) for the effects of the higher multipole terms. Cutoff rigidities appropriate

for the eccentric dipole field model have thus been calculated.[67]

Quenby and Webber[7] provide formulae for a more correct set of P_c values which takes into account not only the dipole field but also the effect of the local magnetic field, weighted according to the average relative importance of the various multipoles as averaged over the earth. The values of rigidity cutoff at the various IGY neutron monitor stations were computed according to Quenby and Webber's formulae by Cogger.[68] It has been shown[69] that the earth's ring current cannot produce drastic reductions of apparent cutoff rigidity for near-equatorially incident particles.

---

[67] Kodama, M., Kondo, I. and Wada, M., J. Sci. Res. Inst. (Japan), 51, 138 (1957).

[68] Cogger, L. L., Atomic Energy of Canada Ltd.-1104, Chalk River Ontario, CRGP-965.

[69] Akasofu, S. and Lin, W. C., Trans. Am. Geophys. Union 43, 461, (1962).

II. Data Examined

Standard local production neutron monitor[1,2] data is examined for this study of the CRDV because it requires correction only for atmospheric pressure[1,2] at the monitor. Meson detectors for example require an additional correction for the (unknown) temperature and pressure distribution aloft. A network of forty-nine standard neutron monitor stations distributed widely over the earth gathered continuous records of counting rates during the eighteen months of the International Geophysical Year (IGY), July 1957 through December 1958. The data, consisting of the number of counts per two hour interval, was submitted to the Japanese IGY World Data Center (WDC).[3] Several stations performed pressure corrections, using their two-hourly barometer readings, and their local value for the pressure coefficient. The remaining stations sent their barometer data to the WDC, where the correction was performed using a common pressure coefficient of 0.96%/mmHg for all those stations. In effect, the WDC then expressed the 2-hourly counting rates in tenths of percent of each station's average counting rate, by taking for most stations

$$1000 \ln\left(\frac{\text{bi-hourly counting rate}}{\text{long term average counting rate}}\right)$$

Since the departures from the average are usually only a few percent and $\ln(1+x) \approx x$ for $x \ll 1$, this gives the same number as

---

[1]Simpson, J. A., Fonger, W. and Trieman, S. B., Phys. Rev. 90, 934 (1953).
[2]Arthur, W., The Cosmic Ray Increase of 1960, (Ph.D. thesis, New York University)
[3]Cosmic Ray Intensity During the IGY, National Committee for the IGY, Science Council of Japan, Tokyo, (1960).

would be obtained if the 2-hourly counting rates were actually expressed as a fraction of the average. The data from two stations were expressed in simple percent of the station's average, by the stations themselves. The WDC then added together the percentage counting rates from the same two hour interval of each of the days in a month for which a complete 24 hour record was available, and divided by the number of complete days included in the month. This gives twelve numbers which represent the daily variation part of the cosmic radiation (DVCR) for an average day of that month. The averaging smooths out or reduces the effective value of any fluctuations which did not occur at about the same time each day.[4]

---

[4]Chapman, S. and Bartels, J., Geomagnetism, Oxford, (1940).

III. Data Reduction Performed

A. Harmonic Analysis

When an entry in any station's original remarks suggested it would be prudent, a day of data was eliminated and the remaining data was re-averaged. The bi-hourly values of the average DVCR for each station and month were then analyzed to obtain the coefficients in

$$\text{DVCR}(t) = y_i = a_o + \sum_{m=1}^{6} a_m \cos m \frac{\pi i}{6} + \sum_{m=1}^{5} b_m \sin m \frac{\pi i}{6} \qquad \text{(III-1)}$$

where for $i = 1,\ldots 12$, $t = 2i-1$ is the Greenwich or "universal" time, UT, in hours.[1] For this a standard routine[2] using discrete sums was performed on IBM 704 and 7090 computers.[3] The coefficients were also expressed in the form

$$\text{DVCR}(t) = a_o + \sum_{m=1}^{6} n_m \sin m\,(t-\phi_m). \qquad (2)$$

The phase angles ϕ_m were converted to local time LT in hours by

$$\phi_{m_{LT}} = \phi_m + \text{Longitude}. \qquad (3)$$

This phase time is 6/m hours before the peak time. For recognition of stations and months showing a strongly first harmonic CRDV,

---

[1] 1 hour = 15°

[2] Willers, F. A., Practical Analysis, Dover, p. 345 (1947).

[3] Program written by E. Mehr, NYU Research Division.

the relative amplitudes

$$\frac{n_m}{n_1}\ ,\ m = 2,\ldots 6$$

were calculated. A very few station-months of data were rejected because their higher harmonics m = 3,...6, were thereby found excessive. A more stringent rejection scheme was attempted but was abandoned because it eliminated meaningful first harmonic data, merely because the stations' second or third harmonics were characteristically high. The sine and cosine coefficients for a harmonic dial[6] in local time were computed by

$$a_{mLT} = n_m \cos \phi_{mLT}$$

$$b_{mLT} = n_m \sin \phi_{mLT} \quad . \tag{4}$$

A sample of the IBM 704 output listing is shown as Table I. Much of this output was also punched on IBM cards to form the input to the next computer program. Averages of n_1, n_2, ϕ_{1LT}, ϕ_{1UT}, ϕ_{2UT} and ϕ_{2UT} were made for a great many groupings of stations and months. Sine functions of the same period are correctly averaged by a vector sum of amplitudes, taking into account their phase angles, divided by the number of entries, N. That is,

$$n_m = \sqrt{\bar{a}_{mLT}^2 + \bar{b}_{mLT}^2} \tag{5}$$

$$\phi_{mLT} = \tan^{-1} \frac{\bar{b}_{mLT}}{\bar{a}_{mLT}} \tag{6}$$

---

[6] See page 18 for reference.

where

$$\bar{X}_{mLT} = \frac{1}{N} \sum_{k=1}^{N} X_{mLT\,k} \,, \quad m = 1,2. \tag{7}$$

where $X = a_{mLT}$, b_{mLT}, n_{mLT}, or ϕ_{mLT} .

These, and the standard deviations

$$\sigma_x = \sqrt{\frac{\sum_{k=1}^{N} (X_k - \bar{X}_k)^2}{N - 1}} \tag{8}$$

were calculated on an IBM 650.[4] Simple arithmetic averages of n_m and ϕ_m were also obtained. Samples of the input and output listings are shown as Table II.

A large Forbush-type decrease (FD) occurring in a month would decrease the daily variation ordinate for the bi-hour in which it occurred, and somewhat for the following hours, even after averaging over one month. The apparent DVCR would then not be the true DVCR.[5] The CRDV involves a peak-to-peak amplitude, or change in ordinate, of 0.6 to 1.0%. A typical FD of 6% would make only a 0.2% change in ordinate and therefore have a small but noticeable effect on n_1 and ϕ_1. Days showing an FD were not removed from the record. A few such days were removed from Zugspitze's data, and the harmonic coefficients were not affected sufficiently to seriously affect the maps and graphs which will be described. It was therefore considered unnecessary to reject all the data for those days. A linear increase in counting rate, such as is

---

[4]Program written by A. Lucas, NYU Research Division.
[5]Carmichael, H., private communication.

Table I

Sample IBM 704 Output
Harmonic Analysis

ZUGSPITZE
SEPT. 1957 IDENT. 1131 LONG. 0.732

-0.6 -0.9 -4.2	-0.1	3.0	4.2	0.3	3.9	4.2	0.8	-2.9	-4.3
CONSTANT TERM	-0.05								
COS	-3.12		-0.01		0.37	0.02		0.31	-0.02
SIN	-3.96		-0.30		0.23	0.19		-0.01	0.
AMPLITUDE	5.47		0.30		0.01	0.19		0.31	0.02
AMPLITUDE NRM	1.00		0.05		0.09	0.03		0.05	0.00
PHASE ANGLE	7.91		4.93		5.50	4.87		2.59	2.00
PHASE ANGLE LT	8.25		5.66		6.23	5.61		3.32	2.73
COSINE COEF. LT	-3.39		-0.30		0.11	0.17		-0.11	-0.01
SINE COEF. LT	5.39		0.05		-0.60	-0.08		-0.28	-0.02
HARMONIC, m =	1		2		3	4		5	6

OCT. 1957 IDENT. 1132 LONG. 0.732

-4.6 -3.2 -1.4	-0.9	0.7	1.5	3.8	2.7	2.9	1.2	-0.7	-2.6
CONSTANT TERM	-0.05								
COS	-2.41		-0.46		-0.09	0.15		0.41	-0.17
SIN	-2.45		-0.23		-0.45	0.00		-0.15	0.
AMPLITUDE	3.44		0.54		0.45	0.15		0.44	0.17
AMPLITUDE NRM	1.00		0.16		0.13	0.04		0.13	0.05
PHASE ANGLE	8.03		2.69		2.86	3.50		2.34	2.00
PHASE ANGLE LT	8.76		3.58		3.59	4.23		3.07	2.73
COSINE COEF. LT	-2.28		-0.16		-0.45	-0.04		-0.28	-0.07
SINE COEF. LT	2.58		0.51		0.14	-0.14		-0.34	-0.15

Table II

Sample IBM 650 Input-Output
Vector Averaging of Harmonic Coefficients

	FIRST HARMONIC CRDV						SECOND HARMONIC CRD/2V				RELATIVE AMPLITUDES					IDENTIFICATIONS		
	COS COEF	SIN COEF	PHASE ANGLE	AMPL	COS COEF. L	SIN COEF. L	AMPL	PHASE ANGLE	COS COEF. L	SIN COEF. L						LONG.	CO-LAT	MONTH
	1/10 %	1/10 %	hrs,LT	1/10 %	1/10 %	1/10 %	1/10 %	hrs,LT	1/10 %	1/10 %						hrs	#	# #
	A_{1UT}	B_{1UT}	ϕ_{1LT}	n_1	A_{1LT}	B_{1LT}	n_2	ϕ_{2LT}	A_{2LT}	B_{2LT}	$\frac{n_3}{n_1}$	$\frac{n_3}{n_1}$	$\frac{n_4}{n_1}$	$\frac{n_5}{n_1}$	$\frac{n_6}{n_1}$	ϕ	θ	P_c h
1	1,960,9	8,864,9	9.43	3,47	02,720,9	02,156	0.5	8.6	.10CR	.54CR	.16	.	.	.	.	1		.7,21,16,6,707
1	44449	31029	606	541	027839	04650	09	11	79	56	18	1			100			721166708
1	51219	39609	624	647	035919	05386	03	58	29CR	5	5							721166709
1	26139	24549	876	344	022799	02580	05	35	16CR	51	16	1			205			721166710
1	25609	22219	846	338	020379	02709	09	90	2	95CR	28	1			2			721166711
1	19119	18419	866	265	017029	02035	07	58	73CR	6	28	1			101			721166712
1	23789	26949	896	359	025219	02561	04	98	21	44CR	14				102			721166801
1	28619	23819	838	372	021759	03021	07	91	4	71CR	19	1	1		1			721166802
1	39529	29239	816	491	026399	04147	08	20	40	76	18	1			1			721166803
1	16599	47529	1045	503	046249	01981	03	114	36	10CR	8	1			2			721166804
1	27849	14639	758	314	012659	02880	04	70	38CR	24CR	15	1	1		3			721166805
1	44059	43819	872	621	040619	04701	05	102	35	47CR	10				2			721166806
1	23819	5159	654	243	003479	02412	09	89	2CR	91CR	37							721166807
1	15309	20259	926	253	019139	01668	12	100	63	108CR	49							721166808
1	26879	40299	948	484	038319	02963	06	66	56CR	19CR	12							721166809
1	10079	25649	1030	275	024879	01184	05	92	6	56CR	20							721166810
1	29879	29399	870	419	027229	03186	03	92	4	56CR	8							721166811
1	18229	26109	940	3,18	024769	02001	0.6	5.7	64CR	8	20							721166812
18,48	8.85	6,9,49	9.71	8,9,1	5.7.54				46,17	3,9,0	05	2.221						
											2							
											4,53CR							
											3,41							

721 [illegible]

[illegible]

[illegible]

[illegible]

KEY TO OUTPUT FORMAT

IDENT. OF LAST INPUT CARD		ϕ_{1UT}	n_{1UT}	ϕ_{1LT}	n_{1LT}	ϕ_{2LT}	n_{2LT}
IDENT.	N	A_{1UT}	B_{1UT}	$\lvert\phi_{1LT}\rvert$	$\sigma\, A_{1UT}$	$\sigma\, B_{1UT}$	$\sigma\, \lvert\phi_{1LT}\rvert$
IDENT.	N	A_{1LT}	B_{1LT}	$\lvert n_1\rvert$	$\sigma\, A_{1LT}$	$\sigma\, B_{1LT}$	$\sigma\, \lvert n_1\rvert$
IDENT.	N	A_{2LT}	B_{2LT}	$\lvert n_2/n_1\rvert$	$\sigma\, A_{2LT}$	$\sigma\, B_{2LT}$	$\sigma\, \lvert n_2/n_1\rvert$

THE LAST 2 DIGITS INDICATE DECIMAL POINT POSITION.
NEGATIVE NUMBERS ARE INDICATED BY N, 9, CR, OR * FOLLOWING THE DIGITS.

approximated by the exponential return to normal that occurs during the several days following an FD would affect[6] the harmonic coefficients by adding a saw-tooth waveform to the DVCR so that the apparent DVCR includes this saw-toothed waveform. For this reason the recovery periods following the selected removed days of FD were separately analyzed, and so were the remaining days in those months. There was no significant difference between their first harmonic coefficients and those obtained for the entire month.

The fact that the DVCR ordinates represent averages over the separate two-hour intervals, rather than instantaneous values, reduces the first harmonic coefficients by[6]

$$\frac{\sin\left(2\frac{\pi}{12}\right)}{2\left(\frac{\pi}{12}\right)} = .954 \qquad (9)$$

so that all CRDV amplitudes n_1 found herein must be multiplied by $(.954)^{-1}$ to obtain the true amplitude. This provides an increase which is very small compared to random errors. It will be accounted for in the end. Similarly, the second harmonic amplitudes are to be multiplied by $(.826)^{-1}$.

III. B. Dependences Found

The CRDV amplitude n_1 and peak time were found to depend on geomagnetic latitude λ, figure 1, and less strongly upon longitude and month. In figures 1 to 5, and 10 the small circles represent vector averages for one station over several months, the large

---

[6]Chapman and Bartels, Geomagnetism, Oxford (1940).

circles represent vector averages over several months for two or more stations, and the crosses represent arithmetic averages over the same groupings. The arithmetic average amplitudes are necessarily larger than or equal to the vector averaged amplitudes. The corresponding circles and crosses plotted closer together indicate smaller spread in the phase angle of the averaged sine functions. This closeness helps indicate that the data grouping is appropriate. The straight envelope lines on the graphs are at one standard deviation σ, equation (8), above and below the arithmetic average. This spread includes not only random errors, but also systematic dependences on month, and for figure 1 on longitude as well. Dark smooth curves show the relationships presented.

The curves become smoother and more clearly exhibit the main features of the relationships when they are plotted against geomagnetic cutoff rigidity P_c. Here P_c is regarded as a parameter indicating effective position in the actual field. P_c increases from the poles to the equator. Figure 2 shows n_1 and ϕ_1 averaged over 0.2 BV/c intervals of P_c as calculated for the eccentric dipole field model.[7] This combines the data for northern and southern hemispheres. The Quenby-Webber rigidities[8] are more representative of the actual field of the earth. Their use shifts the P_c values of many points, and changes somewhat the grouping of the stations (Tab. III) into rigidity intervals, thereby altering the average amplitudes and peak times shown and making smoother curves, as in figures 3 and 8, result, especially when northern and southern hemispheres are treated separately. The P_c and n_1 values at the six relative extremums of n_1 which are found as one proceeds from the Arctic

---

[7] Kodama, M., Wada, M., and Kondo, I., J.Sci.Instr. 51, 138, (1957).
[8] Quenby, J. J., and Webber, W. R., Phil. Mag., 4, 90, 1959.

TABLE III

NEUTRON MONITOR STATIONS
which have been averaged together for plotting at the same Quenby-Webber cutoff rigidity P_c, and those plotted separately

Northern (and Equatorial) Stations (P_c)	Plotted at P_c
Thule (0.00), Resolute Bay (0.00)	0.00 BV/c
Murchison Bay (0.06), Heiss Is. (0.07) Churchill (0.11)	0.1
College	0.48
Deep River (0.87), Sulphur Mt. (0.94), Ottowa (0.96)	0.9
Mt. Washington (1.16), Uppsala (1.17), Yakutsk (1.19)	1.17
Chicago	1.54
Leeds	1.71
Lincoln (1.99), London (2.16)	2.08
Herstmonceux (2.30), Gottingen (2.38)	2.34
Climax	2.77
Weissenau (3.22), Zugspitze (3.33)	3.3
Berkeley	4.01
Pic du Midi	4.30
Rome	5.04
Alma Ata	5.47
Mt. Norikura	9.13
Makapuu Point	11.03
Huancayo	14.18
(Kampala)	14.51
Ahmedabad	14.58
(Lae)	14.89
Kodaikanal	17.56

Southern (and Equatorial) Stations

Mawson	0.57
Mt. Wellington (Hobart)	1.71
Invercargill (Awarua)	1.81
Wellington	3.20
Sydney	4.03
Hermanus	4.94
Ushuaia	5.89
Buenos Aires	10.70
Rio de Janeiro	11.47
Mina Aguilar	12.45
(Kampala)	14.51
Lae	14.89
(Kodaikanal)	17.56

The locations of the above stations can be found in reference (II-3) . All other stations listed there have been plotted on the monthly CRDV contour maps but omitted from the plots against P_c since they have data for very few of the included months.

TABLE IV

PERSISTENT PRINCIPAL VALUES IN THE INTEGRAL SPECTRUM OF CRDV AMPLITUDE n_1 AS A FUNCTION OF CUTOFF RIGIDITY, P_c

P_c Values Used	Months Included	Stations Included	Arctic n_1 %	Small Peak n_1 %	Small Peak P_c BV/c	Rel. Min. n_1 %	Rel. Min. P_c BV/c	Main Peak n_1 %	Main Peak P_c BV/c	Rel. Min. n_1 %	Rel. Min. P_c BV/c	Equatorial n_1 %
Centered dipole	July 1957-June 1958	All	.11	.35	1.1	.23	1.7	.49	4.0	(Fluctuates)		
Eccentric dipole			.11	.35	1.1	.27	2.2	.43	4.0	.2	12.	.3
Quenby-Webber			.12	.35		.25	2.1	.49	4.0	.15	6.0	.3
	July 1957-Dec 1958 (IGY)	All	.13	.33	0.9	.24	1.7	.45	4.3	.22	5.5	.26
	Sept, Oct, Nov 1957&1958& Mar, Apr, May 1958		.12	.31	1.2	.27	2.0	.45	4.3	.20	5.7	.275
		N. Hem	.12	.31	1.2	.26	1.7	.45	4.3	.22	5.5	.275
		N. Hem Alt 750	.12	.295	1.	.26	1.7	.43	4.0	.25	5.0	.26
	Sept, Oct, Nov 1957 and 1958	N. Hem	.17	.37	1.2	.25	2.2	.42	3.3	.22	5.5	.275
		N. Hem Alt 750m	.14	.34	1.2	.30	2.2	.43	3.2	.25	5.0	.28
		All	.17	.37	1.2	.30	2.1	.42	3.3	.19	5.7	.28
		S. Hem All	.18	None shown				.5	3.	.18	6.	.28
	Sept, Oct, Nov 1957&1958 Mar, Apr, May 1958	S. Hem All	.2					.5	3.	.15	5.	.275
	Oct. 57-Feb58	N. Hem	.1	.4	1.7	.2	2.8	.42	4.	.21	5.5	.4

to the equator are shown in Table IV. Also shown are a single maximum and relative minimum in the southern hemisphere, where there are not enough stations to show as much detail as is found in the north. The persistence of these values despite considerable changes in the months which are averaged together, and whatever set of P_c values is used, indicate that the two main peaks and troughs are real. The reality of these features should be questioned because it is possible to take a constant n_1 of 0.3% staying just within the envelope limits of $\pm \sigma$, almost all the way to the Arctic where n_1 definitely falls steeply to 0.1% or less. Many prior investigators of CRDV have used a flat spectrum of this type. The detailed main features are not obvious until after some smoothing of data by taking averages such as have been described. Also, no stations have been eliminated by a severe data rejection scheme, as was done by several prior[9,10,11] investigators. In this study, careful attention is paid to such details as the double peak of amplitude, and much new knowledge of the CRDV is obtained thereby.

The peak time is seen to have a minimum near the equator, and to increase almost monotonically with latitude, or decreasing P_c. Strong dependence of n_1, n_2 and ϕ_{1LT} upon the stations' local position in the actual geomagnetic field as well as its latitude in the main dipole field has already been seen from the smoothness of their relationship to the Quenby-Webber P_c, as compared with their relationship to the eccentric dipole P_c. This local field dependence is better exhibited by isoplot (contour) maps of n_1, n_2 and ϕ_{1LT}, figures 6, 9 and 7, as functions of latitude and

---

[9] Venketesen, D., Rao, U. R., McCracken, K. G., J. Geophys. Res. 67, 3590, (1962).

[10] Katzman, J., Venketesen, D., Can. J. Phys. 38, 1011, (1960).

[11] Duggal, S. P., Nagashima, K., and Pomerantz, M. A., J. Geophys. Res. 66, 1970, (1961).

longitude. These CRDV maps have been made for all individual months, and for averages over several months. They all correspond very closely to isoplot maps of the horizontal or vertical intensity of the geomagnetic field at the earth's surface. On figure 6 the double peak in the northern hemisphere and a simple peak in the southern hemisphere can be traced around the world, as indicated by the heavy black lines. The troughs are similarly traced by the heavy dashed lines. The equatorial flat of n_1 shows a dark equatorial ridge line across India, Africa and South America, but a dashed equatorial trough line across most of the Pacific. The monthly n_1 maps show clearly a northern peak line and sometimes indicate that it is a double peak. They show generally only a single trough near the equator, such as figure 6 shows in the Pacific, but some months show the double trough at India and the Indian Ocean with a small equatorial maximum in between, as shown on figures 5 and 6. Figure 7 and all the other monthly or average maps of ϕ_{1LT} show a minimum near the equator, with no well-defined maxima near the poles. All these ridge and trough lines are due to the main dipole field. Their departures from curves of constant magnetic latitude indicate the effect of non-dipole terms of the geomagnetic field. This is also indicated by ridge and trough lines which run approximately north-south on the CRDV maps, crossing the northern and southern peak zones and sometimes crossing the equator. The geomagnetic dipole equator is shown as a light dashed curve for comparison with the CRDV equators.

The only serious ambiguities in CRDV first harmonic peak time occur in the Arctic where the amplitude is negligibly

small, and for several months at Hermanus, Capetown, South Africa, where a magnetic anomaly is located. Here the peak time, about 03 hours LT, is almost twelve hours away from the peak time of neighboring stations. In drawing contours of peak time this must be shown as very early, or as very late. The choice between very early and very late was made in such a way as to obtain best agreement of the resulting contours with the contours for those months when no ambiguity arose.

Figure 8 shows ridge and valley lines of relative maxima and minima of the Quenby-Webber cutoff rigidities drawn in geographic coordinates. The maxima and minima which are oriented roughly North-South have been obtained at constant geomagnetic (dipole) latitude in the table in Quenby and Webber's paper,[8] and drawn upon the map of the Quenby-Webber rigidity contours taken from the same table. The P_c values would not show any such extremums if the field were a dipole field. These zones are very similar to the ones on the CRDV maps for the months of symmetrical impact and most other months. This indicates that the relative maxima and minima crossing the impact zones from North to South on the CRDV maps are due to and indicative of the non-dipole features of the earth's field.

III. C. Second Harmonic CRDV

The second harmonic CRDV amplitudes n_2 are plotted against Quenby-Webber P_c in figure 10. These values are obtained after correction for atmospheric pressure. Northern and southern data are separated and shown "back to back" so as to display n_2

from the Arctic through the equatorial region to the Antarctic. A north-south anisotropy is thus shown. In general, n_2 in the south is about twice n_2 in the north. The equatorial maximum of .3% in n_2 appears south of what is normally regarded as the equator, that is, either the geographic equator, the centered dipole equator, the geomagnetic dip equator, or the Q-W rigidity equator. Huancayo, on the centered dipole equator, at P_c = 14.15 BV/c and n_2 of only .045%, is definitely north of the equatorial peak of second harmonic CRDV. This is shown by the isoplot map of n_2, figure 9. Comparison with figure 8 shows that a conspicuous saddle point of the n_2 contours coincides the only saddle point of the P_c contours, and that Huancayo is the only equatorial station near that saddle point. It is therefore not surprising that Huancayo's second harmonic is far less than that of the other equatorial stations. Not only does a true second harmonic CRDV exist after pressure correction, but its contours and extremum lines match those of the Quenby-Webber rigidity more precisely than any first harmonic CRDV contours and extremum lines in the equatorial region, especially regarding the equatorial maxima east of Kodaikanal, and the equatorial saddle point east of Huancayo, and the north-south ridge and valley lines, respectively, extending therefrom.

III. D. Annual Variation of CRDV Amplitude and Phase

The mean sidereal day is about four minutes shorter than the mean solar day. Within a day therefore, a harmonic analysis based on either day as period would give about the same amplitude and phase, whether the actual period of the CRDV was one solar day

or one sidereal day, or whether both periodicities were present. If both periodicities are present they could be added vectorially to get the resulting observed CRDV since their periods are almost identical. A variation whose period is one sidereal day has a vector representation which rotates at one revolution per year on a solar time dial. If it is added vectorially to the representation of a variation whose period is one mean solar day the resulting locus is a circle. The radius of the circle is the amplitude of the sidereal diurnal periodicity and its displacement from the origin is the amplitude of the mean solar diurnal periodicity.

In figure 11 the monthly change of amplitude and phase are shown for one year for North America. The polar plot shows an annual circling of the vector over the first 12 months. This is consistent with a constant vector in local time plus a rotating vector which changes its phase, with the correct sense, through 24 hours each year, and is therefore constant in sidereal time. Similar analysis has been carried out for many regions of the earth, Table V. Most regions confirm this apparent cosmic ray stellar diurnal variation. None deny its existence. The data has been smoothed to eliminate some monthly fluctuations for some regions of the world whose data only poorly showed the stellar diurnal variation. The result is that the stellar diurnal variation is shown more clearly in those regions. Fourier analysis in two directions gives the Lissajous figure of best fit as an ellipse, the semi-major and semi-minor axes of which correspond to amplitudes of 0.13% and 0.076%. Thus 0.08% is an estimate of the amplitude of the stellar diurnal variation in cosmic radiation. Superposed on this approximate circling is a monthly fluctuation in amplitude

and in phase due in part to monthly change of the angle between the dipole axis and the incident beam, as indicated on the right side of the figure and in figure 8 in the paper by Kelsall.[12] The fluctuations in total proton flux over the whole earth for a spectrum of E^{-5} closely resemble the observed monthly fluctuations except for small phase shifts which can be caused by the beam not coming directly from the sun, or anti-sun direction, and some irregular fluctuations, which may be statistical but which are due in part to monthly shifting of the impact zones relative to individual stations. There are also superposed random fluctuations in amplitude and phase of the apparent CRDV due to such events as solar flares and Forbush-type decreases in the cosmic radiation.

A similar Lissajous analysis was performed to find a universal time component, which would be caused by oscillation of the impact zones due to diurnal change in the angle between the incident beam and the rotating dipole axis. The effect is masked by a longitude dependence due to the eccentricity of the earth's dipole field, but its .1% amplitude is discussed on page 83.

III. E. Relationship to Other Variables

By plotting n_1 and ϕ_{1LT} against altitude of station within geographic regions of similar position in the geomagnetic field, it was found that the CRDV is independent of station altitude, or depth in the atmosphere.

The diurnal variation (DV) in atmospheric pressure is related to but is not the cause of the observed CRDV. There exists at the top of the atmosphere over several stations an almost purely sinusoidally (first harmonic) CRDV. The not purely sinusoidal DV

---

[12] Kelsall, T., J. Geophys. Res. 66, 4047 (1961).

in pressure, or thickness of absorbing air, masks that CRDV so that it is not observed in the raw data recorded at ground level. For Zugspitze the DV of the nucleon counting rates uncorrected for pressure variation did not resemble a sine curve. Neither did the pressure DV. Yet after the effects of that pressure variation were removed from the data the CRDV emerged as a reasonably smooth sine curve. It follows that while atmospheric pressure variation does not cause the CRDV, it does hide the CRDV, unless it is properly corrected for. Improper pressure correction will cause errors in the reported CRDV.

Since the CRDV as averaged over all stations has its peak time at 1400 hrs LT, it has been suggested by some[13] that the CRDV might be due primarily to the diurnal variation in atmospheric temperature, which peaks at about the same time. This cause is ruled out by the fact that the CRDV at equatorial stations peaks well before noon. Also if the effect were due to meteorological causes, the isoplots of CRDV might be expected to show some relation to weather maps, which they do not.

---

[13]Haymes, R. C., private communication.

Table V

Groups of Neutron Monitor Stations Analyzed to Investigate CRDV in Sidereal Time

Region	No. of Sta.	Stations	Date on which CRDV in ST is in phase with CRDV in LT during July 1957-June 1958
Regions which clearly show a CRDV in ST. throughout IGY			
South America	4	Buenos Aires, Huancayo, Mina Aguilar, Ushuaia	July-Aug
CRDV equator	3	Huancayo, Kodaikanal, Lae	June-Aug June-July
Pacific Ocean	4	Lae, Makapuu Pt., Mt. Norikura, Mt. Wellington	July-Sept June-July
Africa	2	Hermanus, Kampala	Spring
Regions for which a CRDV in S.T. is indicated by the data from 12 or more months of the IGY			
Whole world	25	All that have 18 months of record	June-Oct
North America	9	Berkeley, Climax, Chicago, Churchill, Deep R., Lincoln, Mt. Washington, Ottowa, Sulphur Mt.	Aug. 1
Broad equatorial	6	Ahmedabad, Huancayo, Kampala, Kodaikanal, Lae, Makapuu Pt.	July
Equatorial	4	Ahmedabad, Huancayo, Kodaikanal, Lae	July-Aug
Down Under	2	Invercargill, Mt. Wellington	June-Sept
Asia	2	Alma-Ata, Mt. Norikura	June-Aug
Europe, Smoothed	7	Gottingen, Herstmonceux, Leeds, Rome, Uppsala, Weissenau, Zugspitze	Apr-May
Regions which give only a weak indication of the existence of a CRDV in ST, or which do not deny its existence			
Europe	6	Gottigen, Herstmonceux, Leeds, Uppsala, Weissenau, Zugspitze	
England	2	Herstmonceux, Leeds	
Zugspitze	1	Zugspitze	
India	2	Ahmedabad, Kodaikanal	
Dipole Equator	3	Huancayo, Kampala, Kodaikanal	

IV. Explanation and Analysis

A. General Explanation

The general features of the CRDV dependence on λ or P_c can be explained by the impact zones for a beam of non-interacting particles in excess of the isotropic cosmic radiation at infinity. The assymtotic orbits of such a beam would have to be at nearly 90^o to the earth's rotation axis to produce a CRDV which is nearly symmetrical with respect to the equator. Furthermore there are several reasons to expect that such a beam would be nearly parallel to the ecliptic.[1] The symmetrical impact zones[2] for a beam at $\alpha = 90^o$ therefore are correct for some months and then give the simplest and most illuminating picture of the world-wide λ and time dependence of the CRDV. If the rigidity spectrum of the anisotropy beam falls off steeply from some peak value just above a low rigidity cutoff, as the spectrum for the isotropic cosmic radiation is believed to do,[3] then there will be two CRDV amplitude peak zones as observed in the northern hemisphere and two in the southern, at the rigidity which lies just above the spectral cutoff. Examine for example the impact zones for 5 Bev on Kelsall's figure 6a. These center at about 45^o and 57^o geomagnetic latitude and are at an early and a late impact time, respectively. The impact times of these zones would be 03 and 09 hours LT if the anisotropy came from the sun, which it does not, and if the difference between geomagnetic and geographic longitude is for this purpose ignored. A station, in the course of its daily rotation, will pass through these two zones and thus experience two pulses of cosmic radiation in excess of the usual average counting rates as shown in figure 13. These pulses

---

[1] Dattner, A. and Venketesan, D., Tellus 11, 239, 1959.
[2] Kelsall, T., Jour. Geophys. Res. 66, 4055, 1961.
[3] Quenby, J. J., and Webber, W. R., Phil. Mag. 4, 657, 1959.

will be due to particles from two different rigidity intervals, for example, around 5 BV/c in the early zone at $\lambda = 45^{\circ}$ and around 10 BV/c or more in the late zone at $\lambda = 45^{\circ}$. The observed CRDV does not peak between 03 and 09 hours LT because the beam does not come from the sun. The λ dependence of the observed CRDV peak time is due to the fact that the impact zones are at later times at middle and high latitudes than at low latitudes, and to weighting factors for the early and late zones. These factors, Y_e and Y_L will be derived in the next section. The second harmonic CRDV can be partly explained by the existence of two impact zones, early and late, in each hemisphere. The shape of the pulses experienced as a station passes through the impact zones, together with the fact that the early and late zones are not spaced exactly 12 hours apart, will give rise to higher harmonics. The non-dipole terms in the geomagnetic field account for the local details of the zones of high or low amplitude.

The earth's rotation varies α, thus causing the position of the impact zones to depend on Universal Time (UT). Thus a detector kept at constant LT (by not rotating with the earth) would experience a small CRDV dependent on UT, as impact zones for different rigidities passed over the detector.

IV. B. A Theory for Obtaining the Rigidity Spectrum of the CRDV

The curves of CRDV amplitude versus P_c show the integral spectrum of particle momentum per unit charge responsible for the CRDV. In differentiating these curves to find the differential spectrum, account must be taken of rigidity-dependent neutron monitor counting efficiencies, S(P,X), as is usual for the spectral analysis of the total cosmic radiation, and also of a variable focusing factor f(P), and other factors imposed by the interaction between a collimated beam and the main field of the earth. For purposes of spectral analysis the main field will be taken to be that of a uniformly magnetized spherical earth, a centered-dipole field. However, the most accurate description of the integral rigidity spectra is obtained by using the most accurate available values for P_c at each observing station. For this purpose the Quenby-Webber P_c will be used. Where it is necessary to compare with the P dependence of impact zones in a centered dipole field, comparison will be made at corresponding cutoff rigidities. If the anisotropy were perfectly collimated, an unlikely situation, then the observed CRDV at individual stations would have a double-pulse form. The almost perfect sine form of the CRDV at several stations, notably Zugspitze, indicates that the anisotropy is not well collimated. An anisotropy which at remote distances from the earth varies sinusoidally with direction in momentum space[4] can be written

$$\left(J(P) + j_o(P) \cos \theta'\right) d\Omega \, dP \qquad \text{(IV-1)}$$

giving the flux of particles per unit time per unit area within the rigidity interval dP around P, coming from within the solid angle

---

[4]Nagashima, K., V. R. Potnis, and Pomerantz, M., Nuovo Cim. 19, 292-330, 1961.

$d\Omega$ around the direction θ' measured from the axis of anisotropy, as shown in figure 14. $J(P)$ is the differential spectrum for the isotropic cosmic radiation (usually regarded as the total cosmic radiation), and $j_o(P)$ is the differential spectrum responsible for the CRDV. This distribution will now be normalized to agree with the flux $j(P)$ in an equivalent collimated beam.

$$\left(J(P)+j_o(P)\cos\theta'\right)d\Omega dP\,\widehat{\theta'\phi'}\cdot d\vec{A}=\left(J(P)\cos\theta'+j_o(P)\cos^2\theta'\right)d\Omega\,dP dA$$

is the number of particles per unit time within the rigidity interval dP passing through an area $d\vec{A}$ oriented along the axis of anisotropy. The total flux per unit rigidity interval, from all directions is therefore

$$j(P)=\int_0^{2\pi}d\phi'\int_0^{\pi}\left(J(P)\cos\theta+j_o(P)\cos^2\theta'\right)\sin\theta'\,d\theta'$$

$$j(P)=\frac{4\pi}{3}\;j_o(P) \qquad (2)$$

After traversing the dipole field this anisotropic flux will arrive at the top of the atmosphere in two impact zones in the northern and two in the southern hemisphere. The DVCR flux within these zones will be

$$\eta\, f\left(P,\theta,\alpha(t)\right)\; j(P)dP$$

where η is a unit step function which indicates where and when a station is within an impact zone. This gives a DVCR in excess of the average counting rate of

$$y(\theta,t,x)=\sum_z \int_0^{2\pi}\int_0^{\frac{\pi}{2}}\int_{P_c(\theta,\zeta,\mu)}^{\infty} \rho(\zeta,\mu,P,\theta)\eta\left(P,\theta,t,\alpha(t)\right)f\left(P,t,\alpha(t)\right)\cdot S_z\left(P,\frac{x}{\cos\zeta}\right)j_z(P)\,dP\sin\zeta\,d\zeta\,d\mu \tag{3}$$

at depth x in the atmosphere. Here ρ is an appropriate function showing the distribution of particles over direction of incidence at the location θ. All interactions with atmospheric particles, and the relationship between the fluxes j_z of cosmic ray particles of various atomic numbers z at the top of the atmosphere and the response of the detector at the earth's surface, are specified by[3] the factors $S_z\left(P,\frac{x}{\cos\zeta}\right)$. The local time t is regarded as a difference of either geographic or geomagnetic longitude since these differences are nearly the same. Contributions from particles reaching the atmosphere not directly over the station are included by the integration over the hemisphere above the horizon. This integral is analogous to the usual[5,6] form for the total omnidirection cosmic radiation counting rate

$$I(\theta,x)=\sum_z \int_0^{2\pi}\int_0^{\frac{\pi}{2}}\int_{P_c(\theta,\zeta,\mu)}^{\infty} S_z\left(P,\frac{x}{\cos\zeta}\right)J_z(P)\,dP\,\sin\zeta\,d\zeta\,d\mu \tag{4}$$

Rather than integrate the above it is customary[6,7] to approximately relate the vertical flux per unit solid angle

$$I_v(\theta,x)=\sum_z \int_{P_c(\theta,\zeta=0)=P_c(\theta)}^{\infty} S_z(P,x)J_z(P)\,dP \tag{5}$$

---

[5]Simpson, J. A., Fonger, W. and Trieman, S.B., Phys. Rev. 90, 934, (1954).
[6]Arthur, W., Doctoral Thesis, New York University, 1962.
[7]Brown, R. R., Nuovo Cim. 16, 956, (1957).

to the omnidirectional counting rate by the Gross transformation[5]

$$I = 2\pi I_v \left(\frac{L}{L+x} \right) \tag{6}$$

where L is the mean free path of the cosmic ray particles in the atmosphere. The vertical flux can be written[3]

$$I_v(\theta,x) = \int_{P_c(\theta)}^{\infty} S(P,x)\ J(P)dP \tag{7}$$

where S(P,x) is a gross specific yield function relating the proton part J(P) of the total cosmic ray flux to the counting rate of the detector.[3] It is this S(P,x)J(P) which is tabulated and graphed in the paper by Quenby and Webber.[3] If $P_c(\theta,\zeta,\mu)$ were independent of ζ, μ and S were independent of x, ζ the Gross transformation would be simply

$$I = \int_{\Omega} d\Omega\ I_v = 2\pi I_v \quad .$$

the term L/(L+x) is a reduction by atmospheric absorption and does not include the allowed cone[8] effects of P_c variation. In similar fashion, the difficulties of integrating over the unspecified distribution ρ will here be avoided by making a Gross transformation to get

$$y(\theta,t,x) = \frac{L}{x+L} \sum_z \int_{P_c(\theta)=P_c(\theta,\zeta=0)}^{\infty} \eta\left(P,\theta,t,\alpha(t)\right) f\left(P,\alpha(t)\right) S_z(P,x)\, j_z(P)dP \tag{8}$$

---

8 Lemaitre, G. ., and Vallarta, M. S., Phys. Rev. 50, 49, (1936)

The double-pulsed form of the DVCR is expressed by the explicit dependence of η upon t. Within the early impact zone $\eta = 1$ when

$$P_o(\theta,\alpha(t)) < P < P_1(\theta),\ t_o(\theta,\alpha(t)) < t < t_1(\theta,\alpha(t)).$$

Within the late impact zone $\eta = 1$ when

$$P_2(\theta,\alpha(t)) < P < P_3(\theta,\alpha(t)),\ P > P_4(\theta,\alpha(t)),\ t_2(\theta) < t < t_3(\theta).$$

Otherwise, $\eta = 0$. These P limits for $\alpha = 90^\circ$ are shown in figure 12 as taken from table 6 in Kelsall's paper[2] for $\zeta \leq 45^\circ$. Comparison of this figure with a similar graph (not shown) for $\alpha = 100^\circ$ reveals that P_1 does not change much as α changes from 77.5° to 102.5° during one rotation of the earth, nor does P_o, except for an oscillation at the equator that is second harmonic in t, but P_2, P_3, and P_4 make a large oscillation. Examination of Kelsall's impact zone maps reveals that the limits t_o and t_1 make a large oscillation but t_2 and t_3 do not change much as α varies during a day. In the early zone, $t_o < t < t_1$

$$y_e(\theta,t,x) = \frac{L}{x+L} \sum_z \int_{P_{oc}(\theta)}^{P_1(\theta)} f_e(P,\alpha(t)) S_z(P,x) \cdot j_z(P)dP \quad . \tag{9}$$

In the late zone, $t_2 < t < t_3$

$$y_L(\theta,t,x) = \frac{L}{x+L} \sum_z \left(\int_{P_2(\theta,\alpha(t))}^{P_3(\theta,\alpha(t))} f_L(P,\alpha(t)) S_z(P,x) j_z(P)dP + \int_{P_4(\theta)}^{\infty} f_L(P,\alpha(t)) S_z(P,x) j_z(P)dP \right) . \tag{10}$$

At all other times $DVCR(\theta,t,x)=y(\theta,t,x)=0$.

$P_{oc} = P_o$ or P_c, whichever is greater. Both y_e and y_L vary only slightly with t during their time interval where it is brief, since α then does not change much. The pulses can therefore be approximated as rectangular by dropping the α dependence. This approximation will be close except for the late zone at low latitudes where the pulse duration $\tau_L = t_3 - t_2$ is large. However, since the integrand for the late zone is less than the integrand for the early zone at most P values within their range, the error is small. The limits t_o and t_1 also change during the time interval between them. The early pulse begins at local time $t_o = t_o(\theta,\alpha(t'_o))$ where t'_o is the corresponding UT, and similarly ends at $t_1 = t_1(\theta,\alpha(t'_1))$. The effect is that the pulse duration $\tau_e = t_1 - t_o$ should not be obtained from a single impact zone map for a single value of α, but t_1 and t_o should be separately obtained. Since τ_e is only approximately known anyhow this small change will be ignored and both τ_e and τ_L will be obtained from Kelsall's tables[2] for $\alpha = 90^o$. An approximate $y(\theta,t,x)$ consisting of two brief rectangular pulses of height y_e and y_L, duration τ_e and τ_L and center to center time separation $\Delta\psi$ is Fourier analyzed to obtain first harmonic coefficients

$$a_1 = \frac{1}{\pi}\int_{-\tau_e/2}^{\tau_e/2} y_e \sin t\, dt + \frac{1}{\pi}\int_{\Delta\psi-\tau_L/2}^{\Delta\psi+\tau_L/2} y_L \sin t\, dt$$

$$= -Y_L \sin \Delta\psi \qquad (11)$$

$$b_1 = \frac{1}{\pi}\int_{-\tau_e/2}^{\tau_e/2} y_e \cos t\, dt + \frac{1}{\pi}\int_{\Delta\psi-\tau_L/2}^{\Delta\psi+\tau_L/2} y_L \cos t\, dt$$

$$= Y_e + Y_L \cos \Delta\psi \tag{12}$$

where $Y_{e,L} = \frac{2y_{e,L}}{\pi} \sin \frac{1}{2}\tau_{e,L}(\theta)$ (13)

and t, τ, and ψ are in hours or in degrees, where 1 hour = 15°. The first harmonic amplitude of the CRDV is given by

$$c_1^2 = a_1^2 + b_1^2$$

$$c_1 = \sqrt{Y_e^2 + 2Y_eY_L \cos \Delta\psi + Y_L^2} \quad . \tag{14}$$

It will now be shown that an uncollimated anisotropy of the same total flux gives a sine form CRDV of essentially the same amplitude as c_1 just calculated for the double-pulse form CRDV. Eq(1), the anisotropy $j_o(P) \cos \theta'$ previously normalized, will be written

$$j_o(P) \sin \theta \cos \phi = j(P,\theta,\phi) \tag{15}$$

in transformed coordinates in rigidity (momentum) space such that the polar axis is parallel to the earth's dipole axis. The angles θ and ϕ are then the geomagnetic assymptotic colatitude and longitude of the particle orbit. A simpler anisotropy

$$j(P,\phi) = j_E(P) \cos \phi \tag{16}$$

with equatorial assymptotic latitude will be treated. It ignores some spread in the latitude of the predicted CRDV amplitude peak zones. To normalize this to agree with j(P), the total flux per unit rigidity interval through an area $\vec{dA}$ oriented along the axis x of anisotropy is obtained as

$$j_x(P)dA = \int_0^{2\pi} \vec{j}(P,\phi)\cdot\vec{dA}\, d\phi$$

$$j(P)dA = \int_0^{2\pi} j_E(P)\cos^2\phi d\phi\, dA$$

or

$$j(P) = \pi j_E(P) \tag{17}$$

Using $j(P) = \frac{4\pi}{3} j_o(P)$, (Eq. 2) this becomes

$$j_E(P) = \frac{4}{3} j_o(P) \tag{18}$$

so that the flux at large distance from the earth is

$$j(P,\phi)dPd\phi = \frac{4}{3} j_o(P)\cos\phi\, dP\, d\phi \tag{19}$$

within the increment $d\phi$ in direction angle. From a broad beam at each assymptotic direction ϕ a portion is selected by the geomagnetic field and focussed to a pair of impact zones in each hemisphere for each P of (pulse) width τ_e and τ_L after deflections ψ_e and ψ_L. At any local time t in geomagnetic coordinates a station will be within the late impact zones for assymptotic directions $\left(\phi_1 - \frac{1}{2}\tau_L\right) < \phi < \left(\phi_1 + \frac{1}{2}\tau_L\right)$ and simultaneously within the early impact zones for $\left(\phi_2 - \frac{1}{2}\tau_e\right) < \phi < \left(\phi_2 + \frac{1}{2}\tau_e\right)$ and will receive

at the top of the atmosphere a contribution

$$f(P)\frac{4}{3}j_{oz}(P)\cos\phi\, d\phi\, dP \quad . \tag{20}$$

From the early zones over the station at t the total contribution to the DVCR detected at the surface is

$$\frac{L}{x+L}\sum_z \int_{P_c(\theta)}^{P_1(\theta)} \int_{\phi_2(\theta)-\frac{1}{2}\tau_e(\theta,P)}^{\phi_2(\theta)+\frac{1}{2}\tau_e(\theta,P)} \frac{4}{3} f_e(P)S_z(P,x)j_{oz}(P)\cos\phi\, d\phi\, dP \tag{21}$$

which is

$$\left(\cos\phi_2\right)\frac{L}{x+L}\sum_z \int_{P_{oc}(\theta)}^{P_1(\theta)} \frac{8}{3} f_e(P)S_z(P,x)j_{oz}(P)\sin\frac{1}{2}\tau_e(P,\theta)dP \; . \tag{22}$$

From the late zones over the station at t the total contribution is

$$\frac{L}{x+L}\sum_z \left\{ \int_{P_2(\theta)}^{P_3(\theta)} \int_{\phi_1(\theta)-\frac{1}{2}\tau_L(P,\theta)}^{\phi_1(\theta)+\frac{1}{2}\tau_L(P,\theta)} \frac{4}{3} f_L(P)S_z(P,x)j_{oz}(P)\cos\phi\, d\phi\, dP + \int_{P_4(\theta)}^{\infty} \int_{\phi_1(\theta)-\frac{1}{2}\tau_L(P,\theta)}^{\phi(\theta)+\frac{1}{2}\tau_L(P,\theta)} \frac{4}{3} f_L(P)S_z(P,x)j_{oz}(P)\cos\phi\, d\phi\, dP \right\} \tag{23}$$

which is

$$\left(\cos \phi_1\right) \frac{L}{x+L} \sum_z \left\{ \int_{P_2(\theta)}^{P_3(\theta)} \frac{8}{3} f_L(P) S_z(P,x) j_{oz}(P) \sin \tfrac{1}{2} \tau_L(\theta,P) dP + \int_{P_4(\theta)}^{\infty} \frac{8}{3} f_L(P) S_z(P,x) j_{oz}(P) \sin \tfrac{1}{2} \tau_L(\theta,P) dP \right\} \tag{24}$$

The total DVCR (θ,t,x) is the sum of these two contributions. The CRDV differential spectrum $j_{oz}(P)$ for each particle type z will be written as a fraction $k_z(P)$ of the differential spectrum $J_z(P)$ for the total isotropic cosmic radiation,

$$j_{oz}(P) = k_z(P) J_z(P) \quad . \tag{25}$$

Since $$\phi_2 - \phi_1 = \Delta\psi = \psi_e - \psi_L \tag{26}$$

it is possible to introduce

$$\phi_1 = t' \quad , \quad \phi_2 = t' + \Delta\psi \tag{27}$$

where $$t' = t + \text{constant} \ . \tag{28}$$

Letting $$F_{e,L} \equiv \frac{8}{3} \sin \tfrac{1}{2} \tau_{e,L}(P,\theta) f_{e,L}(P,\theta) \sum_z S_z(P,X) k_z(P) J_z(P) \tag{29}$$

The sum of the contributions to the CRDV counting rate becomes

$$\mathrm{DVCR}(\theta,t,x) = \frac{L}{x+L} \left\{ \int_{P_{oc}(\theta)}^{P_1(\theta)} F_e dP \cos(t' + \Delta\psi) + \left[\int_{P_2(\theta)}^{P_3(\theta)} F_L dP + \int_{P_4(\theta)}^{\infty} F_L dP \right] \cos t' \right\} \tag{30}$$

with the Σ now under the integral sign. These two components have different amplitudes and phases but the same period (1 day) and can be added vectorially to obtain the resultant amplitude c_1. As in Quenby and Webber[3] a set of coefficients K_z is introduced such that

$$J_z(P) = K_z J_1(P) \ , \ J(P) \equiv J_1(P) \ . \tag{31}$$

It is now assumed that the CRDV differential spectrum $j_{oz}(P)$ is the same fraction $K(P)$ of the omnidirectional cosmic ray differential spectrum $J_z(P)$ for all atomic numbers z, that is $k_z(P) = k(P)$. Then

$$k_z(P)J_z(P) = k(P)K_z(P)J(P) \tag{32}$$

and

$$\sum_z S_z(P,x)k_z(P)J_z(P) = \sum_z K_z S_z(P,x)k(P)J(P)$$

$$= S(P,x)k(P)J(P) \tag{33}$$

where

$$S(P,x) = \sum_z K_z \ S_z(P,x) \tag{34}$$

is the gross S defined by Quenby and Webber[3] to relate the proton part $J(P)$ of the primary cosmic ray flux to the total counting rate of the detector. Then

$$F_{e,L} = \frac{8}{3} \sin \frac{1}{2} \mathcal{T}_{e,L}(P,\theta) f_{e,L}(P) S(P,x) J(P) k(P). \tag{35}$$

The $\sum_z$ has not been omitted, it has been formally performed. Now let

$$Y_e \equiv \frac{L}{L+x} \int_{P_{oc}(\theta)}^{P_1(\theta)} F_e \, dP \ , \tag{36}$$

$$Y_L = \frac{L}{L+x}\left\{ \int_{P_2(\theta)}^{P_3(\theta)} F_L dP + \int_{P_4(\theta)}^{\infty} F_L dP \right\} . \tag{37}$$

These integrals can be written more compactly by noting that outside of the above integrated ranges of P,θ, the factor $\sin \frac{1}{2}\tau_{e,L}(P,\theta)$ in the integrand is zero. With this understanding

$$Y_e = \frac{L}{x+L} \int_{P_c(\theta)}^{\infty} F_e dP \tag{38}$$

$$Y_L = \frac{L}{x+L} \int_{P_c(\theta)}^{\infty} F_L dP \; . \tag{39}$$

The law of cosines gives

$$c_1^2 = Y_e^2 + Y_L^2 - 2Y_eY_L \cos(\pi - \Delta\psi)$$

or

$$c_1 = \sqrt{Y_e^2 + 2Y_eY_L \cos\Delta\psi + Y_L^2} \tag{14}$$

and from the law of sines

$$\sin\epsilon = \frac{Y_L \sin\Delta\psi}{\sqrt{Y_e^2+2Y_eY_L\cos\Delta\psi+Y_L^2}} \tag{40}$$

which gives the time lapse ϵ from the center of the early zone to the peak time.

This is identical to the result for the collimated beam, except that here the 2 sin $\frac{\tau}{2}$ in Y is under the integral sign where it properly belongs.

Observed CRDV amplitudes n are given in this paper as fractions of the total omnidirectional cosmic ray counting rate I:

$$n_1(\theta) = \frac{c_1(\theta)}{I(\theta)} \quad . \tag{41}$$

The factors which depend on colatitude θ in this analysis based on a dipole field model, depend also on longitude in the actual field of the earth.

$P_c(\theta)$ is a monotonic function so that

$$n_1(\theta) = n_1\left(P_c(\theta)\right) \tag{42}$$

is single-valued. Then

$$\frac{dn_1(\theta)}{dP_c(\theta)} \frac{dP_c}{d\theta} = \frac{dn_1}{d\theta} \tag{43}$$

and

$$n_1\left(P_c(\theta)\right) I\left(P_c(\theta)\right) = \frac{L}{x+L} \left\{ \left[\int_{P_c}^{\infty} F_e \, dP \right]^2 + 2\cos\Delta\psi \int_{P_c}^{\infty} F_e \, dP \int_{P_c}^{\infty} F_L \, dP + \left[\int_{P_c}^{\infty} F_L \, dP \right]^2 \right\}^{\frac{1}{2}} . \tag{44}$$

By use of the Gross transformation, eq. 6,

$$2\pi I_v \left(\frac{L}{x+L} \right) = I$$

this can be written

$$2\pi I_v\left(P_c(\theta)\right)n_1\left(P_c(\theta)\right)=\left\{\left[\int_{P_c}^{\infty}F_e\,dP\right]^2+2\cos\Delta\psi\int_{P_c}^{\infty}F_e\,dP\int_{P_c}^{\infty}F_L\,dP+\left[\int_{P_c}^{\infty}F_L\,dP\right]^2\right\}^{\frac{1}{2}}. \quad (45)$$

Differentiating this gives an integral equation

$$(2\pi I_v)^2 n_1\frac{dn_1}{dP_c}\frac{dP_c}{d\theta}+(2\pi n_1)^2 I_v\frac{dI_v}{dP_c}\frac{dP_c}{d\theta}=\left(\int_{P_c}^{\infty}F_e\,dP+\cos\Delta\psi\int_{P_c}^{\infty}F_L\,dP\right)\frac{d}{d\theta}\int_{P_c}^{\infty}F_e\,dP$$

$$+\left(\cos\Delta\psi\int_{P_c}^{\infty}F_e\,dP+\int_{P_c}^{\infty}F_L\,dP\right)\frac{d}{d\theta}\int_{P_c}^{\infty}F_L\,dP+\int_{P_c}^{\infty}F_e\,dP\int_{P_c}^{\infty}F_L\,dP\;\frac{d}{d\theta}\cos\Delta\psi\,. \quad (46)$$

This form is a bit more complicated than the usual technique[3] in which the derivative with respect to P_c of the known total (integral) cosmic ray spectrum is set equal to the differential proton spectrum multiplied by the specific counting efficiency $S(P_c,x)$. If the $\sin\frac{1}{2}\tau$ factor in F is regarded as dependent on θ then

$$\frac{d}{d\theta}\int_{P_c(\theta)}^{\infty}F_{e,L}\,dP=-\frac{8}{3}\sin\tfrac{1}{2}\tau_{e,L}(P_c,\theta)f_{e,L}(P_c)S(P_c,x)J(P_c)k(P_c)\frac{dP_c}{d\theta}$$

$$+\frac{8}{3}\int_{P_c(\theta)}^{\infty}\frac{\partial}{\partial\theta}\sin\tfrac{1}{2}\tau_{e,L}(P,\theta)f_{e,L}(P)S(P,x)J(P)k(P)\,dP\,, \quad (47)$$

where the first term is zero for the late zone integral since $\sin\frac{1}{2}\tau_L(P_c,\theta)=0$ for all θ. The θ dependence of $\sin\frac{1}{2}\tau$ is only very approximately known over much of the range of the variables. Regarding $\sin\frac{1}{2}\tau(P)$ as independent of θ amounts to squaring up the impact zones for each energy into rectangular blocks in latitude and longitude or local time extent. A similar squaring up in

local time and pulse height has already been performed in order to yield the expression for the CRDV amplitude, and hence a concomitant complete squaring off of the impact zones is reasonable for calculation purposes. With that approximation

$$\frac{d}{d\theta}\int_{P_{oc}}^{\infty} F_e\,dP = \frac{d}{d\theta}\int_{P_{oc}(\theta)}^{P_1(\theta)} \frac{8}{3}\sin\tfrac{1}{2}\tau_e(P) f_e(P) S(P,x) J(P) k(P)\,dP$$

$$= \frac{8}{3}\sin\tfrac{1}{2}\tau_e(P_1) f_e(P_1) S(P_1,x) J(P_1)\frac{dP_1}{d\theta}\, k(P_1)$$

$$-\frac{8}{3}\sin\tfrac{1}{2}\tau_e(P_{oc}) f_e(P_{oc}) S(P_{oc},x) J(P_{oc})\frac{dP_{oc}}{d\theta}\, k(P_{oc}) \qquad (48)$$

where $P_{oc} = P_o$ or P_c, whichever is greater and

$$\frac{d}{d\theta}\int_{P_c}^{\infty} F_L\,dP = \frac{d}{d\theta}\int_{P_2(\theta)}^{P_3(\theta)} \frac{8}{3}\sin\tfrac{1}{2}\tau_L(P) f_L(P) S(P,x) J_o(P)\,dP + \frac{d}{d\theta}\int_{P_4(\theta)}^{\infty} \frac{8}{3}\sin\tfrac{1}{2}\tau_L(P) f_L(P) S(P,x) j_o(P)\,dP$$

$$= -\frac{8}{3}\sin\tfrac{1}{2}\tau_L(P_2) f_L(P_2) S(P_2,x) J(P_2)\frac{dP_2}{d\theta}\, k(P_2)$$

$$+\frac{8}{3}\sin\tfrac{1}{2}\tau_L(P_3) f_L(P_3) S(P_3,x) J(P_3)\frac{dP_3}{d\theta}\, k(P_3)$$

$$-\frac{8}{3}\sin\tfrac{1}{2}\tau_L(P_4) f_L(P_4,x) J(P_4)\frac{dP_4}{d\theta}\, k(P_4)\, S(P_4,x)\,. \qquad (49)$$

If, over a particular range of θ, as for $\lambda < 56^\circ$, some of the limits P_3, P_4 do not exist, then for example, $P_3 = \infty$ and $dP_3/d\theta = 0$ so its term drops out. Substitution of either of these forms for

the θ derivative of the integral can lead to an iteration scheme for solving for $k(P)$ where $P_c > P_o$, but taking τ independent of θ is preferable where $P_c < P_o$.

At $\lambda > 53^o$ the atmospheric cutoff rigidity[9] of 3 BV/c equals $P_1(\theta)$ so that $Y_e = 0$ and the integral for c_1 becomes

$$2\pi I_v(\theta) n_1(\theta) = \int_{P_2(\theta)}^{P_3(\theta)} F_L dP + \int_{P_4(\theta)}^{\infty} F_L dP \qquad (50)$$

and $\epsilon = \Delta\psi$, which are exact relationships.
Then, taking τ_L as independent of θ

$$2\pi I_v \frac{dn_1}{dP_c}\frac{dP_c}{d\theta} + 2\pi n_1 \frac{dI_v}{dP_c}\frac{dP_c}{d\theta} = -\frac{8}{3}\sin\tfrac{1}{2}\tau_L(P_2)f_L(P_2)S(P_2,x)J(P_2)\frac{dP_2}{d\theta}k(P_2)$$

$$+\frac{8}{3}\sin\tfrac{1}{2}\tau_L(P_3)f_L(P_3)S(P_3,x)J(P_3)\frac{dP_3}{d\theta}k(P_3)$$

$$-\frac{8}{3}\sin\tfrac{1}{2}\tau_L(P_4)f_L(P_4)S(P_4,x)J(P_4)\frac{dP_4}{d\theta}k(P_4) \qquad (51)$$

The variables $I_v(P_c)$, $S(P,x)$, $J(P)$, and P_c at the locations of the stations are available from the papers of Quenby and Webber.[3,10] The variables $\tau(P)$, $\Delta\psi(\theta)$, $P_o(\theta)$, $P_1(\theta)$, $P_2(\theta)$, $P_3(\theta)$, $P_4(\theta)$ and $f(P)$ are taken from Kelsall's[2] tables 5 and 6.

---

[9] Montgomery, D.J.X., Cosmic Ray Physics, Princeton, 1949, p. 351.
[10] Quenby, J. J., and Webber, W. R., Phil, Mag. 4, 90, (1959).

$$f(P) = \frac{1}{2} f_{\alpha=90^o} + \frac{1}{2} f_{\alpha=100^o} \qquad (52)$$

is used as representing the average value of f on a day when the impact zones are most nearly symmetrical ($\alpha \approx 90^o$). $dP/d\theta = -dP/d\lambda$ is obtained from the Störmer expression (eq. I-2) for $P_c(\lambda)$ as

$$\frac{dP_c}{d\theta} = \frac{377}{360} \sin\lambda \cos^3\lambda \quad \frac{BV/c}{\text{degree}} . \qquad (53)$$

Approximate values are available for every variable except the distribution function k(P), which is sought.

Since the known terms in this integral equation are approximate, an approximate equation will suffice at least for the zeroth and first approximation solutions at $\lambda < 53^o$. This is obtained by assuming in the expression for n_1 that $Y_e = Y_L$. This is reasonable over the range $0^o < \lambda < 50^o$, and is satisfied exactly at $\lambda = 41^o$. Then

$$c_1 = \sqrt{2}\, Y \sqrt{1 + \cos\Delta\psi} \quad . \qquad (54)$$

Now replace $2Y \approx Y_e + Y_L$

and

$$c_1 = (Y_e + Y_L) \cos\tfrac{1}{2}\Delta\psi \qquad (55)$$

$$c_1(\theta) \approx \frac{L}{x+L} \cos\tfrac{1}{2}\Delta\psi(\theta) \left\{ \int_{P_c(\theta)}^{P_1(\theta)} F_e\, dP + \int_{P_2(\theta)}^{\infty} F_L\, dP \right\} . \qquad (56)$$

Even if the above equality of early and late pulses is not approximately met, the error in n_1 incurred by using this formula is less than 10% if $Y_L/Y_e = 2$ or $\frac{1}{2}$ and less than 30% if $Y_L/Y_e = 100$ or 1/100. This approximation leads also to the simplification

$$\sin\epsilon \approx \frac{2Y_L \sin\frac{1}{2}\Delta\psi}{Y_e + Y_L}$$

or very roughly

$$\epsilon \approx \frac{Y_L}{Y_e+Y_L}\Delta\psi$$

for ϵ near to $\frac{1}{2}\Delta\psi$, but these are not used for calculation. The amplitude relation becomes approximately

$$2\pi I_v(P_c(\theta))n_1(P_c(\theta)) = \cos\tfrac{1}{2}\Delta\psi(\theta)\left\{\int_{P_c(\theta)}^{\infty} F_e dP + \int_{P_2(\theta)}^{\infty} F_L dP\right\} \tag{57}$$

and differentiating gives

$$\frac{2\pi I_v}{\cos\frac{1}{2}\Delta\psi}\frac{d\eta_1}{dP_c}\frac{dP_c}{d\theta} + \frac{2\pi n_1}{\cos\frac{1}{2}\Delta\psi}\frac{dI_v}{dP_c}\frac{dP_c}{d\theta} - \frac{2\pi I_v n_1 \frac{d}{d\theta}\cos\frac{1}{2}\Delta\psi}{(\cos\frac{1}{2}\Delta\psi)^2} = \frac{d}{d\theta}\int_{P_c(\theta)}^{\infty} F_e dP + \frac{d}{d\theta}\int_{P_2(\theta)}^{\infty} F_L dP, \tag{58}$$

which can be solved for the unknown function k(P) contained in F by a straightforward iteration process. For this purpose a zeroth approximation to k(P) is needed at $P \gtrsim 6$ BV/c and is chosen so as to satisfy a further simplified form of this equation which is approximately valid at low geomagnetic latitude.

Over the region $10 < P_c < 18$ BV/c, n_1 is found to be nearly constant so the dn_1/dP term is zero. For $P_c < 12$ BV/c, $\Delta\psi$ is nearly constant, so the $d \cos \frac{1}{2}\Delta\psi/d\theta$ term is zero also. Thus the two terms

$$\frac{2\pi I_v(\theta)}{\cos \frac{1}{2}\Delta\psi(\theta)} \left(\frac{dn_1}{d\theta} - \frac{n_1(\theta)}{\cos \frac{1}{2}\Delta\psi(\theta)} \frac{d}{d\theta} \cos \frac{1}{2}\Delta\psi \right) \approx 0 \tag{59}$$

for $10 < P_c(\theta) < 12$ BV/c. This subsidiary equation has the solution $n_1(\theta)/\cos \frac{1}{2}\Delta\psi(\theta) =$ constant so that it is not necessary to separately assume n_1 and $\Delta\psi$ are constant in order to assert that

$$\frac{2\pi n_1(\theta)}{\cos \frac{1}{2}\Delta\psi(\theta)} \frac{dI_v}{dP_c} \frac{dP_c}{d\theta} \approx \frac{d}{d\theta} \left\{ \int_{P_c(\theta)}^{\infty} F_e dP + \int_{P_2(\theta)}^{\infty} F_L dP \right\}, \quad 10 < P < 12 \frac{BV}{c} . \tag{60}$$

At these low latitudes $P_3 = P_4$ and it will be assumed for the zeroth approximation solution $k_o(P)$ that $P_c = P_o$ and $P_1 = P_2$.

F_e and F_L can then be written as $F(P)$ since the early and late zones don't have overlapping ranges of P. Then using eqs. 57,38,39 as

$$n_1 = \frac{\cos \frac{1}{2}\Delta\psi}{2\pi I_v} \int_{P_c}^{\infty} F dP$$

equation 60 becomes

$$\frac{\frac{d}{d\theta}\int_{P_c(\theta)}^{\infty} FdP}{\int_{P_c(\theta)}^{\infty} FdP} \approx \frac{1}{I_v(\theta)} \frac{dI_v}{d\theta}$$

or, substituting equations 35 and 7

$$\frac{\frac{d}{d\theta}\int_{P_c(\theta)}^{\infty} 2 \sin \tfrac{1}{2}\tau(P)f(P)S(P,x)J(P)k_o(P)dP}{\frac{d}{d\theta}\int_{P_c(\theta)}^{\infty} S(P,x)J(P)dP} = \frac{\int_{P_c(\theta)}^{\infty} 2\sin\frac{\tau}{2} fSJk_o dP}{\int_{P_c(\theta)}^{\infty} SJdP} \qquad (61)$$

which gives

$$\sin \tfrac{1}{2}\tau(P_c)f(P_c)k_o(P_c) = \frac{3n_1}{8 \cos \frac{1}{2}\Delta\psi}$$

which is constant for all $10 < P_c < 12$ BV/c, so that there

$$k_o(P) = \frac{3n_1}{8 \cos \frac{1}{2}\Delta\psi f(P) \sin \frac{1}{2}\tau(P)} \qquad (62)$$

$$k_o(P) \approx 0.004 \qquad (63)$$

Four forms divisible into two major classes are used to obtain $k_{i+1}(P)$ from $k_i(P)$ as solutions of the simplified equations 51&66, each valid over a separate interval of P_c. The first class applies where $Y_e = 0$. It assumes τ is independent of θ or λ.

At $\lambda > 56^\circ$, $P_c < 1.4$ BV/c, $3 < P_2 < 4.6$ BV/c

$$k_{i+1}(P_2) = \frac{\left\{ \begin{array}{l} -\frac{3\pi}{4} I_v \frac{dP_c}{d\theta} \frac{dn_1}{dP_c} + \frac{3\pi}{4} n_1 SJ(P_c, x_o) \frac{dP_c}{d\theta} \\ \\ + \sin \frac{1}{2} \tau_L(P_3) f_L(P_3) SJ(P_3, x_o) \frac{dP_3}{d\theta} k_i(P_3) \\ \\ - \sin \frac{1}{2} \tau_L(P_4) f_L(P_4) SJ(P_4, x_o) \frac{dP_4}{d\theta} k_i(P_4) \end{array} \right\}}{\sin \frac{1}{2} \tau_L(P_2) f_L(P_2) SJ(P_2, x_o) \frac{dP_2}{d\theta}} \qquad (64)$$

is a solution to the exact equation, 51.

For $56^\circ > \lambda$ and $P_1(\theta) < 3$ BV/c or $k_1(P) = 0$ for $P \leq P_1(\theta)$,

$P_c \geq 1.4$ BV/c, $P_2 \geq 4.6$ BV/c

then $P_3 = P_4$ and

$$k(P) = \frac{-\frac{3\pi}{4} I_v \frac{dP_c}{d\theta} \frac{dn_1}{dP_c} + \frac{3\pi}{4} n_1 SJ(P_c, x_o) \frac{dP_c}{d\theta}}{\sin \frac{1}{2} \tau_L(P_2) f_L(P_2) SJ(P_2, x_o) \frac{dP_2}{d\theta}} \qquad (65)$$

is a solution to the exact eq. (51) which requires no iteration and is independent of the trial function $k_i(P)$. These two solutions

are joined by requiring continuity of the solution. The second class of solution is approximate and applies where $Y_e \neq 0$, at higher P_c. Again assuming τ is independent of θ or λ, then

For $50.7^\circ \rangle \lambda$, $P_c \rangle 2.4$ BV/c

$$k_{i+1}(P_{oc}) = \frac{\left\{ \begin{array}{l} -\frac{\frac{3}{4}\pi I_v}{\cos\frac{1}{2}\Delta\psi}\frac{dP_c}{d\theta}\frac{dn_1}{dP_c} + \frac{\frac{3}{4}\pi n_1}{\cos\frac{1}{2}\Delta\psi} SJ(P_c,x_o)\frac{dP_c}{d\theta} \\ -\left(\frac{3}{4}\pi I_v n_1 \frac{d}{d\lambda}\cos\frac{1}{2}\Delta\psi\right)/\cos^2\frac{1}{2}\Delta\psi \\ + \sin\frac{1}{2}\tau_e(P_1)f_e(P_1)SJ(P_1,x_o)\frac{dP_1}{d\theta}k_i(P_1) \\ - \sin\frac{1}{2}\tau_L(P_2)f_L(P_2)SJ(P_2,x_o)\frac{dP_2}{d\theta}k_i(P_2) \end{array} \right\}}{\sin\frac{1}{2}\tau_e(P_{oc})f_e(P_{oc})SJ(P_{oc})\frac{dP_{oc}}{d\theta}} \qquad (66)$$

where for $50.7^\circ \rangle \lambda \rangle 40^\circ$, $5.2 \rangle P_c \rangle 2.4$ BV/c, $5.2 \rangle P_o \rangle 3$ BV/c then $P_{oc} = P_o \rangle P_c$, and for $40^\circ \rangle \lambda$, $P_c \rangle 5.2$ BV/c then $P_{oc} = P_c \rangle P_o$.

These two solutions are joined by requiring continuity. Two alternate forms of the second class are valid if τ_L or τ_e are regarded as dependent on θ. These are, for $\lambda \langle 40^\circ$:

$$k_i = \left\{ \frac{-\frac{3}{4}\pi I_v}{\cos\frac{1}{2}\Delta\psi}\frac{dP_c}{d\theta}\frac{dn_1}{dP_c} + \frac{\frac{3}{4}\pi n_1}{\cos\frac{1}{2}\Delta\psi} SJ(P_c,x)\frac{dP_c}{d\theta} \right.$$

Equation (67) continued on next page

$$- \frac{3\pi}{4} I_v n_1 \frac{d}{d\lambda} \cos\tfrac{1}{2}\Delta\psi \Big/ (\cos\tfrac{1}{2}\Delta\psi)^2$$

$$+ \sin\tfrac{1}{2}\tau_e(P_1) f_e(P_1) SJ(P_1, x_o) \frac{dP_1}{d\theta} k_o(P_1) + \int_{P_2(\theta)}^{\infty} \frac{\partial}{\partial\theta} \sin\tfrac{\tau_L(P,\theta)}{2} SJ(P, x_o) k_o(P) dP \Bigg\}$$

$$\sin\tfrac{1}{2}\tau_e(P_c,\theta) f_e(P_c) SJ(P_c, x_o) dP_c/d\theta \qquad (67)$$

and

$$k_{i+1}(P_c) = \Bigg\{ \frac{-\frac{3\pi}{4} I_v(P_c(\theta))}{\cos\frac{1}{2}\Delta\psi(\theta)} \frac{dP_c}{d\theta} \frac{dn_1}{dP_c} + \frac{\frac{3}{4}\pi n_1(P_c) SJ(P_c, x) \frac{dP_c}{d\theta}}{\cos\frac{1}{2}\Delta\psi(\theta)} - \frac{\frac{3\pi}{4} I_v n_1 \frac{d}{d\lambda}\cos\frac{1}{2}\Delta\psi}{(\cos\frac{1}{2}\Delta\psi)^2}$$

$$+ \int_{P_c(\theta)}^{P_1(\theta)} \frac{\partial}{\partial\theta} \sin\tfrac{1}{2}\tau_e(P,\theta) f_e(P) SJ(P, x) k_i(P) dP$$

$$+ \int_{P_2(\theta)}^{\infty} \frac{\partial}{\partial\theta} \sin\tfrac{1}{2}\tau_L(P,\theta) f_L(P) \quad SJ(P) k_i(P) dP \Bigg\}$$

$$\sin\tfrac{1}{2}\tau_e(P_c,\theta) f_e(P_c) SJ(P_c, x_o) \frac{dP_c}{d\theta} \qquad (68)$$

These two forms are used to check the accuracy of the previous more approximate forms, equations 64, 65 and 66, numerically.

The exact class of solutions $k_i(P_2)$ gives values over the range $3 < P < 6.3$, and the approximate class gives values over $3 < P < 11$ BV/c. Because of possible errors in the known functions yielding the "exact" solutions (as well as errors in the functions yielding the approximate solutions), the approximate solution is not ignored over the range $3 < P < 6.3$ BV/c for the purpose of

choosing the best fitting solution to the foregoing equations. That solution is used as the first trial for $k_i(P)$ in the iteration process for solving the exact equation for $k_{i+1}(P_{oc})$ for $P_c \rangle 2.4$ BV/c, which is equation 46 in the form

$$k_{i+1}(P_{oc}) = \left\{ \begin{array}{l} -\frac{3}{2}\pi^2 I_v^2(P_c) n_1(P_c) \frac{dn_1}{dP_c} \frac{dP_c}{d\theta} \\ \\ +\frac{3}{2}\pi^2 n_1^2(P_c) I_v(P_c) SJ(P_c, x_o) \frac{dP_c}{d\theta} \\ \\ -\frac{3}{8} Y_{ei} Y_{Li} \frac{d}{d\lambda} \cos\Delta\psi \\ \\ +(Y_{ei}+Y_{Li}\cos\Delta\psi)\sin\frac{1}{2}\tau_e(P_1) f_e(P_1) SJ(P_1, x_o) \frac{dP_1}{d\theta} k_i(P_1) \\ \\ -(Y_{Li}+Y_{ei}\cos\Delta\psi)\sin\frac{1}{2}\tau_L(P_2) f_L(P_2) SJ(P_2, x_o) \frac{dP_2}{d\theta} k_i(P_2) \end{array} \right\}$$

$$(Y_{ei}+Y_L \cos\Delta\psi)\sin\frac{1}{2}\tau_e(P_{oc}) f_e(P_{oc}) SJ(P_{oc}, x_o) \frac{dP_{oc}}{d\theta} \qquad (69)$$

which applies when the $F(P_{oc})$ term $\rangle$ $F(P_2)$ term or $F(P_1)$term.

Here

$$Y_{ei} = \int_{P_{oc}(\theta)}^{P_1(\theta)} \frac{8}{3} \sin \frac{1}{2} \tau_e(P,\theta) f_e(P) SJ(P,x_o) k_i(P) dP \quad , \tag{70}$$

$$Y_{Li} = \int_{P_2(\theta)}^{\infty} \frac{8}{3} \sin \frac{1}{2} \tau_L(P,\theta) f_L(P) SJ(P,x_o) k_i(P) dP \quad . \tag{71}$$

Some choice must be made of months to be included in the spectral analysis. As will be discussed in section VI which considers the direction of the incident beam responsible for the CRDV, the impact zones are reasonably symmetric in the months September, October, November, March, April and May, when $\alpha \approx 90^\circ$. There exists a small but fairly consistent difference between Fall and Spring values of n_1 and ϕ_{1LT}, as was discussed in paragraph IIID. For this reason six Fall months of $\alpha \approx 90^\circ$ have been selected for spectral analysis, omitting the three Spring months. Only northern hemisphere data is used. Due to the scarcity of stations in the southern hemisphere and to the fact that few of them operated for all eighteen months, not as much detail shows (Fig. 4) in the south as in the north. What detail does show there agrees well with the northern data. Not only was the CRDV data found to be independent of altitude, but it will be shown analytically that this independence is expected. For this reason data from stations of all altitudes enters the spectral analysis. The principal change which would be produced by the elimination of high altitude stations is further flattening of the broad equatorial region of almost constant n_1.

The approximate equations (63) and then (66) which is a form of (58), followed by (69) which is a form of the exact equation (46) are used in solving the exact equation (45) in order to yield k(P) for $P > 3$ BV/c. These equations apply at $P_c > 2.4$ BV/c, or over the main peak and the equatorial flat of n_1. Equations (66) and (69) are valid iteration formulae provided that the term in P_{oc} exceeds the terms in P_2 or P_1. Otherwise these terms are interchanged and the equation provides values of k(P) at P_2 or P_i, not P_o or P_c. Eq. 66 gives a solution which converges quickly, by the third iteration, and shows k(P)=0 for $P < 3.8$ BV/c spectral cutoff, a peak from 3.8 to 5.5 BV/c, peaked at k(5.4)=0.0296, and low values ranging from k(6)=.001 to $k(P > 10)$=.006 at $P > 6$. This solution is inserted as the first trial k_1 in the solution of eq. 69, which requires calculation of trial values Y_{ei} and Y_{Li} by eqs. 70, 71. It is thus found that $Y_{ei} \ll Y_{Li}$ for $P_c > 6$ BV/c, so that eqs. 50, 51 apply there almost exactly, and give k(P) for $12.9 < P_2 < 17.7$ BV/c. They show k(P) is almost constant, $k(P) \approx .004$, at high P, with a small rise to .005 around P = 15 BV/c. Equations 66, 51 and 69 indicate $k(P) \approx$ constant at moderately high $10 < P < 20$, and eq. 50 is then used to adjust that constant to the result $k(P > 6) = .0037$ which gives the correct (observed) $n_1(P_c)$ at $P_c > 6$ BV/c. Eq. 45 gives the same value. Equation 69 does not converge in an osculating manner, but oscillates. That is, if a trial solution k_i is put in which is too low, the resulting k_{i+1} will be too high. In order to obtain convergence, therefore, the trial solution $k_i(P)$ is replaced by one intermediate in value between $k_i(P)$ and $k_{i-1}(P)$, thus damping the oscillation. Six such iterations produced convergence. The resulting $k_{i+1}(P)$ are integrated in eqs. 70,71 in order to satisfy eq. 45. In this way the solution converges to a peak from 3.8 to

5.7 BV/c, peaked at k(5.4)=.068, k(p>5.7)=.0037, and k(P)=0 for P<3.8 BV/c spectral cutoff, as shown in fig 16 . Equation 50 is a form of eq. 45 which applies at P_c<2.2 BV/c, over the small peak of n_1, and eq. 51 in the forms 64, 65 is used to solve it for k(P) for 3<P_2<6.3 BV/c. It gives k(P)=0 for P<3.85 BV/c spectral cutoff, and shows a peak between 3.9 BV/c and 6.0 BV/c peaked at k(5.3)=0.0125, with very low k just above 6 BV/c, as shown in fig 16 . Both the small peak and the main peak in $n_1(P_c)$ thus result from a single peak in the differential spectrum k(P), located between about 3.8 BV/c and about 6 BV/c, and peaked at 5.3 or 5.4 BV/c. However, the values from the small peak and from the main peak of n_1 disagree by a factor of 5.38 as to the value of k at the peak. This discrepancy is largely due to uncertainty in the "known" functions $\Delta\psi(\theta)$, $I_v(P_c)$, $\tau(P)$, f(P), SJ(P), $P_o(\theta)$, and $P_2(\theta)$. The values of $I_v(P_c)$, $SJ(P_c)$, and $dP_2/d\theta$ are especially poor for low P_c at the small peak. The discrepancy is also due to uncertainty in the values of $n_1(P_c)$, σ for which is large, as shown in fig 5 . The height k discrepancy can be greatly reduced, to a factor of about 3, simply by taking the bend in $n_1(P_c)$ at P_c= 5.4 BV/c to be less sharp. The peak in the solution k(P) of eq. 46 will then be less sharp, and lower. An attempt was made to take $f_e(P) \neq f_L(P)$ but to estimate them each from the values of f(P) tabulated by Kelsall together with the impact zone information given in his table 6, but the discrepany was then larger than when $f_e=f_L=f$ was taken directly by interpolating (graphically) from Kelsall's table 5.

For 7<P_c<11 BV/c the values used for $\Delta\psi$ are guided by the almost constant small second harmonic relative amplitude, equation (90) . At P_c<7 BV/c, $\Delta\psi$ can be obtained rather precisely from the sharply defined impact zones. Values of τ are taken to have a simplified dependence on P, and no dependence on θ.

The fact that one peak in k(P) leads to two peaks in $n_1(\lambda(P_c))$ is due principally to the limits P_o, P_1, P_2, P_3 as functions of λ, shown in figure 15. At $\lambda < 38^\circ$, the k peak is outside the limits of integration of Y_e and Y_L. When $39^\circ < \lambda < 52^\circ$, corresponding to $5.5 > P_c > 2.2$ BV/c, the k peak, and therefore a peak in F(P), eq. 35, is within the limits P_o and P_1 of integration for the early impact zone, thus producing large Y_e and the main peak of n_1. When $52^\circ < \lambda < 53^\circ$, corresponding to $P_c \approx 2.1$, the k peak is outside the limits of integration for Y_e and Y_L, in fact $Y_e = 0$, so n_1 is small, producing the relative minimum n_1 between the peaks. When $54^\circ < \lambda < 62^\circ$, corresponding to $1.9 > P_c > 0$ BV/c, the k peak is within the limits P_2 and P_3 of integration for the late impact zone, thus producing especially large Y_L and the small peak of n_1. Y_L is rather large at all λ due to large τ_L and the absence of an upper limit of integration at $\lambda < 55^\circ$, hence the n_1 peak due to large Y_L is smaller than the n_1 peak due to large Y_e, which is zero or almost zero elsewhere.

The k(P) peak is skewed, falling more steeply at its high P end, and so that the peak lies at the P value just below the P_c value at the relative minimum n_1 just south of the main peak. The spectral cutoff, k(P)=0, occurs at a P value P_o about 0.5 BV/c above the P_c value at the top of the main peak of n_1. Thus the k(P) peak locations and spectral cutoff limits for periods other than September, October, and November, 1957 and 1958 can be obtained from table IV.

Although the integral spectrum $n_1(P_c)$ can be perfectly fitted by a k(P) which is constant (k=.0037) for $P > 6$ BV/c, it is possible also to fit a k(P) which rises slightly from 6 BV/c to 15 BV/c, and then falls off as

$$k(P) = A\left(\frac{15}{P}\right)^{m}, \quad P \rangle 15 \frac{BV}{c} \quad , \tag{72}$$

$$A = k(15)$$

where m is very small. The constants A and m are chosen so as to yield the same values for Y_L, Y_e, and n_1 as are obtained from the constant k.

At high rigidity, using eq. 25, the CR flux (eq. 1) can be written as

$$(1+0.0037 \cos \theta') \, J(P) \, d\Omega \, dP, \quad P \rangle 6 \frac{BV}{c} \tag{73}$$

or, using eqs. 25 and 72, as

$$(1+15^{m} \, k(15) P^{-m} \cos \theta') \, J(P) \, d\Omega \, dP, \quad P \rangle 15 \frac{BV}{c} \quad , \tag{74}$$

both in good agreement with the observed CRDV amplitudes. At lower rigidities the anisotropic part k(P) J(P) must be more elaborately specified, as shown in fig. 16 , in order to describe the spike between 3.8 and 6 BV/c which is at least 3 and possibly 18 times as great as the anisotropy at $P \rangle 6$ BV/c.

The small rise in k(P) near 15 BV/c was found after smoothing flat the fluctuations in $n_1(P_c)$ near the equator, which are due partly to an unremoved longitude dependence, shown in fig. 12. The k(P) found indicates $\alpha = 0^{\circ}$ in late December. When $n_1(P_c)$ is plotted for October 1957 through February 1958 or for December 1957 through January 1958, then a pronounced rise in $n_1(P_c)$ shows at 14,5 BV/c, suggesting a higher rise in k(P). Also the two peaks of n_1 are then bifurcated or jagged.

The functions $\frac{8}{3} \sin \frac{1}{2}\tau_{e,L}(P)\ f(P)\ S(P,x_o)J(P)=F_{e,L}/k(P)$ eq.(35), used in obtaining the foregoing solutions are shown in figures 17a and 17b, for low P. Integrations over them were performed graphically or by the trapezoidal rule. At high P, the integrations were performed analytically, using

$$\sin \frac{1}{2}\tau_e = 0.2 \ , \ P > 6 \text{ BV/c} \tag{75}$$

$$\sin \frac{1}{2}\tau_L(P) = 0.03(P-5), \ 8 < P_2 < 25 \text{ BV/c} \tag{76}$$

$$= 0.6 \ , \ P = P_2 > 25 \text{ BV/c} \tag{77}$$

$$f(P) = 2.1-.0225P, \ 10 < P < 49 \text{ BV/c} \tag{78}$$

$$= 1 \ , \ P > 49 \text{ BV/c} \tag{79}$$

$$S(P,x_o)J(P) = 200\ P^{-1.5} \ , \ P > 10 \text{ BV/c} \tag{80}$$

Because of the maxima in F_e and F_L at 4.2 BV/c and 3.8 BV/c respectively, a simpler form such as

$$k(P) = AP^{-m} \tag{81}$$

with m = 0 , 0.4 , or 1 will also give two peaks in the integral spectrum of height and slope different than those observed, but the spectral cutoff must be at $P=3.85\pm.5$ BV/c to agree with the location of the two peaks. This cutoff is lower than those found from the simpler theories.

IV. C. Altitude Independence of CRDV

The principal dependence of both c_1, (eq. 44), and I, (eqs. 6 and 5) upon altitude or upon atmospheric depth x occurs in the common factor (1+x/L), so that their ratio n_1,(eq. 41), is practically independent of x. Slight x dependence enters through the factor S(P,x) which is integrated over different limits in eqs. 5 and 44. Complete independence of x requires either the condition that

$$P_o \lesseqgtr P_c \ , \ P_1 = P_2 \tag{82}$$

with P_3 and P_4 playing no role, so that the limits are the same in the two integrals, or else it requires the assumption that

$$\frac{\delta S(P,x)}{S(P,x)} = \frac{1}{S(P,x)} \frac{\partial S(P,x)}{\partial x} \delta x = K(x, \delta x) \tag{83}$$

which is nearly satisfied by Quenby and Webber's values for S . Then the change in vertical intensity

$$\begin{aligned} \delta I_v = \frac{\partial I_v}{\partial x} \delta x &= \int_{P_c}^{\infty} J(P) \ \delta S(P,x) dP \\ &= \int_{P_c}^{\infty} K(x, \delta x) J(P) S(P,x) dP \\ &= K(x, \delta x) I_v \ . \end{aligned} \tag{84}$$

Similarly, the change in n_1 is

$$\delta n_1 = \delta x \frac{\partial n_1}{\partial x} = -\frac{\cos\frac{1}{2}\Delta\psi}{2\pi I_v^2} \frac{\partial I_v}{\partial x} \delta x \left\{ \int_{P_c}^{\infty} F_e dP + \int_{P_2}^{\infty} F_L dP \right\}$$

$$+ \frac{\cos\frac{1}{2}\Delta\psi}{2\pi I_v} \left\{ \int_{P_c}^{\infty} \frac{8}{3} \sin\tfrac{1}{2}\tau_e(P,\theta) f_e(P) J(P) \delta S \, dP \right.$$

$$\left. + \int_{P_2}^{\infty} \frac{8}{3} \sin\tfrac{1}{2}\tau_L(P,\theta) f_L(P) J(P) \, \delta S \, dP \right\} \tag{85}$$

Then, substituting the preceeding two expressions yields

$$\frac{\partial n_1}{\partial x} \delta x = -\frac{\cos\frac{1}{2}\Delta\psi}{2\pi I_v} K(x,\delta x) \, \delta x \left\{ \int_{P_c}^{\infty} F_e dP + \int_{P_2}^{\infty} F_L dP \right\} + \frac{\cos\frac{1}{2}\Delta\psi}{2\pi I_v} K(x,\delta x) \delta x \left\{ \int_{P_c}^{\infty} F_e dP + \int_{P_2}^{\infty} F_L dP \right\}$$

or

$$\frac{\partial n_1}{\partial x} = 0. \tag{86}$$

Thus the percent amplitude, 100 n_1, of the CRDV, is expected to be approximately independent of altitude, insofar as the condition (eq. 83) upon S is met. The slight x dependence depends on the values of P_1, P_2, P_3 and P_4, which depend on θ. Hence the x dependence can be different for different groups of stations. It was found that n_1 increased slightly with altitude for some groups of stations and decreased slightly for others. The condition (eq. 82) for complete x independence is met in a centered dipole

field at $\lambda = 36^{o}$, $P_c = 6.5$ BV/c. The almost complete independence of the CRDV at all λ permits spectral analysis using data from all altitudes, as was done, using $X = X_o$ for sea level in the function $S(P,x)$ throughout the analysis.

IV. D. An Explanation of the Second Harmonic of the CRDV

A CR anisotropy which is purely first harmonic in assymptotic longitude, such as eq. 19 , produces a DVCR, eq. 30, which is purely first harmonic in LT, despite the fact that there are two impact zones at each latitude. In order to have a second harmonic CRDV (CRD/2V) observed anywhere, the CR anisotropy must have an assymptotic longitude dependence which is more narrowly collimated than the $\cos\phi$ dependence of eq. 19. Even then the CRD/2V will not be observed at all stations.

A perfectly collimated anisotropy includes all components in a Fourier analysis over assymptotic longitude. This is the model discussed on pages 28 through 34, leading to two sharp rectangular (Fig. 13) pulses of DVCR, eqs. 9 and 10. For them the second harmonic Fourier coefficients are found, in a manner similar to that used for eqs. 11-14, to be

$$a_2 = \frac{1}{\pi}\int_{-\tau_e/2}^{\tau_e/2} y_e \sin 2t\, dt + \frac{1}{\pi}\int_{\Delta\psi-\tau_L/2}^{\Delta\psi+\tau_L/2} y_L \sin 2t\, dt$$

$$= (1/\pi)\sin\tau_L \sin(2\Delta\psi)$$

and similarly

$$b_2 = (1/\pi)\left\{ \sin\tau_e + \sin\tau_L \cos(2\Delta\psi)\right\} \quad .$$

Then, using $c^2 = a^2 + b^2$ and eq. 14 without the approximation of eq. 13, since τ_L is not small at low λ,

$$\frac{n_2}{n_1} = \frac{c_2}{c_1} = \frac{1}{2}\left\{ \frac{(y_e \sin\tau_e)^2 + 2y_e y_L \sin\tau_e \sin\tau_L \cos(2\Delta\psi) + (y_L \sin\tau_L)^2}{(y_e \sin\tfrac{1}{2}\tau_e)^2 + 2y_e y_L \sin\tfrac{1}{2}\tau_e \sin\tfrac{1}{2}\tau_L \cos\Delta\psi + (y_L \sin\tfrac{1}{2}\tau_L)^2} \right\}^{\frac{1}{2}} \tag{87}$$

This gives $n_2/n_1 = 1.1$ at $\lambda = 0^\circ$ and $n_2/n_1 = 0.1$ at $\lambda > 23^\circ$, as observed in the IGY data. Even when $y_e = 0$, so that there is only one rectangular pulse, eq. 87 gives $n_2/n_1 \approx 1$ for a pulse of infinitesimal duration τ_L. It is evident that n_2/n_1 depends not only on the form of longitude dependence of the CR anisotropy, but also on the pulse shape and the pulse spacing $\Delta\psi$ of the associated CR pulses at the ground. Examination of the actual pulse shapes, as given by Kelsall's[2] table 6, indicates that at low λ the pulse for 50 Bev is broad and very nearly rectangular, and that the broad rectangular pulse approximation is not terrible at 25 Bev. A single broad rectangular pulse, of large τ_L, does give $n_2 > 0$ at low λ, and a second pulse $Y_e \ll Y_L$ but at an appropriate $\Delta\psi$ gives an enhanced $n_2 \approx n_1$. The values of $\Delta\psi$ are again taken from Kelsall's table 6. At high λ, $\Delta\psi \approx 94^\circ$ so that the second pulse makes n_2 much less than it would be for a single rectangular pulse.

At $39^{\circ} < \lambda < 51^{\circ}$, within the main peak zone of n_1, both τ_e and τ_L are small so that eq. 13 and

$$(1/\pi)\, y_{e,L} \sin \tau_{e,L} \approx Y_{e,L}$$

hold. At these λ it was found in the solution of eq. 69 that $Y_e \approx Y_L = Y$, as in eq. 14, so that

$$c_2 \approx \sqrt{2}\, Y \sqrt{1 + \cos\,(2\Delta\psi)}$$

$$c_2 \approx (Y_e + Y_L) \left| \cos \Delta\psi \right| \quad . \tag{88}$$

The relative amplitude than becomes

$$n_2/n_1 \approx \left|\cos \Delta\psi\right| \Big/ \cos \tfrac{1}{2}\Delta\psi \quad . \tag{89}$$

The approximations in eqs. 14 and 88 were found to give errors less than 50%, and their ratio may be expected to differ from eq. 87 by even less. Eq.89 does in fact agree very well with the observed n_2/n_1 at all λ. It is to be remembered that eqs. 87 and 89 were derived for a perfectly collimated anisotropy, and must be modified for some other assymptotic longitude dependence. For example, $n_2/n_1 \equiv 0$ when that dependence is of form $\cos \phi$.

Another contribution to an enhanced CRD/2V at low λ is suggested by eqs. 9 and 10. Diagrams such as figure 15 showing the P limits P_c, B_o, P_1, P_2,...for $\alpha = 90^{\circ}$ and 100° clearly show a semidiurnal oscillation of $P_o(\theta)$ at low λ, with $P_o(\theta)$ unchanging at high λ. It is not clear whether they also show a semidiurnal oscillation of P_2, the lower limit for y_L, since the P limit

diagrams are taken from Kelsall's table 6, which gives numbers only at 10 and 25 Bev. P_2 at $\lambda \approx 0$ remains just below 25 BV/c. If it is assumed that both the lower limits of integration P_o and P_2 have a semi-diurnal oscillation at very low λ, this will produce a CRD/2V which has a fixed phase in UT and which will enhance the CRD/2V of fixed phase in LT which is introduced by the pulse shape and spacing. To show this take $y_e \approx 0$, as found at low λ from eq. 70 and the solution to eq. 69, and take

$$P_2 = \overline{P_2} + b \cos 2(t' - \beta) \tag{90}$$

where t' = UT. Modification of eq. 10 gives

$$y_L = \overline{y} + \Delta P_2 \left[\frac{d}{dP_2} \int_{P_2(\theta, \alpha(t'))} \frac{L}{x+L} f(P, \;) S(P, x_o) J(P) k(P) dP \right]_{\overline{P_2}} \tag{91}$$

so that

$$y_L = \overline{y} + B \cos 2 (t' - \beta) \tag{92}$$

and

$$a_2 = \frac{1}{\pi} \int_{-\tau/2}^{\tau/2} \overline{y} \sin 2 t \, dt + \frac{1}{\pi} \int_{-\tau/2}^{\tau/2} B \cos 2 (t' - \beta) \sin 2 t \, dt \, .$$

Using LT

$$t = t' + \varphi \tag{93}$$

this becomes

$$a_2 = B \sin(2\varphi + 2\beta) \left[\tau - \frac{1}{2} \sin 4\tau \right] / 2\pi$$

Similarly

$$b_2 = (\bar{y}/\pi)\sin\tau + (B/2\pi)\cos(2\varphi+2\beta)\left[\tau + \tfrac{1}{2}(\sin 4\tau)\right] .$$

Thus, if B = 0, then

$$c_2 = \left(\bar{y}\sin\tau_L\right)/\pi$$

which equals c_1 for small τ but if $B \neq 0$ then c_2 can be larger or smaller, depending on the longitude φ, at $\lambda \approx 0^\circ$:

$$c_2^2 = B^2\left\{\left[\tau^2 + \tfrac{1}{4}\sin^2 4\tau\right] + \tau\sin 4\tau\cos(4\varphi+4\beta)\right\}/4\pi$$

$$+ (B\bar{y}/\pi^2)\left[\tau + \tfrac{1}{2}\sin 4\tau\right]\sin\tau\cos(2\varphi+2\beta) + (\bar{y}\sin\tau/\pi)^2 . \qquad (94)$$

The assymptotic longitude dependence of the CR anisotropy is not purely first harmonic, since a CRD/2V is observed at some equatorial stations. This is quite plausible, since cos ϕ gives a large angular spread for the beam. It is to be noticed that n_1 is essentially the same for zero angular spread, eq. 14, or for a cos ϕ dependence, eq. 44, so k(P) as determined by eq. 45 or 69 is unaffected by the conclusion that cos ϕ is not the complete assymptotic longitude dependence.

IV. E. Application of Liouville's Theorem

It is commonly asserted, in studies of the isotropic CR and of the CRDV anisotropic CR,[10] that Liouville's Theorem[11] demands

---

[10] Rao, U. R., McCracken, K. G. and Venkatesan, D., J. Geophys. Res. 68, 345 (1963).

[11] Goldstein, H., Classical Mechanics, Addison-Wesley, (1950).

that the CR flux at the top of the atmosphere equals zero for $P < P_c$, and equals the CR flux at infinity for $P > P_c$. If correct, this statement would forbid CR focusing by the geomagnetic field, and require f = 1 in eqs. 3 through 71. For a somewhat collimated anisotropic CR beam, the assertion is not correct, and focusing actually does occur as found by Kelsall.[2]

Liouville's theorem states that the density of points is constant in a 6N dimensional phase space where each point represents all the coordinates $\vec{q}$ and momenta $\vec{p}$ of an entire system of N particles. The theorem can be applied to the isotropic CR case by taking each CR particle as an independent system, not interacting with its fellows, so that the phase space is six dimensional. Next the fact that p^2 is constant for a charged particle in a magnetic field is introduced in order to make an assertion about the volume in the three dimensional p space occupied by the N particles. The ordinary assertion for the isotropic CR case is that all directions of velocity are equally populated, so that for particles within dp around p the volume in p space is the constant $4\pi\ p^2\ dp$.

Consider now an anisotropic CR particle beam at infinite distance from the geomagnetic field center, collimated so that not all directions of $\vec{p}$ are equally populated. In fact, for a mono-directional, mono-energetic assymptotic beam such as treated by Kelsall, the volume in p space is zero, or if we treat an interval dp around the constant $\vec{p}$, then it is an infinitesimal sphere $4\pi(dp)^3/3$. After deflection by the geomagnetic field, the particle momenta do not all have the same direction, in fact the beam is converging. The volume in p-space is then a much larger shell $\Delta\Omega\, p^2\ dp$. Liouville's theorem requires that the volume in phase space be constant, so that the enlargement of the volume in p space requires a contraction in q space, thus increasing the particle density ρ in q space. Since v^2 is constant this increases the flux

$\vec{j} = \rho \vec{v}$ over the value it had at remote distances. Thus Liouville's theorem not only permits, but it demands geomagnetic focusing of an originally collimated charged particle beam. A similar discussion applies to the beam in a cathode ray tube, where magnetic focusing is also possible. Those papers on the CRDV which ignore magnetic focusing factors are making a substantial error at rigidities below 6 BV/c.

V. Use of the CRDV as a Field Probe

A. Assymptotic Direction of Incident Beam

Information regarding the directions of the interplanetary (IP) and perhaps interstellar magnetic fields may be deduced from the direction of the axis of CR anisotropy responsible for the CRDV. This is the direction of the assymptotic orbit at the center of the beam, at a distance sufficiently remote from earth so as to be not yet significantly deflected by the earth's dipole field. To obtain this direction, A, the CRDV peak times are compared with the impact deflections ψ_e and ψ_L and the predicted peak times

$$\Phi_{theor} = -\psi_e + \epsilon + 12 \quad \text{hrs} \tag{V-1}$$

corresponding to a perfectly collimated assymptotic beam from 12 hours LT, perpendicular to the dipole axis ($\alpha = 90^\circ$).[1]

For the first approximation the above comparison was made using peak times from all months of the IGY, and without knowledge of the spectrum k(P). Eq. IV-40 could then not be evaluated and $\epsilon \approx \frac{1}{2}\Delta\psi$ was obtained by taking the centroid of the zone area at each energy in Kelsall's figure 6. The comparison

$$A = 12 + \Phi_{obs} - \Phi_{theor} \tag{2}$$

then gave $A \approx 20$ hours, LT. The corresponding months of nearly symmetrical impact zones, when $\alpha \approx 90^\circ$, are November and May. For the second approximation, data might be taken from these three IGY months only. It is desirable, however, to average over more

---

[1] Kelsall, T., J. Geophys. Res. 66, 4055, (1961).

than three months data to remove random monthly fluctuations. The zero-th approximation CRDV spectrum, $k_o J(P)=9000\ k_o P^{-2.5}$, has high values at low rigidity, so that $Y_e \gg Y_L$ is possible, and then $A \approx 24$ hrs LT. Then equinoctial months would give the most symmetrical impact zones, and so they were included in the averages for the second approximation. For continuity of record the intervening three months October and April were also included. The ϕ_{1LT} versus latitude, or versus P_c, curves obtained for these nine months of symmetric impact agree closely with the curves for all eighteen IGY months. Therefore, the second approximation for A, using the same values of ϵ as the first approximation, gave the same result.

The differential spectrum k(P) stated on pages 56, 58 is based upon data from the months which would give almost symmetric impact, if the first approximate A is correct. That spectrum is used to evaluate eq. IV-40 and therefore the predicted peak time, eq. 1, at various latitudes, using the impact times ψ from a zone map for $\alpha = 90^\circ$ as drawn from Kelsall's[1] table 6 for $\zeta \leq 45^\circ$. This Φ_{theor} is compared with the ϕ_{1LT} curves for the same months using eq. 2 to obtain the third approximation for A. At most values of P_c, $\epsilon \approx \Delta\psi$ and A = 17 to 17.6 hrs is obtained. However over the main peak of n_1, $Y_e \approx Y_L$ so $\epsilon < \Delta\psi$ and the Φ_{theor} are somewhat earlier than elsewhere. Eq. 2 applied to data in this region thus gives $A > 18$ hrs. If ϵ is here computed using the $Y_{e,L}$ from the k(P) peak of height as found from the main peak region of $n_1(P_c)$, then the predicted Φ_{theor} values over this region are too low (early) to agree with the observed Φ_{1LT}. Better Φ agreement is obtained when a smaller peak height for k(P) is used, such as found from the small peak of $n_1(P_c)$. Thus the height discrepancy found in the peak of k(P), page 56, is partially resolved if k(P) is required to satisfy

eq. IV-40 and V-1 as well as eq. IV-45.

North of 68° latitude not only is $Y_e = 0$, but only the very high energy part of the late zone, $P \rangle P_4$, contributes. The peak time is then the not sharply defined centroid for high $P \rangle P_4$ and large τ_L, which occurs a little later than the low rigidity late zones. CRDV peak times in the Arctic are therefore exceptionally late.

The fact that the source beam responsible for the CRDV may have a component from a direction opposite the sun's direction can be ascribed to a few related causes. They are the geomagnetic envelope due to the confinement of the geomagnetic field by the solar wind plasma, and the possibility that the sun casts a "shadow" for cosmic rays upon the earth. Our attention has focused upon the geomagnetic envelope. The significant feature is not the "tail" which stands away from the sun, but the "head" which faces the sun.[2] Here the horizontal component of the geomagnetic field is increased over its dipole value, while in the tail it is decreased. This increased field on the sunward side blocks out some of the otherwise isotropic galactic cosmic radiation, thus leaving an excess from the side away from the sun.

That enhancement will cause a diurnal variation of the cutoff rigidity at an observing station of form

$$P_c(\theta)=\overline{P}_c(\theta)\left\{1+\sum_i R_i(\theta)\cos i(t-\beta_i)+\sum_j R_j(\theta)\cos j(t'-\gamma_j)\right\}. \qquad (3)$$

The UT=t' dependence is introduced by variation of α as the earth rotates. Inserting this P_c in eq. (IV-7) and using eq . (IV-80) gives

---

[2]Suggested by A. Beiser, private communication

$$I_v(\theta) = + 200 \left[P^{-0.5}/0.5 \right]_{P_c}^{\infty}$$

$$= 400 \, \overline{P}_{c\,(\theta)}^{-0.5} \left\{ 1+\sum_k R_k(\theta) \cos k\,(t-\delta_k) \right\}^{-1/2}$$

$$= 400 \, \overline{P}_{c\,(\theta)}^{-0.5} \left\{ 1-\frac{1}{2} R_1(\theta) \cos\,(t-\delta_1) - \frac{1}{2} R_2(\theta) \cos 2(t-\delta_2) + \ldots \right\} \qquad (4)$$

This gives a diurnal and semi-diurnal variation in the observed cosmic ray counting rate I, due to no anisotropy in the cosmic radiation. If the ratio R_1 is independent of θ or P_c, then $n_1(P_c)$ is independent of P_c. There is no reason to expect that $R_1(\theta)$ has a peak, and especially not a double peak, at high λ. Thus the DV in P_c can not be entirely responsible for the CRDV, but it can make a substantial contribution. A CRDV vector due to DV in P_c must then be added to the CRDV vector due to an anisotropic CR beam. This vector addition could produce a large shift in the apparent source direction A with only a small increase in amplitude n_1, and thus be responsible for the reported A $>$ 18 hrs.

A discrepancy between CRDV peak times observed at several P_c and peak times predicted from the k(P) presented can be ascribed partly to the possibility that A depends on P. It is also partly due to an unremoved longitude dependence as shown in fig. 12, especially at Makapuu (P_c = 11), and Lae (P_c = 14.9). If A = 18 hrs then $\alpha \approx 90^\circ$ on December 21. Little P_c dependence is shown by CRDV peak times for October 1957 through February 1958 averaged, after the U.T. dependence is considered.

V. B. Earth's Magnetic Field

The earth's quadrupole field is more significant than is indicated by the frequently stated[3] fact that its average value at the earth's surface is only 7% of that of the dipole field. There are places on earth's surface near the dipole equator where the quadrupole field strength is nearly half the dipole field strength. At the dipole poles, the quadrupole field strength is almost zero, so its average strength is comparatively small. A similar statement applies to some of the higher multipole field strengths.

On maps of the horizontal and vertical intensity (H and Z) of the earth's magnetic field, zones of relative maxima and minima of H and Z can be drawn. A CRDV relative maximum should occur where the dip is large, that is, wherever a minimum line for H nearly coincides with a maximum line for Z. There are two such places in the southern hemisphere and two in the northern, and they coincide the observed maxima of n_1 for months of symmetric impact. This occurs because CR orbits, for rigidities not very much above P_c at high λ, finish by spiraling tightly around geomagnetic field lines.[3] Larger dip angles for field lines at a given λ bring in particles of lower rigidity. Since $S(P,x)\ J(P)$ peaks at low rigidity this provides larger I where the dip is larger. Since $f(P)S(P,x_o)J(P)k(P)$ is even more sharply peaked at low P, increased dip in the region of the n_1 peak zones will increase c_1 faster than I, so that $n_1 = c_1/I$ is largest where the dip is greatest.

---

[3]Quenby, J. J. and Webber, W. R., Phil. Mag. 4, 90, (1959).

Similarly, A CRDV relative minimum should occur where the dip is small, that is, wherever a maximum line for H coincides a minimum line for Z. There are just two such places in the north and none in the south. These coincide the minima of n_1 for months of symmetric impact. This shows that the CRDV amplitude is indicative of some of the details of the earth's magnetic field maps.

Eqs. IV-14, 40, and 45 show that the CRDV peak time Φ_{1LT} is related to the amplitude n_1 through Y_e and Y_L. It follows that relative maxima and minima (ridges and valleys) on isoplot (contour) maps of Φ_{1LT} (Fig. 7) as well as of n_1 (Fig. 6) are indicative of similar relative extremums in the earth's magnetic field maps. Similarly, an isoplot map of the CRD/2V amplitude n_2 shows (Fig 10) an equatorial maximum which is indicative of the geomagnetic equator.

Most of the CRDV maps show four zones in the north. These are two North-South oriented ridge lines of relative maximum amplitude and also of phase, and two North-South valley lines of relative minimum amplitude and also of phase. Many of the maps also show four such lines in the south. These zones can be explained by a superposition of the earth's dipole plus quadrupole fields. The dipole field direction is from south to north near the dipole equator. The four quadrupole "poles" are situated near the dipole equator. These are the locations where the quadrupole terms of the scalar potential of the geomagnetic surface-measured field achieve their greatest magnitude, positive or negative. Above a positive such pole the quadrupole field is essentially radially up, thus making the field lines of the dipole plus quadrupole field dip more in the south and less in the north. This causes a CRDV relative maximum near a region south of the plus quadrupole pole and a relative minimum near a region north of the plus pole. Similarly

above a negative pole of the quadrupole the field lines of the combined field dip more in the north and less in the south. This causes a CRDV relative maximum near a region north of the negative quadrupole pole and a relative minimum near a region south of the negative quadrupole pole. Using this reasoning four quadrupole polar regions were obtained from the CRDV amplitude contour maps for November 1957 and 1958 and May 1958. These regions will be called the "apparent quadrupole poles." They agree within 15° with the locations of the quadrupole poles obtained from the spherical harmonic coefficients of the geomagnetic scalar potential.

V. C. Orbits in Dipole Plus Quadrupole Field

Cosmic ray orbits are governed by

$$q\vec{v} \times \vec{B} = \frac{d}{dt}(m\vec{v}) \tag{5}$$

where

$$m = m_o \Big/ \sqrt{1 - v^2/c^2} \tag{6}$$

$$v^2 = \text{constant} \tag{7}$$

$$\vec{B} = -\mu_o \vec{\nabla} V \tag{8}$$

$$V = a \sum_{n=1}^{\infty} \sum_{m=0}^{n} (a/r)^{n+1} \left(g_n^m \cos m\phi + h_n^m \sin m\phi\right) P_n^m(\cos\theta) \tag{9}$$

a = radius of earth

ϕ = longitude, θ = colatitude

$q = Ze/c$ = charge in ab.e.m.u. (10)

so that $\mu_o = 1$.

The discussion of the preceeding section, VB, ascribes the relative extremums of the CRDV to the dipole and quadrupole components of $\vec{B}$, and so the n = 1,2 terms are most significant for describing the CR orbits responsible. The dipole term, in geomagnetic dipole coordinates, is

$$V_1 = a(a/r)^2 \, g_1^o \cos \theta \qquad (11)$$

Because the quadrupole is so oriented that its poles lie near $\theta=\pi/2$ in geomagnetic coordinates the dominant second degree term is m=2. This can be written

$$V_2 = a(a/r)^3 \, h_2^{\,2} \sin 2\phi \, P_2^{\,2} (\cos \theta) \qquad (12)$$

$$= 6a(a/r)^3 \, h_2^{\,2} \sin \phi \cos \phi \sin^2 \theta$$

by a suitable choice of ϕ origin. In rectangular geomagnetic coordinates eqs. 11, 12 become

$$V_1 = a^3 \, g_1^{\,o} \, Z/(x^2 + y^2 + z^2)^{3/2} \qquad (13)$$

$$V_2 = 6a^4 h_2^{\,2} \, xy/(x^2+y^2+z^2)^{5/2} \qquad (14)$$

This dipole plus quadrupole magnetic field is then

$$B_x = (3a^3 g_1^o xz - 6a^4 h_2^2 y)/r^5 + 30a^4 h_2^2 x^2 y/r^7 \quad (15)$$

$$B_y = (3a^3 g_1^o yz - 6a^4 h_2^2 x)/r^5 + 30a^4 h_2^2 xyz/r^7 \quad (16)$$

$$B_z = (3a^3 g_1^o yz - 6a^4 h_2^2 x)/r^5 + 30a^4 h_2^2 xyz/r^7 \quad (17)$$

where $r = (x^2+y^2+z^2)^{1/2}$.

Let

$$dt = (ds)/v$$

by making use of v = constant, eq. 7, so that eq. 5 becomes

$$P\, d^2x/ds^2 = B_z\, dy/ds - B_y\, dZ/ds \quad (18)$$

$$P\, d^2y/ds^2 = B_x\, dZ/ds - B_z\, dx/ds \quad (19)$$

$$P\, d^2Z/ds^2 = B_y\, dx/ds - B_x\, dy/ds \quad (20)$$

where $P = mv/q$.

It is convenient to combine the constants into the Störmer constant[4]

$$S_k = \sqrt{a^3(-g_1^o)q/mv} \quad \text{cm} \quad (21)$$

and a coefficient

$$Q' = 2ah_2^2/g_1^o \text{ , cm} \quad (22)$$

when substituting eqs. 15, 16, 16 into eqs. 18, 19, 20.

---

[4]Montgomery, D. J. X., Cosmic Ray Physics , p. 351, Princeton (1949).

These equations can be put in Stormer units by letting

$$s = S\, S_k \tag{23}$$

$$x = XS_k,\ y = YS_k,\ z = ZS_k \tag{24}$$

$$r = R\, S_k$$

$$Q' = Q\, S_k \tag{25}$$

Then, introducing

$$l = dX/dS \tag{26}$$

$$m = dY/dS \tag{27}$$

$$n = dZ/dS \tag{28}$$

equations 17, 18, 19 become

$$\frac{dl}{dS} = -m\left[(2Z^2-X^2-Y^2)/R^5 + 15\ QXYZ/R^7\right] + n\left[3(YZ-QX)/R^5 + 15\ QXY^2/R^7\right] \tag{29}$$

$$\frac{dm}{dS} = -n\left[3(xZ-QY)/R^5 + 15\ QX^2Y/R^7\right] + l\left[(2Z^2-x^2-Y^2)/R^5 + 15\ QXYZ/R^7\right] \tag{30}$$

$$\frac{dn}{dS} = -l\left[3(YZ-QX)/R^5 + 15\ QXY^2/R^7\right] + m\left[3(xZ-QY)/R^5 + 15\ QX^2Y/R^7\right] \tag{31}$$

with lengths and the coefficient Q in Stormer units. Taking h_2^2/g_1^o ≈ -0.1 then Q = 0.18 Stormer for P = 50.9 BV/c and Q = 0.06 Stormer for P = 5.9 BV/c CR particles. Equations 26-31 can be solved

numerically for CR orbits, using

$$\frac{df}{dS} \Rightarrow \frac{f(S+\Delta S) - f(S)}{\Delta S} \tag{32}$$

and successive approximations[5] (predictor-corrector method). Newton's method[5] of extrapolation was found to give larger errors than successive approximations, where

$$err = l^2 + m^2 + n^2 - 1. \tag{33}$$

Some solutions indicate that orbits from zero assymptotic latitude, ($z = 0$, with $n = 0$,) are deflected by the quadrupole term so as to impact near the dip equator for this field model. Such orbits have been more extensively studied by Ruth Gall[6] using a similar set of equations.

If Q is set equal to zero, the resulting equations for orbits in a dipole field are exactly those solved by Thomas Kelsall,[1] using the Runge-Kutta technique and various initial conditions with $n = 0$ and $R = 10$ Störmer.

---

[5] Margenau, H., and Murphy, G. M., The Mathematics of Physics and Chemistry, Van Nostrand, pp. 482-491, (1956).

[6] Gall, R., J. Geophys. Res. 65, 3545, (1960).

V. D. Effect of the Equatorial Ring Current

The magnetic field above the ionosphere includes the fields of some systems of electric currents flowing in the neighborhood of the earth. A simplification of the field[7] of the equatorial ring current (ERC) will now be used to calculate the order of magnitude of the ERC's contribution to the total deflection of CR particles by the geomagnetic field. In the region near the equator, the ERC field has opposite directions, approximately, inside and outside the current-ring. This decreases the field below the dipole field value over a region near the ring but inside it, $r<r_2$, and increases the field outside the ring, $r>r_2$. In this calculation it will be assumed that for $r<r_1$ the field is nearly the dipole value B_1, for $r_1<r<r_2$ it is $B_1\ b<B_1$, and for $r>r_2$ it is $B_1\ a>B_1$. This approximation fits the values of Akasofu, et al[7] fairly well.

The radius of curvature for a particle of rigidity P is $R = P/B$, so that deflection

$$d\theta = \frac{ds}{R} = \frac{Bds}{P} \quad . \tag{34}$$

In the equatorial plane of a dipole field $B = B_o\ (r_o/r)^3$ so the total deflection for equatorial CR orbits is

$$\Delta\theta = \frac{B_o r_o^3}{P} \int r^{-3}\ ds \tag{35}$$

where $(ds)^2 = (rd\phi)^2 + (dr)^2$. (36)

To get the order of magnitude of the $\Delta\theta$ produced by the ERC field let us take an orbit which is radially directed as it passes the ring, r_2, and assume $ds \approx dr$ for $r_1<r<r_3$. Without the

[7] Akasofu, S.I., Cain, J.C., and Chapman, S., J. Geophys. Res. 66, 4013, (1961).

ERC field the deflection suffered by a CR while traversing from r_3 to r_1 is then

$$\Delta\theta \approx \frac{B_o r_o^3}{P} \int_{r_3}^{r_1} r^{-3}\, dr$$

$$\Delta\theta \approx \frac{B_o r_o^3}{2P}\left(\frac{1}{r_3^2} - \frac{1}{r_1^2}\right) \tag{37}$$

and with the ERC it is

$$[\Delta\theta]_{ring} \approx \frac{B_o r_o^3}{P}\left\{\int_{r_3}^{r_2} a r^{-3} dr + \int_{r_2}^{r_1} b r^{-3}\, dr\right\}$$

$$\approx \frac{B_o r_o^3}{2P}\left\{a\left(\frac{1}{r_3^2} - \frac{1}{r_2^2}\right) + b\left(\frac{1}{r_2^2} - \frac{1}{r_1^2}\right)\right\}. \tag{38}$$

The deflections within the two regions in eq. 38 are almost equal and opposite. Various reasonable values for a, b, r_1, r_2 and r_3, chosen to fit the approximate ERC field[7] make $[\Delta\theta]$ring of eq. 38 differ from $\Delta\theta$ of eq. 37 by as much as 2^o eastward or westward, for $P = P_c = 15$ BV/c. This shift will be smaller for $P \rangle P_c$. Such a shift will shift the direction A of the axis of CR anisotropy by the same few degrees, if unaccounted for in eq. V-1. Since A has been determined only correct to within about 20^o the 2^o shift can be ignored.

Using a closer approximation to Akasofu, Cain and Chapman's approximate values for the ERC field, Dr. Untiedt[8] has more elaborately calculated the shift of the impact point of a 25 Bev proton moving within the z = 0 plane with Störmer parameter $\gamma = -0.7$, due to the introduction of the ERC field in addition to the dipole field. He found a shift of 0.8° towards the east. For $z \neq 0$ he has proposed a set of eight functions to approximate the ERC field within seven different regions of r. These are to be added to eqs. 15-17.

It is probable that the shift caused by the ERC will be larger for CR of P $<$ 15 BV/c which have non-equatorial impact points. For these the amount of the shift can be in latitude as well as longitude. It has been shown[9] that the ERC field does not drastically alter the cutoff rigidity P_c. Latitude shifting by the ERC is therefore small. Even at low P the longitude shifting can only show up in a shift of A. Any such error can be kept near to the plus or minus two degrees found at the equator by weighting the equatorial observed impact times more heavily than the high latitude ones found in the peak impact zone. This weighting will introduce errors larger than 2° however, since ψ_e and ψ_L are only roughly known at $\lambda = 0$.

---

[8]Untiedt, J., Geophysikalisches Institut der Universitat, Gottingen, Germany. (private communication)

[9]Akasofu, S., and Lin, W. C., Trans. A.G.U. 43, 461, (1962).

V. E. Eccentricity of Geomagnetic Field

The fact that the geomagnetic field is rather well represented by an eccentric dipole manifests itself in that the magnetic quantities, H, Z and field-dependent quantities P_c, n_1, ϕ_{1LT} undergo one maximum and one minimum as one goes once around the equator. For n_1, ϕ_{1LT} this is confused somewhat by the CRDV in UT,[10] which causes them to undergo a similar cycle as a function of longitude.[11] The CRDV at the equator was found to be representable (Fig.12) by a vector of length $n_1 \approx .003$ at constant ϕ_{1LT} plus a vector of length $\approx .0012$ which circles in LT as longitude is varied, and in such a sense as to be fixed in UT. The vector of amplitude .0012 is a vector sum of the CRDV vector fixed in UT plus an assymetry vector due to the eccentricity of the dipole. These rotate together in LT at a constant phase difference independent of longitude. The CRDV in UT may therefore be more or less than .12%. In the northern impact zone (at $\lambda = 50^{\circ}$) the circling is at times in such a sense as to deny the existence of a variation in UT, so the field eccentricity evidently dominates.

V. F. Cosmic Ray Anisotropy Fixed in the Galaxy

The regions of the world which show a small CRDV component vector rotating annually in LT in addition to a CRDV component vector fixed in LT are listed in Table V. There agreement within one month is shown that the two vectors were in phase in late July during the IGY. African peak times indicate an earlier phase agreement, but this is to be disregarded since CRDV peak times at Hermanus, where there is a geomagnetic anomaly, often disagreed with expectations and with surrounding stations.

---

[10] Kertz, W., Z. Geophysik 24, 210 (1959).
[11] Kertz, W., private communication, Gottigen (1960).

If the vector rotating in LT and therefore fixed in sidereal time (ST) is a true indication of a CR anisotropy outside the solar system, then this anisotropic flux arrived at the earth's orbit from 14 hrs right ascension (RA) during the IGY. That is, it arrived from a direction in the galaxy which lay between the galactic center and the direction away from which the sun is moving due to galactic rotation. This direction is determined by taking A = 18 hrs and the two flux vectors coming from the same direction on July 21, that is, from the direction to the sun on October 21, which is 13.7 hrs RA. A different value for A results in an equally different direction for the galactic CR anisotropy.

It is possible that a boundary between the interplanetary and galactic magnetic fields exists with a "head" on the side toward which the sun is moving and a "tail" on the opposite side, similar in appearance to the geomagnetic envelope.[12] As discussed on pages 71, 72, this could provide the excess CR flux from the tail side. This component would be added to a component perhaps from the galactic center or elsewhere[13,14] to provide the anisotropy from 14 hrs RA.

The eccentricity of the earth's orbit might conceivably produce the annual change in CRDV in LT, but it evidently does not. In July, when the two CRDV vectors are in phase so that the resultant amplitude n_1 is largest, the earth is near aphelion. If the annual change in CRDV in LT were due to changing distance to the sun then n_1 might be expected to be largest near perihelion. The perihelion and aphelion distances differ by only 4%.

The obliquity of the earth's orbit with respect to the solar equator is another conceivable cause of the observed annual

---

[12] Beard, D. B. and Jenkins, E. B., J. Geophys. Res. 67, 4895, (1962).
[13] Rossi, B., Suppl. Nuovo Cimento 2, X, 275 (1955).
[14] Korff, S. A., Amer. Sci. 45, 293, (1957).

change in CRDV. This effect might be expected to cause two maxima and two minima per year in n_1. This would produce a small CRDV vector component which rotates semi-annually in LT, and not the annually rotating one. Such a semi-annually rotating vector of amplitude $\approx$ .0005 is shown by several groups of stations. This very small effect may indicate that the CR anisotropy in the solar system depends slightly on solar latitude, perhaps as a cosine function for example.

VI. Conclusions

The amplitude and the local time of maximum (peak time) of the cosmic ray nucleon diurnal variation (CRDV) depend on latitude, longitude and month. Relative maxima and minima on their isoplot contour maps correspond to relative extremums in the geomagnetic field at or near the earth's surface, and in the geomagnetic cutoff rigidity. The CRDV map contours indicate that the geomagnetic dipole and quadrupole moments and the eccentricity of the geomagnetic field are significant in influencing the anisotropic part of the cosmic ray flux.

When the amplitudes n_1 of the CRDV of all northern and equatorial neutron monitors are averaged over groups of months within the IGY, and some pairs of stations with similar values of cutoff rigidity P_c are averaged together to smooth the data, then two peaks of n_1 persist at approximately P_c = 1 and 4 BV/c. These are related to a single peak of k(P) in the differential spectrum (4/3) k(P) cos ϕ for the cosmic ray anisotropy. Here k(P) is a fraction of the isotropic cosmic ray flux at infinity and ϕ is the assymptotic longitude with respect to an axis of anisotropy. P is magnetic rigidity, or momentum per unit charge. The k(P) peak lies between P = 3.8 and 5.7 BV/c, and k(P) = 0.0039 $\pm$ 0.002 for $P > 6$ BV/c. At $P < 3.8$ BV/c spectral cutoff, k(P) = 0.

A meaningful semi-diurnal variation in cosmic radiation is found to be strongly dependent upon position on the earth. It indicates that the cosmic ray anisotropy is more narrowly collimated than a cos ϕ dependence. A significant part of the observed semi-diurnal variation is dependent on universal time.

The CRDV is primarily caused by an anisotropy in the cosmic ray flux introduced by some mechanism within the solar

system. This anisotropic flux arrives from an assymptotic direction 75^{o} to 100^{o} east of the sun, in the ecliptic plane. A small CRDV component dependent on local time is introduced by the increased geomagnetic field on the sunward side of the earth, so as to show an apparent excess flux from opposite the sun. If this component were subtracted, the direction of anisotropy stated above would be decreased.

A component of the CRDV is dependent on universal time, with amplitude of about 0.1%. Another component of the CRDV of amplitude 0.1% appears to be dependent on sidereal time, and to be caused by a cosmic ray anisotropic flux in the galaxy which came from 14 hours right ascension during the IGY.

It is possible to ascribe most, if not all, of the spatial variations in cosmic ray diurnal intensity variation on the earth's surface to the spectrum of the cosmic ray anisotropy and to the dipole and higher multipole geomagnetic field components. This suggests that, insofar as the immediate vicinity of the earth is concerned, the external geomagnetic field is fairly satisfactorily represented in its interaction with cosmic rays by the multipole coefficients obtained by analyzing the surface field.

Several mechanisms appear responsible for the cosmic ray anisotropy. Further CRDV investigations should attempt to separate various sources and find their individual spectra and rigidity-dependent axial directions, rather than seek a single source direction.

Bibliography

Alfven, H., Tellus 6, 232-253.

Akasofu, S-I and Chapman, S., J. Geophys. Res. 66, 1321-1350 (1961).

Akasofu, S-I and Lin, Trans. Am. Geophys. Union 43, 461 (1962).

Arthur, W., The Cosmic Ray Increase of 1960, (Ph.D. thesis, NYU).

Bartels, J., Terr. Magn. and Atmos. Elec. 41, 225 (1936).

Beard, D. B., J. Geophys. Res. 65, 3559 (1960).

Beard, D. B. and Jenkins, E. B., J. Geophys. Res. 67, 4895 (1962).

Bercovitch, M., Bull. Am. Phys. Soc. 8, 7, (23 Jan. 1963).

Bethe, H. A., Korff, S. A. and Placzek, G., Phys. Rev. 57, 573 (1940).

Brumberg, E. A., Tellus 8, 216 (1956).

Brumberg, E. A. and Dattner, A., Tellus 5, 135, 269 (1953).

Cain, J. C., Shapiro, I. R., Stolarik, J. D. and Heppner, J. P., J. Geophys. Res. 67, 5055, (1962).

Chapman, S., Akasofu, S-I. and Cain, J. C., J. Geophys. Res. 66, 4013, (1961).

Chapman, S. and Bartels, J., Geomagnetism, Oxford, (1940).

Cogger, L. L., Atomic Energy of Canada Ltd-1104, Chalk River, Ontario, CRGP-965.

Compton, A. H. and Getting, I. A., Phys. Rev. 47, 817 (1935).

Conforto, A. N. and Simpson, J. A., N. Cim. 6, 1952 (1959).

Cosmic Ray Intensity During the IGY, National Committee for the IGY, Science Council of Japan, Tokyo (1960).

Cotten, D., J. Geophys. Res. 66, 2522 (1961).

Dattner, A. and Venkatesan, D., Tellus 11, 116 (1959).

Dattner, A. and Venkatesan, D., Tellus 11, 239 (1959).

Dessler, A. J., Ahluwalia, H. S. and Gottlieb, B., J. Geophys. Res. 67, 3553, (1962).

Dorman, L. I., Cosmic Ray Variations, State Publ. House for Technical and Theor. Lit., Moscow 1957.

Duggal, S. P., Nagashima, K, and Pomerantz, M. A., J. Geophys. Res. 66, 1970 (1961).

Dwight, K., Phys. Rev. 78, 40 (1950).

Elliot, H., Progress on Cosmic Ray Physics 1, p. 453, North Holland Publishing Co., 1952.

Elliot, H., Phil. Mag. 5, 601-619 (1960).

Elliot, H. and Dolbear, D. W. N., J. Atmos. and Terres. Phys. 1, 205 (1951).

Epstein, P. S., Phys. Rev. 53, 862 (1938).

Finch, H. F. and Leaton, B. R., Roy. Astron. Soc. Mon. Not., Geophys. Suppl. 7, 314 (1957).

Firor, J., Phys. Rev. 94, 1917 (1954).

Firor, J., Fonger, W. H. and Simpson, J. A., Phys. Rev. 94, 1031 (1954).

Forbush, S. E., Terr. Magn. 42, 1 (1937).

Forbush, S. E. and Venkatesan, D., J. Geophys. Res. 65, 2213 (1960).

Gall, R., J. Geophys. Res. 65, 3545 (1960).

Goldstein, H., Classical Mechanics, Addison-Wesley (1950).

Heppner, J. P., Ness, N. F., Scearce, C. S. and Skillman, T. L., J. Geophys. Res. 68, 1 (1963).

Hess,, V. F. and Graziadei, H. T., Terr. Magn. 41, 9 (1936).

Hurley, J., Doctoral Thesis, New York University (1961).

Hurley, J., "Interaction Between the Solar Wind and the Geomagnetic Field," NYU Project Report (March 1, 1961).

Janossy, L., Zeit. Phys. 104, 430 (1937).

Jory, F. S., Phys. Rev. 103, 1068 (1956).

Kane, R. P., Proc. Indian Acad. Sci. 52, 69-79 (1960).

Kane, R. P, Indian J. Phys. 35, 213 (1961).

Katzman, J., Can. J. Phys. 37, 1207 (1959).

Katzman, J., Can. J. Phys. 39, 1477 (1961).

Katzman, J. and Venkatesan, D., Can. J. Phys. 38, 1011 (1960).

Kelsall, T., J. Geophys. Res. 66, 4047 (1961).

Kertz, W., Z. Geophysik 24, 210 (1959).

Kodama, M, Kondo, I. and Wada, M., J. Sci. Res. Inst. 51, 138 (1957) Japan.

Korff, S. A., Amer. Scientist 45, 293 (1957).

Lemaitre, G. and Vallarta, M. S., Phys. Rev. 43, 87 (1933).

Lemaitre, G. and Vallarta, M. S., Phys. Rev. 50, 49 (1936).

Lemaitre, G. and Vallarta, M. S., Phys. Rev. 49, 719 (1936).

Lust, R., Phys. Rev. 105, 1827 (1957).

Malinfors, Arkiv. Mat. Astron. Fys, 30A, 12 (1944).

Malinfors, Arkiv. Mat. Astron. Fys. 32, 8 (1945).

Margenau, H. and Murphy, G. M., The Mathematics of Physics and Chemistry, Van Nostrand, Pp. 482-491 (1956).

McCracken, K. G., Doctoral Thesis, University of Tasmania, 1958.

Messerschmidt, W., Naturforschung 15a, 734 (1960).

Millikan, R. A. and Neher, Phys. Rev. 47, 204 (1935); 50, 15 (1936)

Montgomery, D. J. X., Cosmic Ray Physics, p. 351, Princeton (1949).

Nagashima, K., Potnes, V. R. and Pomerantz, M. A., Nuovo Cimento 19, 292-330 (1961).

Parsons, N. R., J. Geophys. Res. 65, 3159 (1960).

Parsons, N. R., Tellus 12, 4 (1960).

Proceedings of the International Conference on Cosmic Rays and the Earth Storm II, Joint Sessions, J. Phys. Soc. Japan 17, Suppl. A-II, 379-504, (1962).

Quenby, J. J. and Thambyahpillai, Phil. Mag. 5, 585.

Quenby, J. J. and Webber, W. R., Phil. Mag. 4, 90 (1959).

Quenby, J. J. and Webber, W. R., Phil. Mag. 4, 654 (1959).

Rao, U. R., McCracken, K. G. and Venkatesan, D., J. Geophys. Res. 67, 3590 (1962).

Rao, A. and Sarabhai, V., Proc. Roy. Soc. 263, 101, 118, 127 (1961).

Rose, D. C., Adv. In Electronics and Electron Phys. 9, 129 (1957).

Rosser, W. G. V., O'Brien, B. J., Van Allen, J. A., Frank, L. A. and Laughlin, C. D., J. Geophys. Res. 67, 4533 (1962).

Rossi, B., Suppl. Nuovo Cimento 2, X, 275 (1955).

Rothwell, P., J. Geophys. Res. 64, 2026 (1959).

Sandstrom, A. E., Am. J. Phys. 29, 187 (1961).

Sandstrom, A. E., Dyring, E. and Lindgren, S., Tellus 12, 332 (1960).

Sandstrom, A. E., Dyring, E. and Lindgren, S., Nature 187, 1099 (1960).

Sandstrom, A. E., and Lindgren, S., Ark. Fys. 16, No. 12 (1959).

Sarabhai, V. and Bhavsar, P. D, Supp. Nuovo Cim. 8, 299 (1958).

Sarabhai, V., Disai, U. D. and Venkatesan, D., Phys. Rev. 99, 1490, (1955).

Sarabhai, V. and Nerurkar, N. V., Time Variation of the Primary Cosmic Rays, Ann. Rev. Nuc. Sci. 6, 1 (1956).

Schluter, J., E. Naturforsch 62, 613 (1951).

Schonland, B. F. J., Delatizky, B. and Gaskell, J., Terr Magn. 42, 137 (1937).

Schwachheim, G. J. Geophys. Res. 65, 3149 (1960).

Simpson, J. A., Phys. Rev. 83, 1175 (1951).

Simpson, J. A., Fonger, W. and Trieman, S. B., Phys. Rev. 90, 934 (1953).

Singer, S. F., Progress in Cosmic Ray Physics, 4, p. 203, North Holland Publishing Co., 1958.

Stern, D., J. Geophys. Res. 67, 2133 (1962).

Stormer, C., Astrophys. Norv. 1, 1 (1936).

Stormer, C., The Polar Aurora, Oxford 1955.

Thompson, J. L., Phys. Rev. 54, 93 (1938).

Thompson, D. M., Phil. Mag. Vol. 6, #64, 573 (1961).

Trieman, S. B., Phys. Rev. 86, 917 (1952).

Vallarta, M. and Godart, O., Rev. Modern Phys. 11, 180 (1939).

Vestine, E. H., Transactions A.G.U. 41, 4 (1960).

Willers, F. A., Practical Analysis, p. 345, Dover 1947.

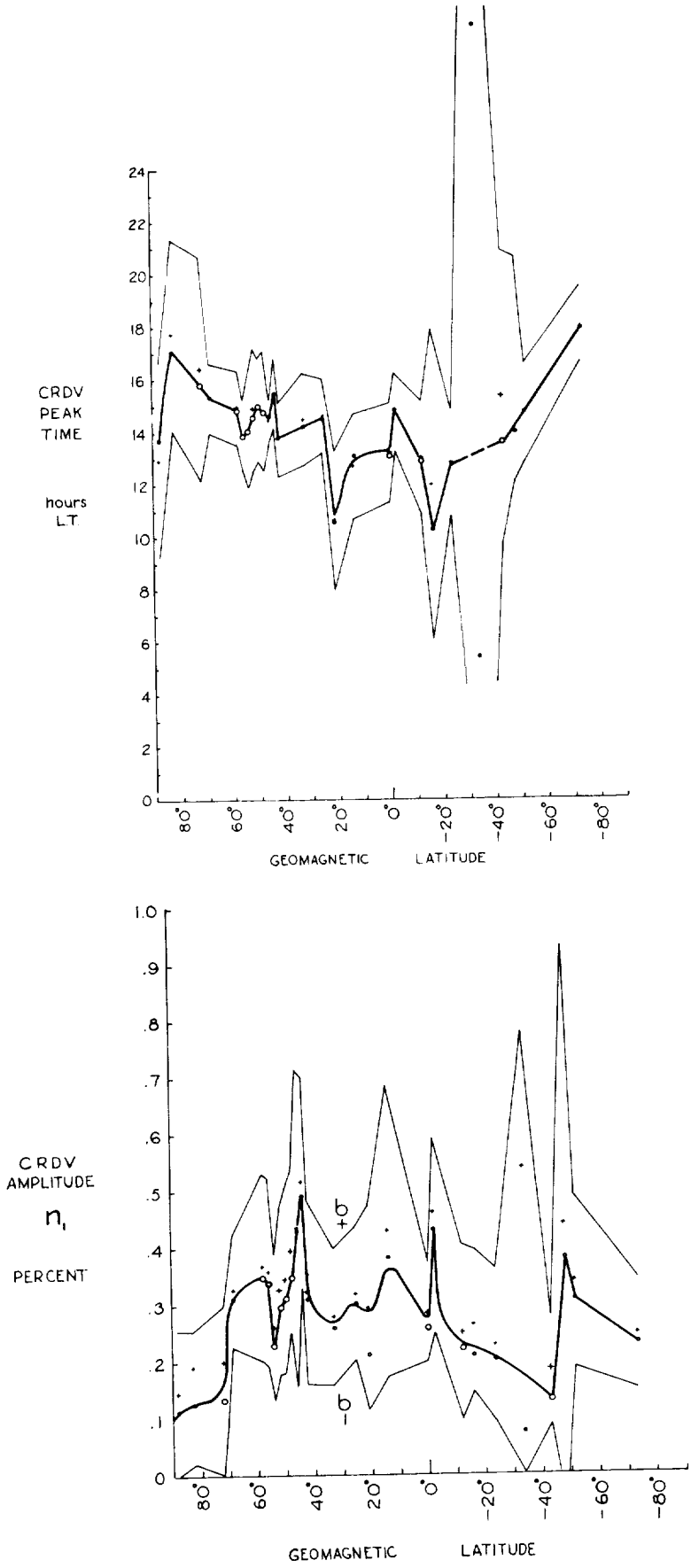

Fig. 1. CRDV AMPLITUDE n_1 AND PEAK TIME VERSUS GEOMAGNETIC LATITUDE
Averaged over the year July, 1957 through June, 1958.

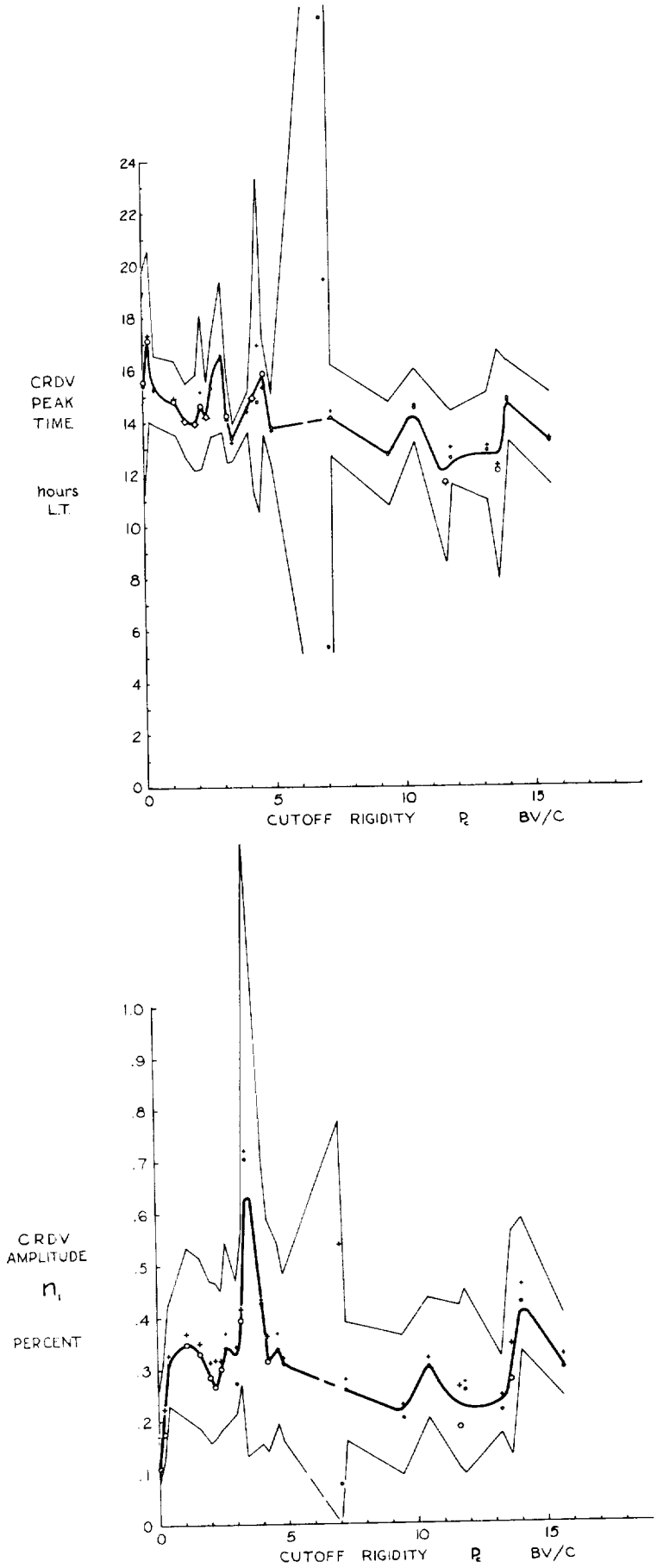

Fig. 2. CRDV AMPLITUDE n_1 AND PEAK TIME VERSUS GEOMAGNETIC CUTOFF RIGIDITY FOR THE ECCENTRIC DIPOLE GEOMAGNETIC FIELD MODEL

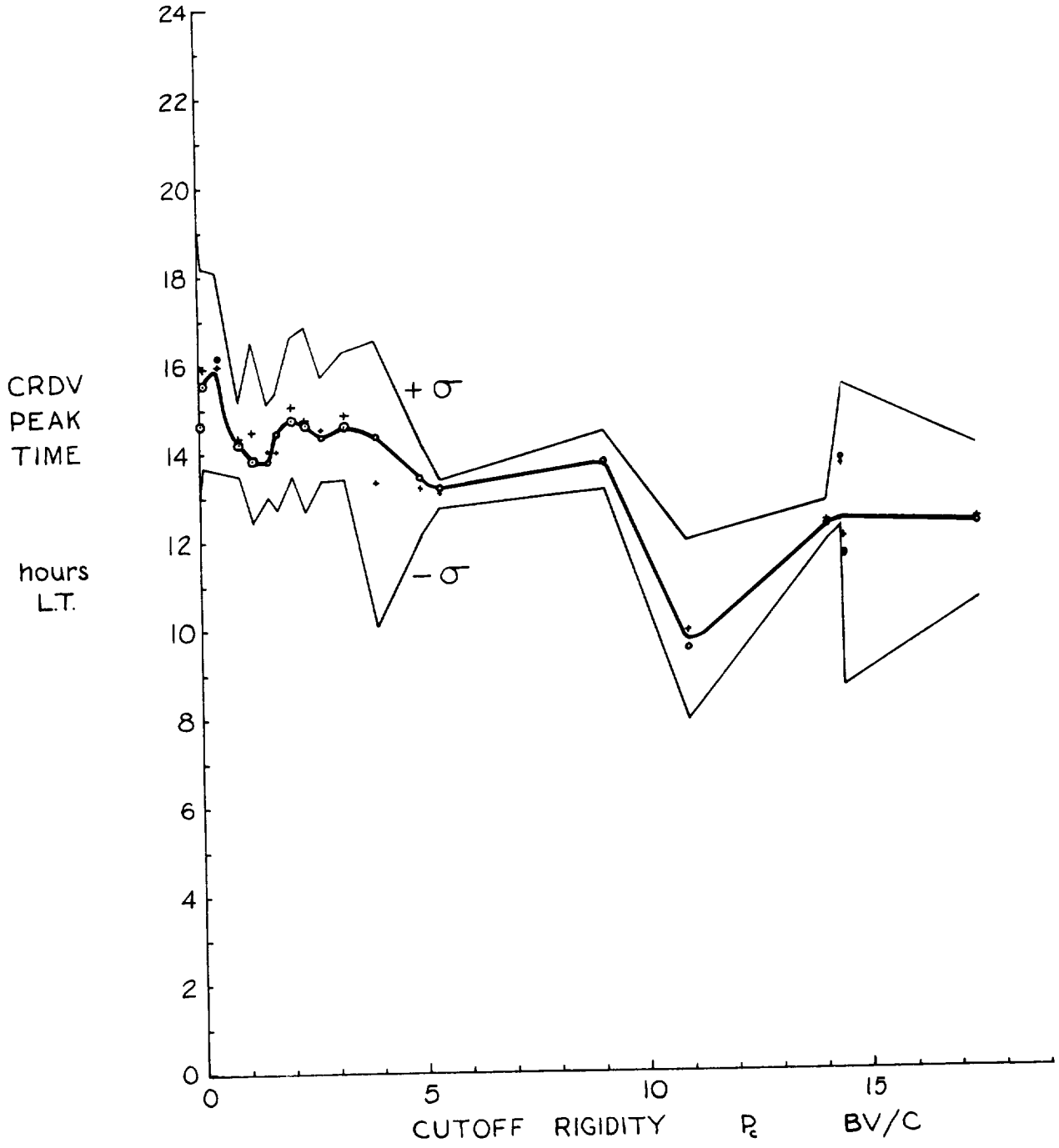

Fig. 3. THE LOCAL TIME OF DIURNAL MAXIMUM (CRDV PEAK TIME) OF THE COSMIC RAY NUCLEON COUNTING RATE PLOTTED AGAINST GEOMAGNETIC CUTOFF RIGIDITY P_c as given by Quenby and Webber. The data shown, from northern and equatorial stations of all altitudes for September, October and November 1957 and 1958, is typical of the entire IGY.

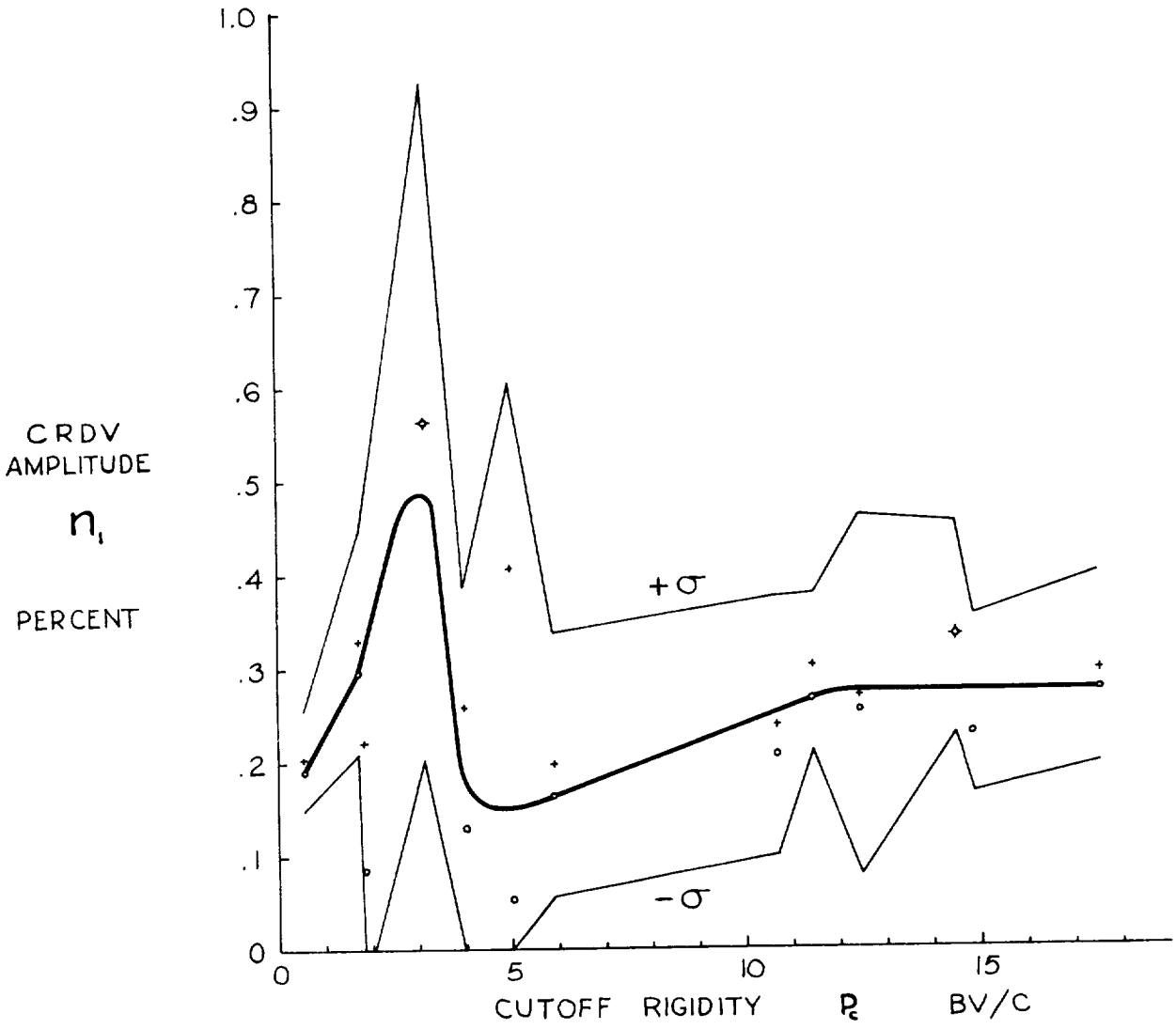

Fig. 4. CRDV AMPLITUDES n_1 IN THE SOUTHERN HEMISPHERE PLOTTED AGAINST GEOMAGNETIC CUTOFF RIGIDITY P_c as given by Quenby and Webber. The data for each station is averaged over at least three of the months September, October, November, 1957 and 1958, and March, April, May, 1958.

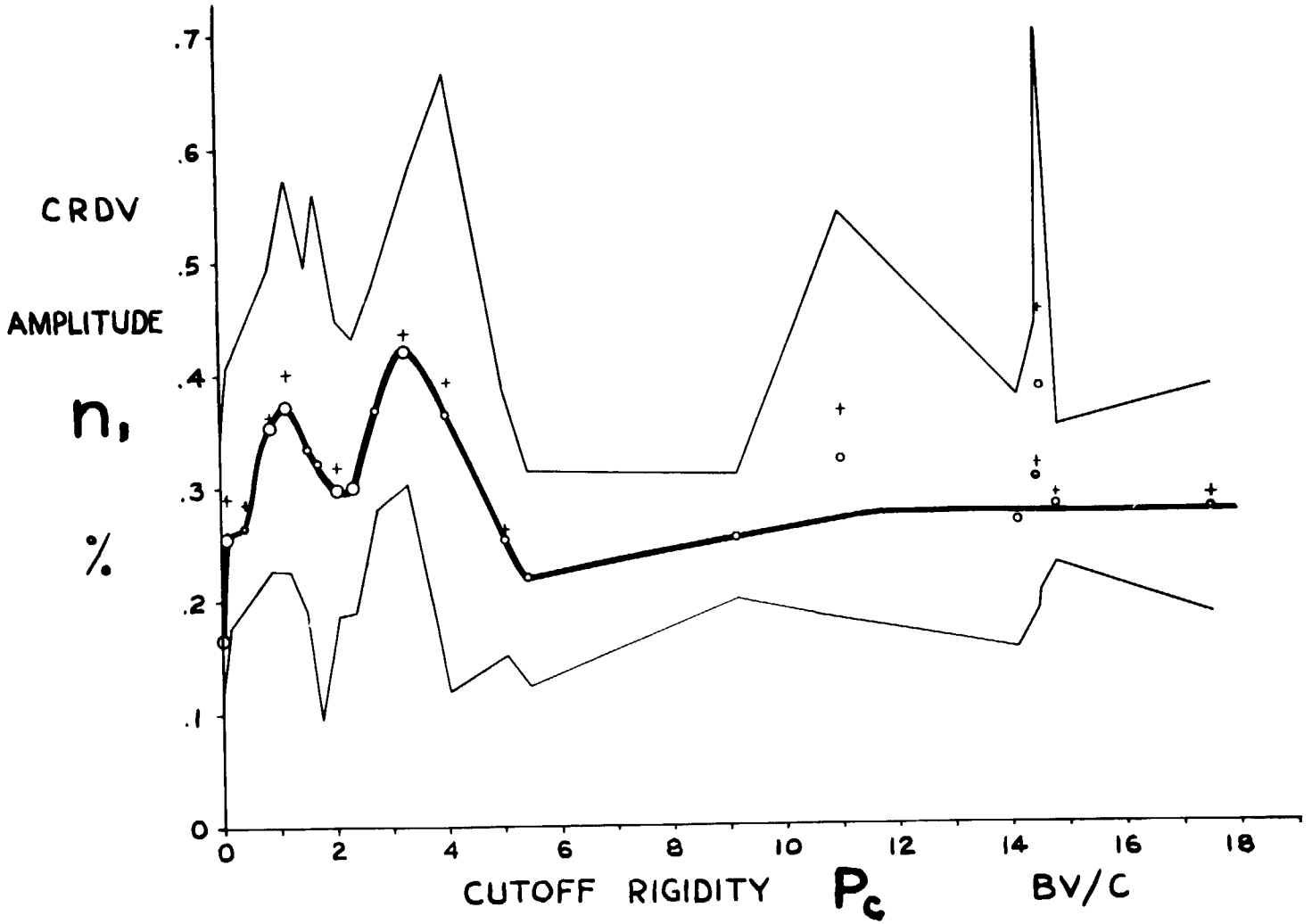

Fig. 5. CRDV AMPLITUDE n_1 VERSUS GEOMAGNETIC CUTOFF RIGIDITY P_c as given by Quenby and Webber. The data shown, from northern and equatorial stations of all altitudes for September, October and November 1957 and 1958, is typical of the entire IGY.

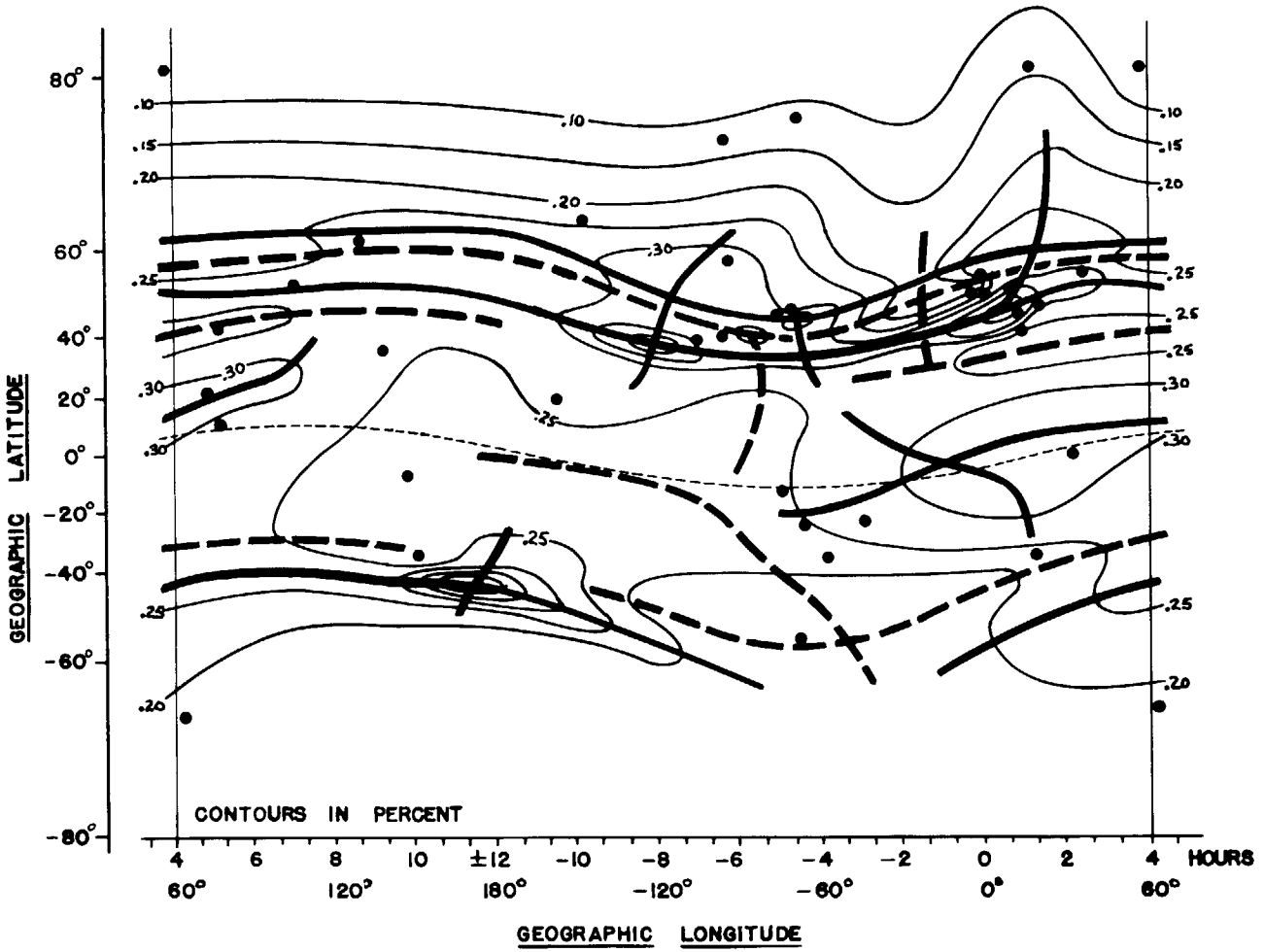

Fig. 6. ISOPLOT MAP OF CRDV AMPLITUDE n_1 averaged over September, October, November, 1957 and 1958 and March, April and May, 1958. Contours are typical of the monthly maps of n_1 for the entire IGY.

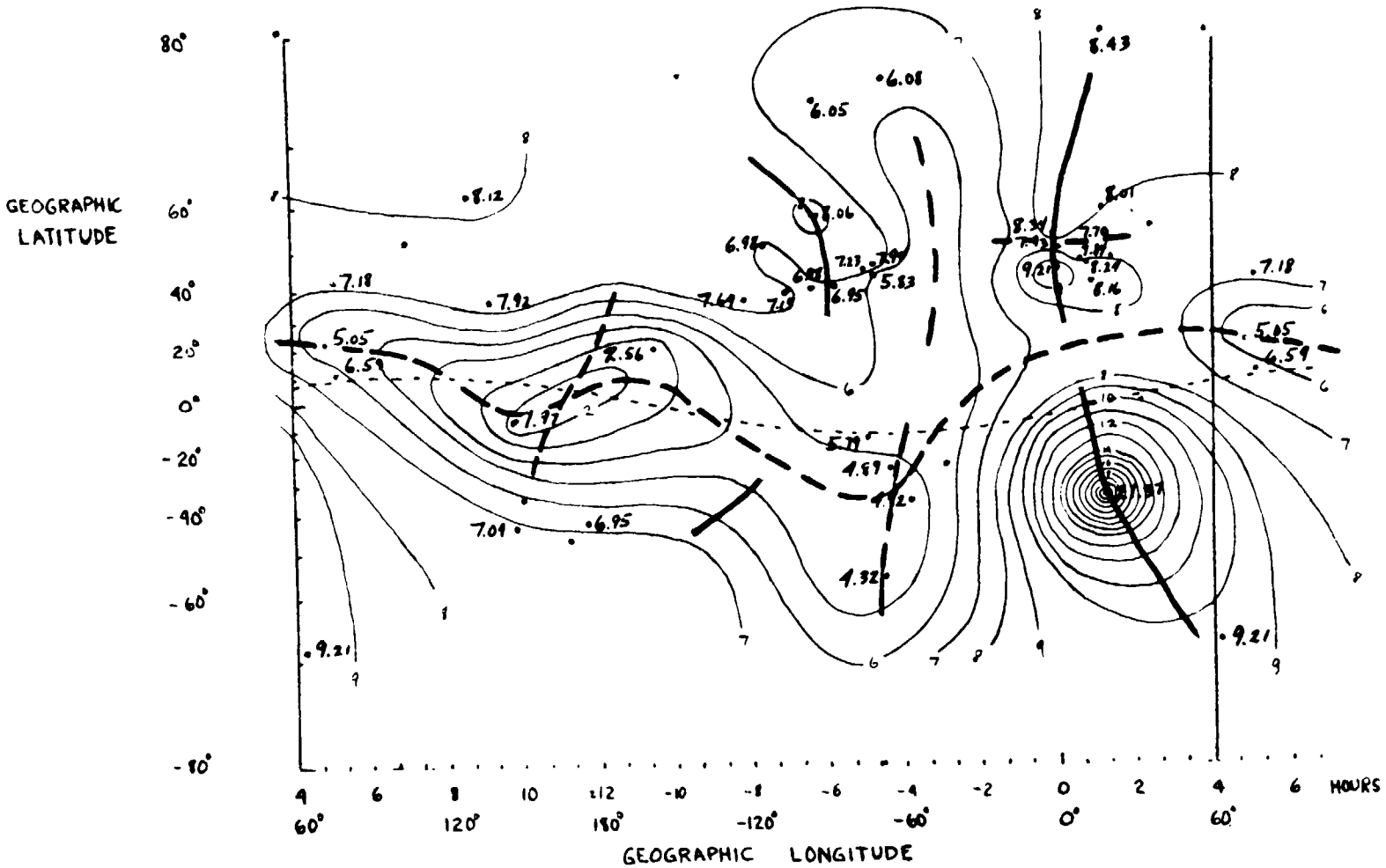

Fig. 7. TYPICAL MONTHLY ISOPLOT MAP SHOWING THE CRDV PHASE ANGLE, that is, the diurnal peak time minus 6 hours, L. T.

SEPT 1957

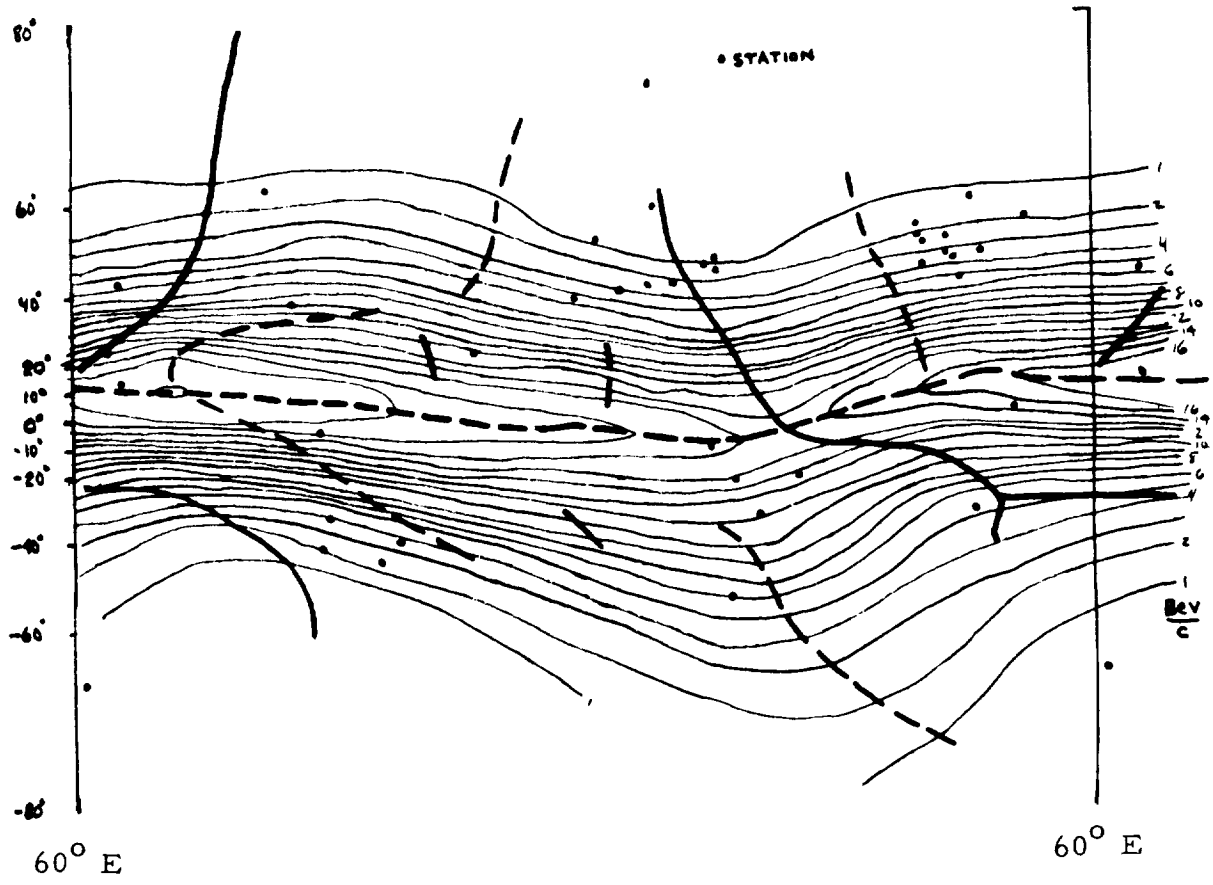

Fig. 8. ISOPLOT MAP SHOWING RELATIVE EXTREMUMS IN THE GEOMAGNETIC CUTOFF RIGIDITY P_c as calculated by Quenby and Webber, in geographic coordinates

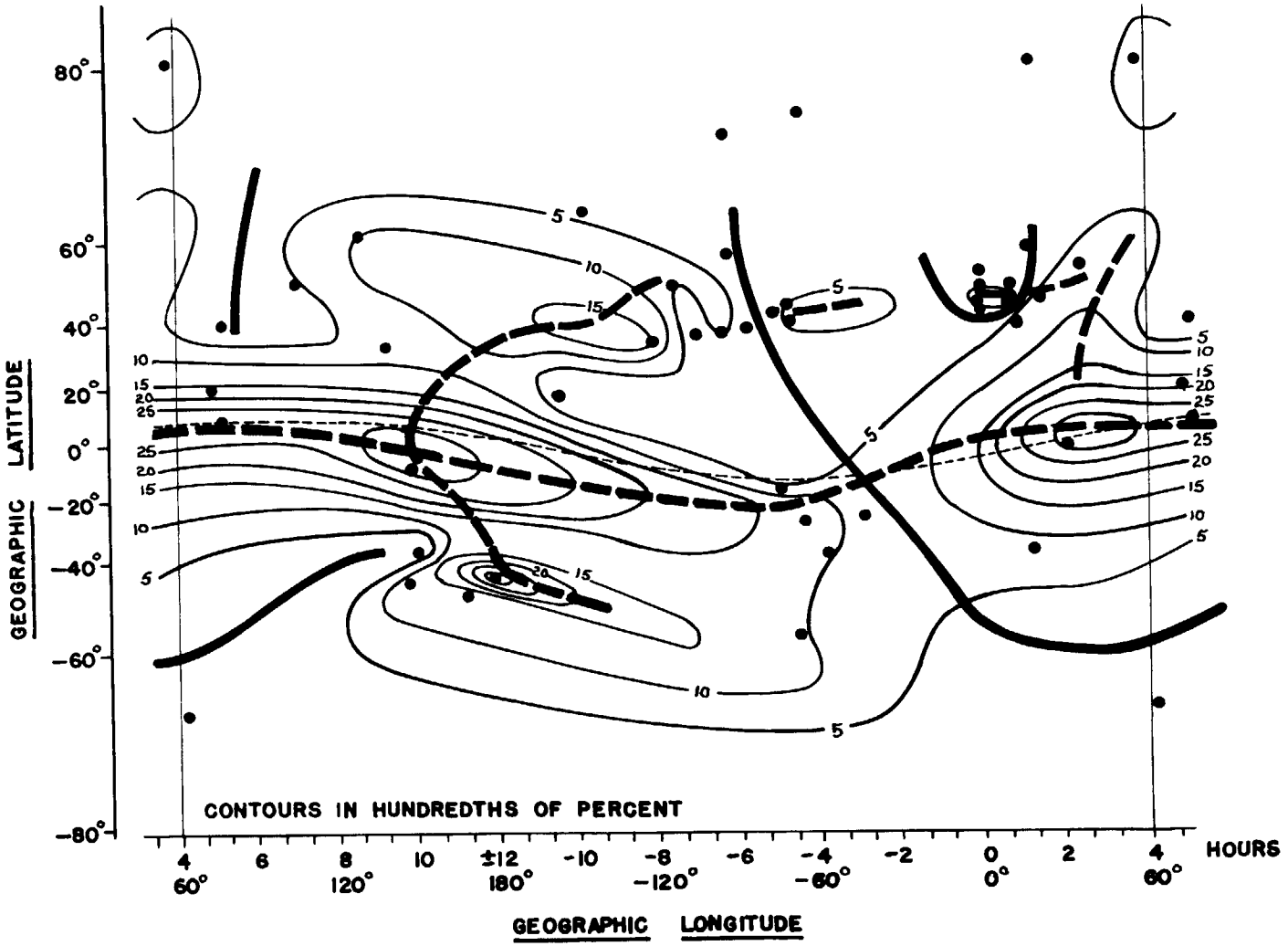

Figure 9: ISOPLOT MAP OF AMPLITUDES OF THE SEMI-DIURNAL VARIATION IN COSMIC RAY NUCLEON COUNTING RATE, averaged over September, October, November, 1957 and 1958 and March, April, and May, 1958. The contours are typical of the monthly maps of n_1 for the entire IGY.

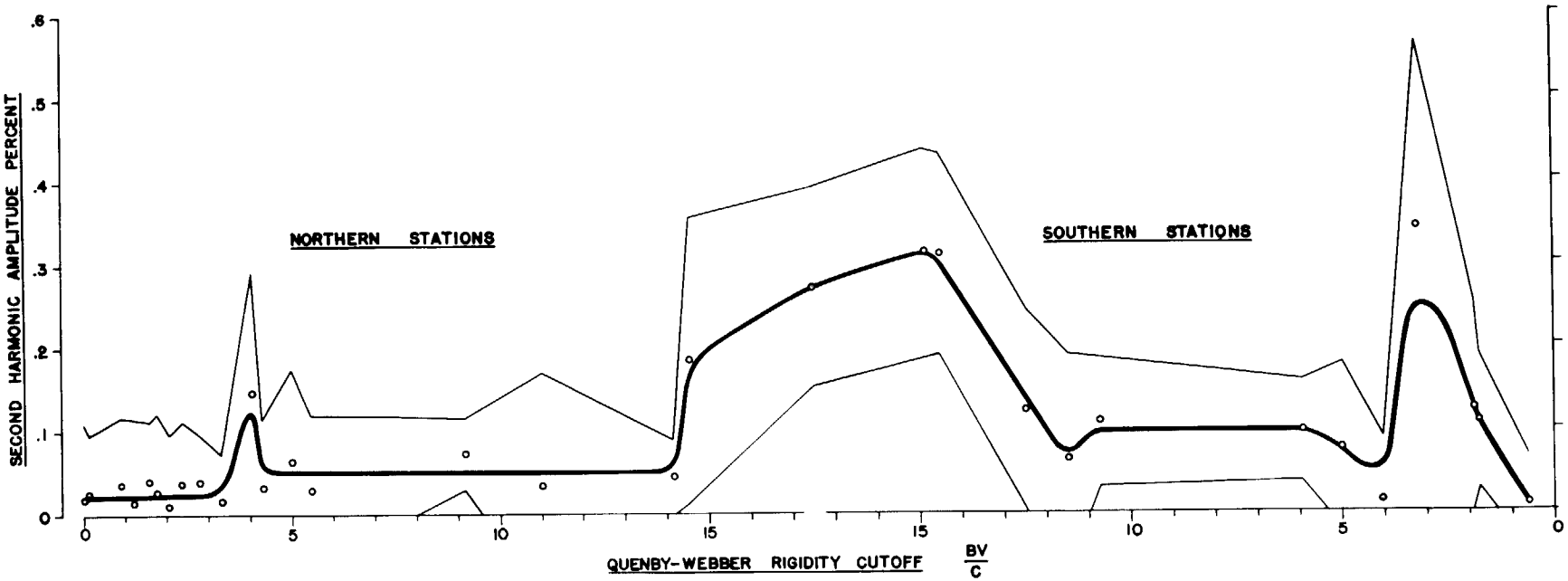

Fig. 10. AMPLITUDE n_2 OF THE SEMI-DIURNAL VARIATION IN COSMIC RAY NUCLEON COUNTING RATE, plotted against Quenby-Webber cutoff rigidity P_c for each hemisphere of the world separately, and placed so as to display the data continuously from North to South. Huancayo is shown on the north (left) side at 14.18 BV/c. The months averaged, September, October, November, 1957 and 1958, and March, April and May 1958, give values typical for the IGY.

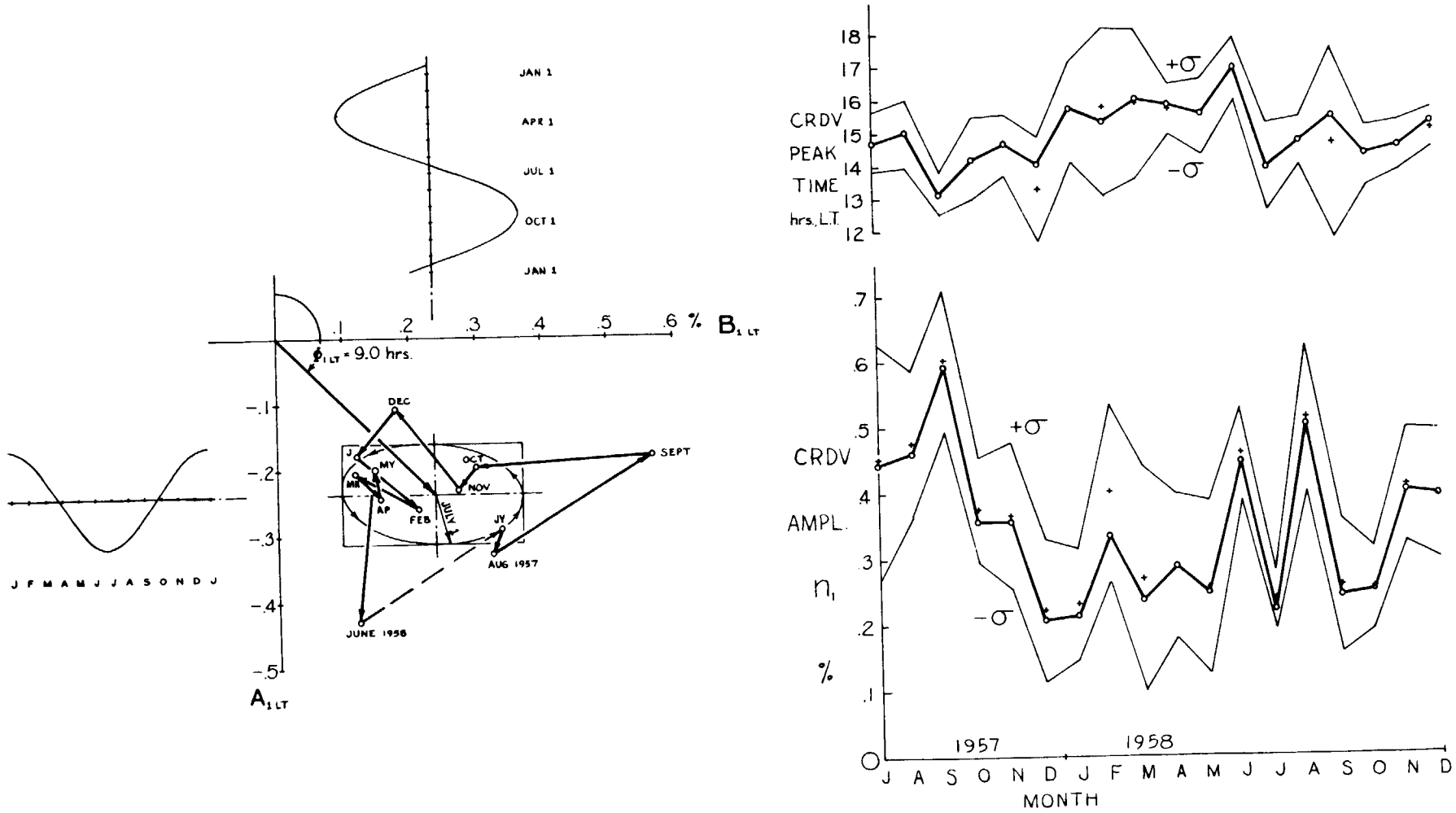

Fig. 11. AN EXAMPLE OF THE ANNUAL VARIATION OF THE CRDV AMPLITUDE AND LOCAL TIME PHASE, and Lissajous-Fourier analysis to determine the amplitude and phase of a CRDV fixed in sidereal time. Data shown is for 9 stations in North America from July 1957 to June 1958.

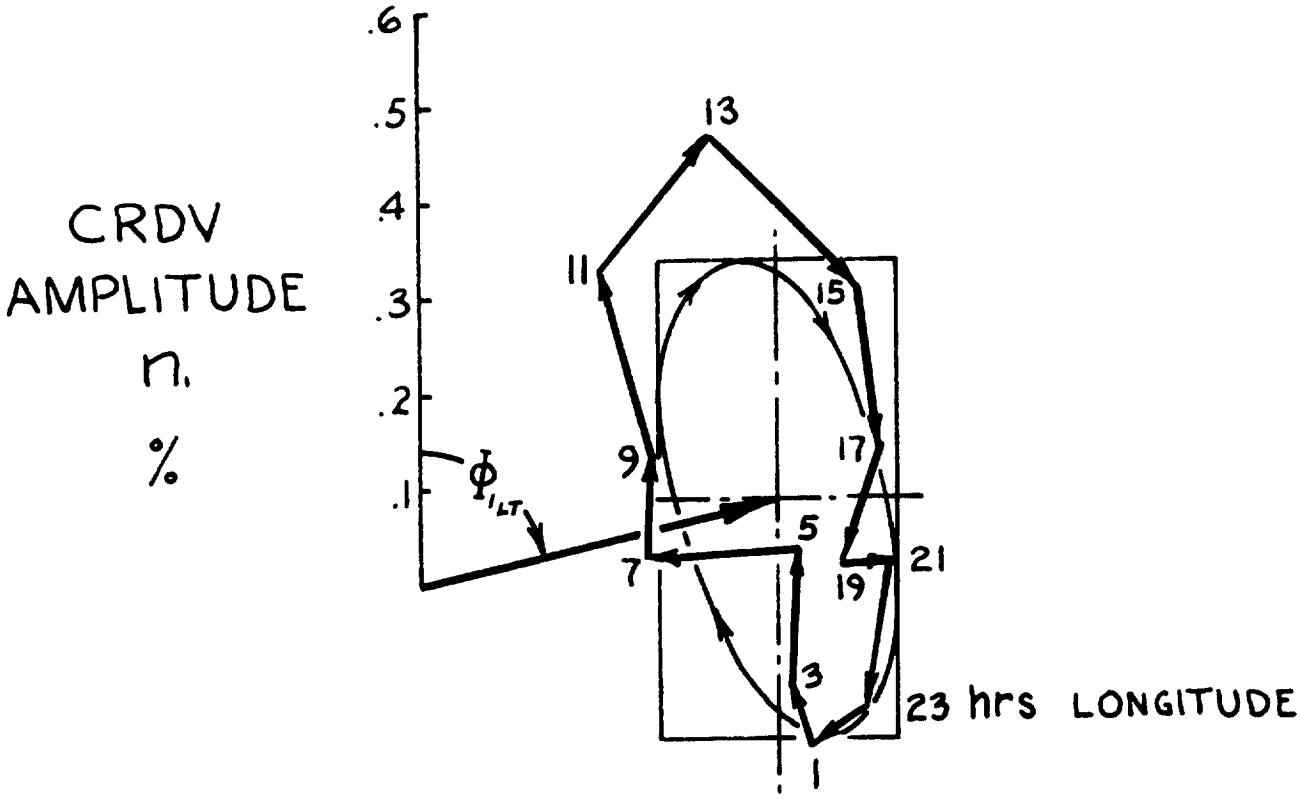

Fig. 12. TYPICAL POLAR PLOT OF THE CRDV AMPLITUDE AND PHASE IN LOCAL TIME. Values shown are read from the amplitude and phase contour maps for September, 1957, at uniform longitude intervals of 2 hours, along the CRDV equator. A Lissajous-Fourier analysis to find a CRDV fixed in Greenwich time is shown.

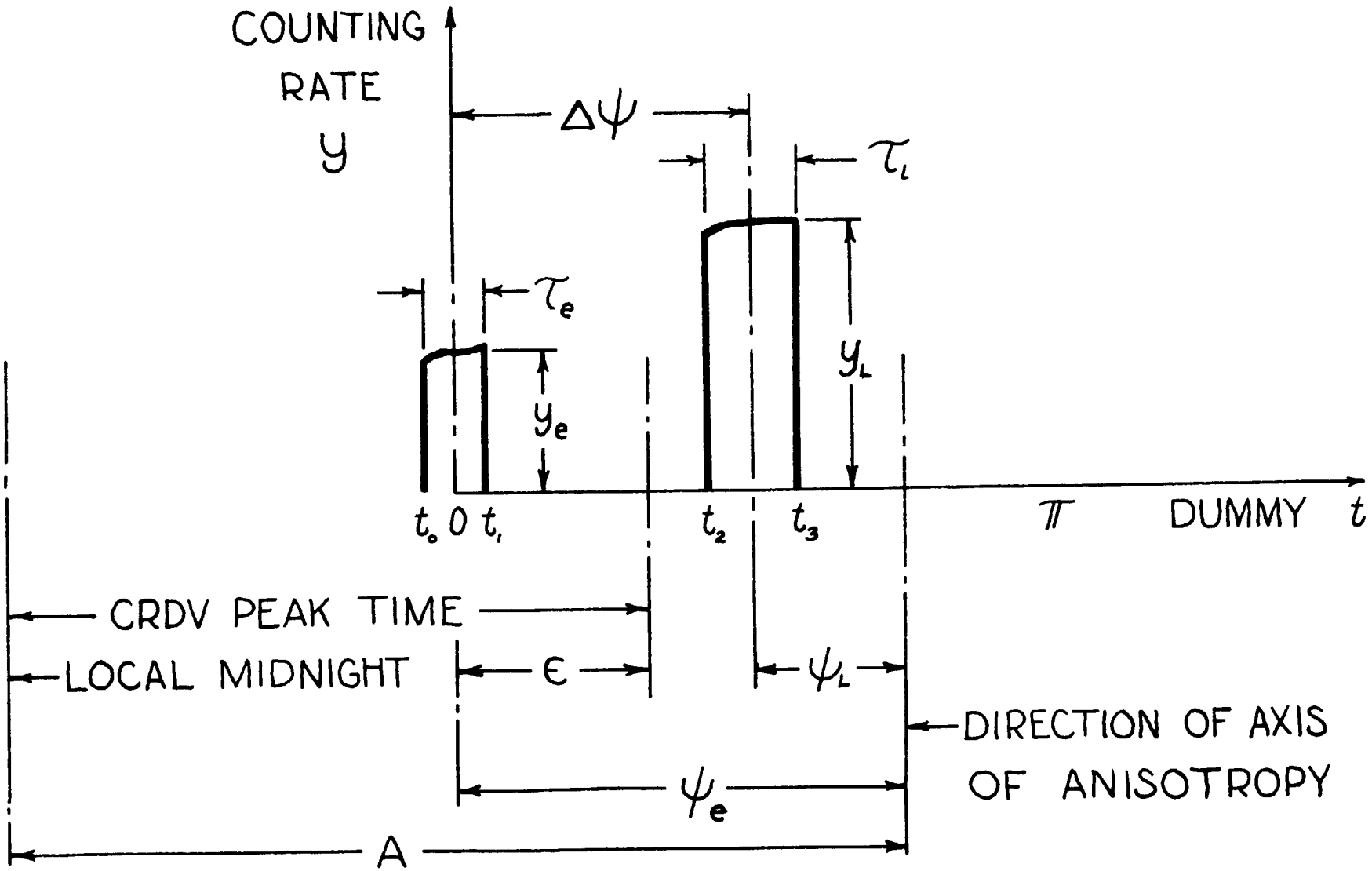

Fig. 13. DOUBLE-PULSE FORM OF DVCR = $y(t, \theta, \alpha)$ SHOWING QUANTITIES USED IN ITS HARMONIC ANALYSIS

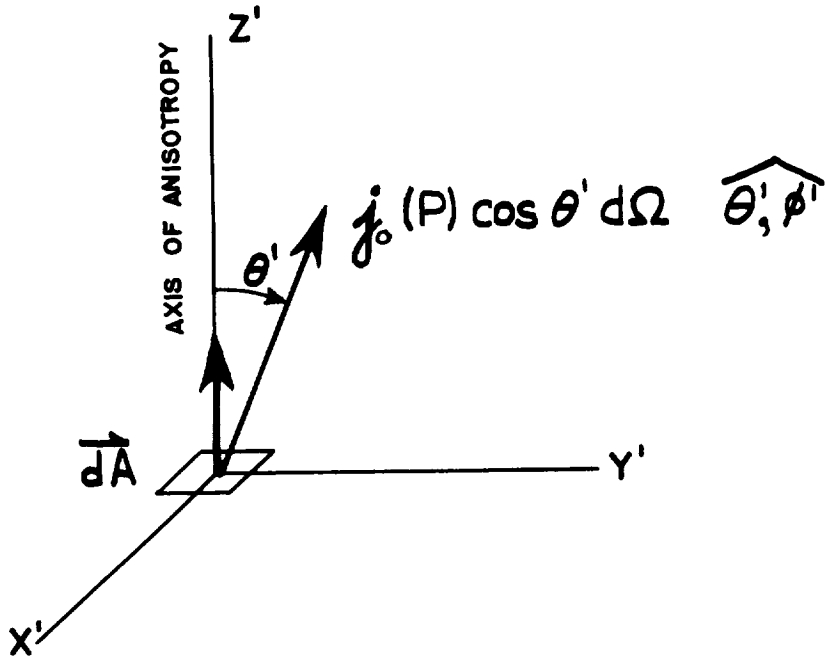

Fig. 14. FLUX VECTOR USED IN ANALYSIS

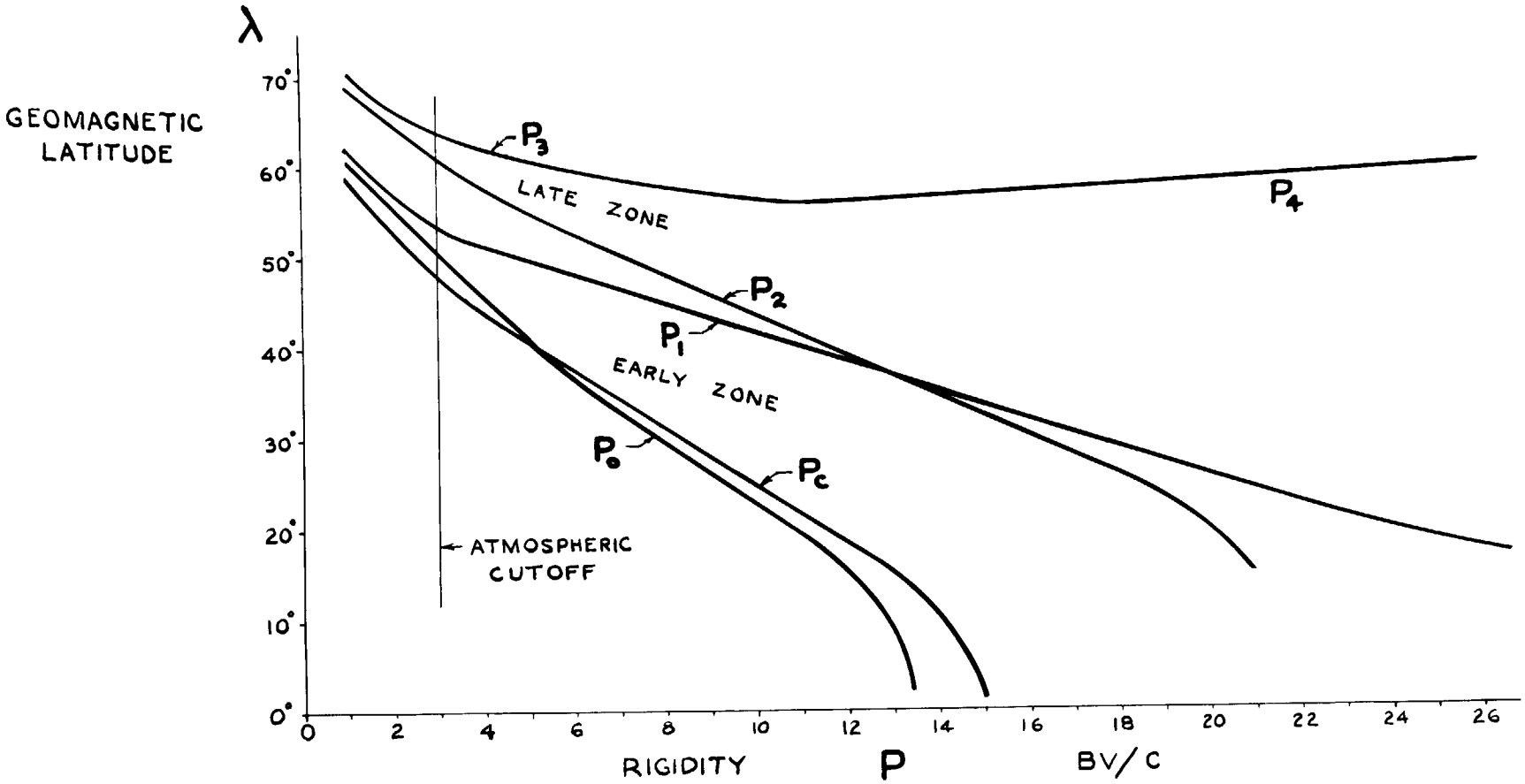

Fig. 15. INTEGRATION LIMITS for rigidity integrals used in this analysis of the CRDV

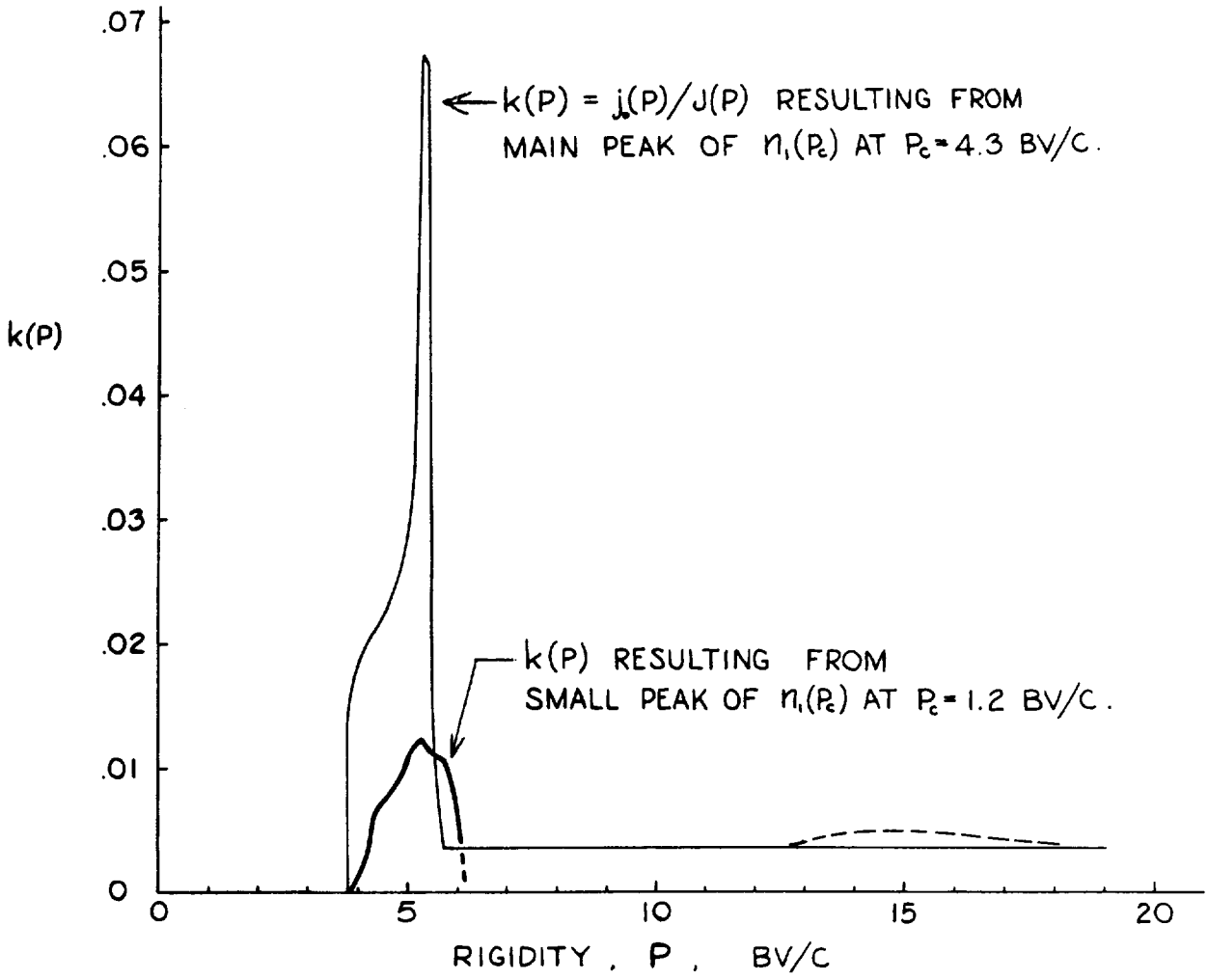

Fig. 16. THE CRDV DIFFERENTIAL SPECTRUM k(P) given as the anisotropic cosmic ray flux in the direction of the axis of anisotropy, per cm^2, per steradian, per second, per unit rigidity interval, divided by the isotropic cosmic ray flux. The anisotropic flux is taken to fall off as the cosine of the angle to the axis of anisotropy.

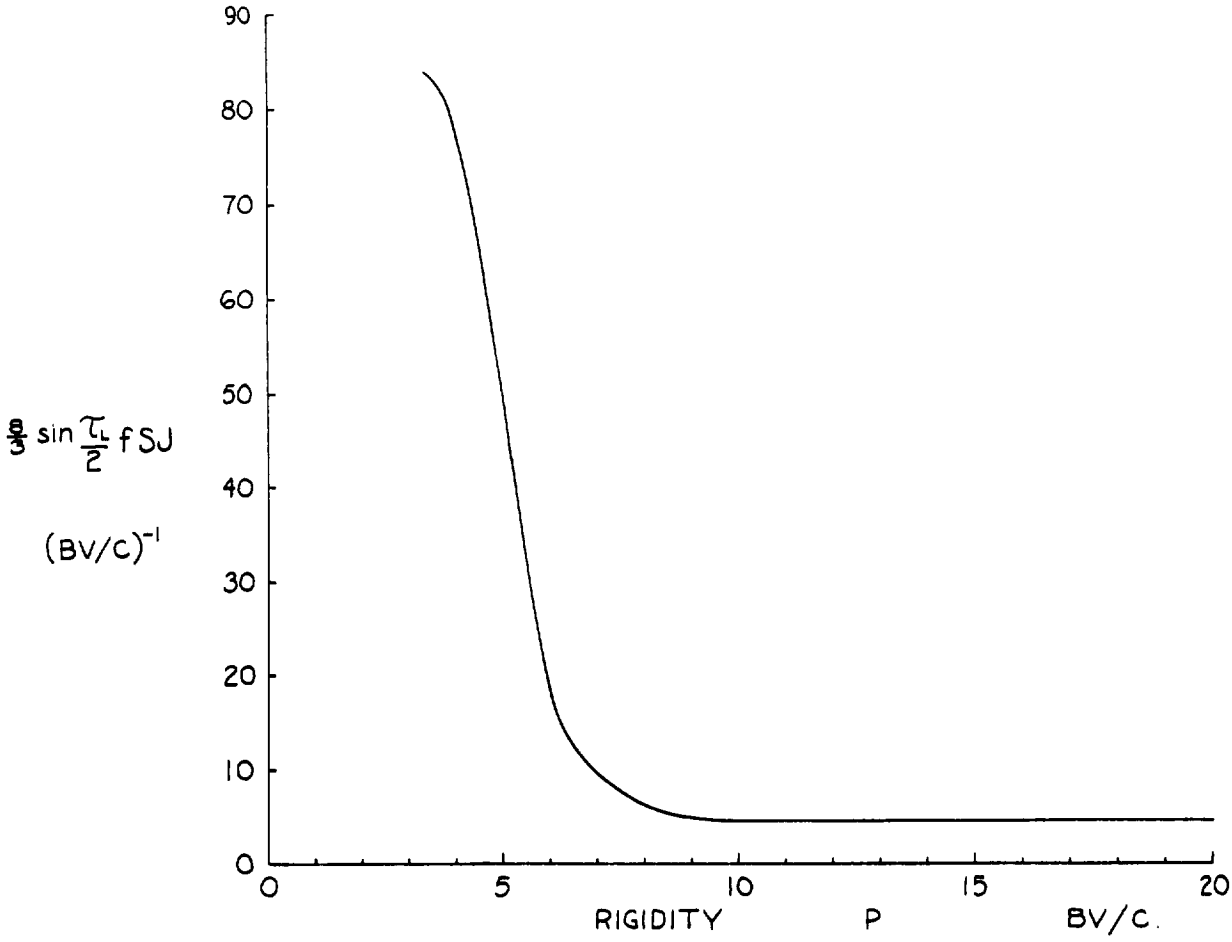

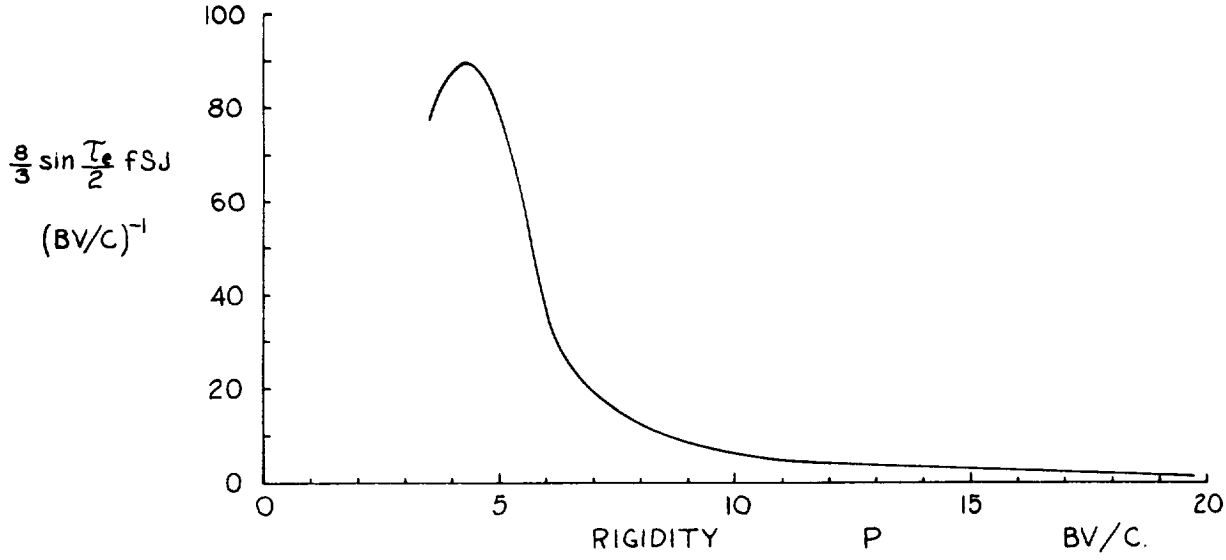

Fig. 17. THE FUNCTIONS $\frac{8}{3}\sin\frac{1}{2}\tau_{e,L}(P)f(P)S(P,X_o)J(P)$ WHICH MULTIPLY k(P) IN THE CRDV SPECTRAL INTEGRANDS $F_{e,L}$ USED. At P>20 BV/c these functions are given analytically in the text.